

DISSERTATION

Titel der Dissertation

Hydrodynamic behaviour of nummulitids

Verfasser

Antonino Briguglio, Dipl- Geol.

Angestrebter akademischer Grad

Doktor der Naturwissenschaften (Dr. rer. nat.)

Wien, im November 2010

Studienkennzahl lt. Studienblatt: A 091 434

Dissertationsgebiet lt. Studienblatt: Paläontologie

Betreuer: Ao. Univ. -Prof. Dr. Johann HOHENEGER

*Omnia suppeditat porro natura neque ulla
res animi pacem delibat tempore in ullo.
At contra nusquam apparent Acherusia templa,
nec tellus obstat quin omnia dispiciantur,
sub pedibus quae cumque infra per inane geruntur.
His ibi me rebus quaedam divina voluptas
percipit atque horror, quod sic natura tua vi
tam manifesta patens ex omni parte resecta est.*

Lucretius: *De rerum natura*, III, 23-3

Acknowledgement

I would like to extend my deepest acknowledgment to my mentor, teacher and supervisor Johann Hohenegger. This dissertation would not have been written without his patience, guidance and encouragement over these three years. For every question I always got an answer, for every request I always got permissions, for every discussion I always got time. To apply my ideas he let me use his experience, to route my young scientific ardour he taught method and reasoning, to correct my mistakes he took time for heated discussions.

I would also like to thank the reviewers for the published portions of this thesis: Joseph Serra-Kiel, Stephan Jorry, Cesare Andrea Papazzoni, Robert Speijer, Jarosław Tyszka. Their reviews were always thorough, detailed, stimulating and full of ideas resulted in great improvements on the publications. Cesare Andrea Papazzoni and James Nebelsick are also deeply acknowledged for agreeing to be reviewers for my dissertation, and for having been in Vienna for my Defence.

I want to thank Stefano Dominici, he spent several days with me in the field and, most important; he shared with me his love for nature, God, science and the Pyrenees.

Peter Pervesler, besides trying teaching me ichnology and the Viennese way of life, was my reference point for regional geology and palaeontology with his incredible cornucopia of ideas and surprises. Martin Zuschin showed me how is possible to combine love for life and passion for science: and he did it everyday, from 7 o'clock to late at night. I have to thank Benjamin Sames, my office mate, to have played with me the part of the young assistant. He challenged me to share an office with a barbarian and we both learnt a lot! Jennifer Sawyer showed me how to earn a PhD living abroad and within three years by sharing with me emotion, fear, passion for palaeontology, dedication and strength with the fastest talking speed ever!

My professional gratitude goes to the Institut für Paläontologie, Universität Wien and its scientific staff for providing me a position as assistant for four years. I have learnt a lot during my stay here. You put me in charge on some teaching and some

Acknowledgement

students; you gave me the chance to do my job always stimulating me in doing more and doing better. I thank Doris Nagel as head of the Department for having given to me this possibility. My stay in the university was homely and warm due to the precious smiles, advices and competence of Klaudia Zetter. Therefore, she gained since the very beginning of my stay in Vienna the appellative of Mamma Zetter. She does not know it yet, but she will figure it out very soon.

I would like to thank all those who, during the last years, have shown interest in my topic, shared their enthusiasm, literature and ideas, gave me tips to improve my work and answered my questions. I had the chance to meet them as persons beyond their scientific value. I will never forget the friendly handshaking of Lukas Hottinger, the generous hugs and smiles of Katica Drobne, the laugh of Willem Renema, the elegance of Ercüment Sirel, the hospitality of Ercan Ozcan, the helpfulness of György Less, the thirst for knowledge of Johannes Pignatti, the accuracy of Joseph Tosquella, the hilarity of Pamela Hallock, the friendship of Botond Kertesz, the vitality of Esmeralda Caus, the heartiness of Ursula Leppig and the style of Carles Ferrandez. I want to thank the colleagues belonging to the G.I.R.M.M. community, particularly Andrea Benedetti and Massimo Di Carlo. Their help, presence and continuous exchanging of opinion were important for my work during the last three years.

I have and I want to thank my parents. They always encouraged my stay abroad and supported it with all a child may need and wish: love, presence and limoncello. As usual, the inspiring muse of all my works is my brother, Runa. Man of science and full of ardour for beauty of nature and for phenomenology, he teaches me everyday curiosity and investigation on the world we have.

The love of a girl, her supporting, sharing and sustaining my anguish, fear, joy, love, passion and progresses produced this work.

Table of Contents

Acknowledgements	V
Table of Contents	VII
Abstract - English	1
Abstract - German	3
Preface	5
Introduction	7
Chapter 1	23
Chapter 2	43
Chapter 3	71
Chapter 4	107
Appendix	167
Curriculum Vitæ	171

Abstract

Larger foraminifera occurred abundantly in many Paleogene shelf carbonate platforms and were influenced by global and local factors. Ecology (e.g. temperature), geology (e.g. sea level changes) and evolution (e.g. population dynamics) affect the abundance and structure of larger foraminiferal communities. Water motion is the most important physical factor in shallow water environments directing the distribution of living individuals, and the distribution of empty shells mainly follows the input produced by water motion. The relationship between the biotic composition and the fossil association must always be taken into account for interpreting the palaeoenvironment. The shape of nummulitids and its relation with systematics on the one and water motion on the other side allows fascinating results. Concerning larger foraminifera, especially nummulitids, shape variation, size and internal structures are highly correlated with taxonomy. These parameters strongly influence the distribution of foraminiferal tests on a slope induced by water motion. Because of these correlations, estimations of palaeodepth can be based on the species distribution in the fossil environment. The calculation to obtain the hydrodynamic answer of nummulitid tests was applied to species belonging to the genera *Nummulites* and *Assilina*, as well as to some operculinids. The value of the hydrodynamic answer of a single test considers size, shape and density, and it is the combination of these variables that express the hydrodynamic behaviour of the specimen. Consequently, the diversity of forms collected within a layer is characterized by the same hydrodynamic behaviour. From a palaeoenvironmental point of view, due to sorting induced by water motion, transported tests with similar hydrodynamic behaviour are deposited in the same hydrodynamic environment. The measured and the calculated parameters allowed the definition of transport / deposition boundary and the location of accumulation areas.

Zusammenfassung

Großforaminiferen unterschiedlicher systematischer Zugehörigkeit bildeten in verschiedenen geologischen Zeiten mächtige Ablagerungen, die sich räumlich weit erstrecken. Solche Ablagerungen von *Nummulites* sind über einen Zeitraum von ca. 30 Millionen Jahren vom Jüngeren Paleozän bis in das Ältere Oligozän immer wieder anzutreffen. Die Interpretation der Umweltbedingungen zum Zeitpunkt dieser Ablagerungen war in den letzten 50 Jahren ein heißer Diskussionspunkt. Dies liegt teilweise in den Schwierigkeiten der Interpretation fossiler Gesteine selbst, insbesondere wenn der aktualistische Bezug durch das Fehlen rezenter vergleichbarer Organismen nicht angewendet werden kann. Ein Weg zur Klärung ist die Untersuchung der hydrodynamischen Eigenschaften von *Nummuliten*-Gehäusen. In den letzten 50 Jahren konnten Sedimentologen in zahlreichen Arbeiten die hydrodynamischen Eigenschaften von Sedimentkörnern erklären, insbesondere was den Transport und die Ablagerung während unterschiedlicher Wasserbewegungen (oszillatorisch oder gerichtet) sowohl im seichten als auch im tieferen Wasser betrifft. Zur selben Zeit erklärten Paläontologen die Verbreitung lebender Groß-Foraminiferen unter Verwendung komplexer statistischer Methoden. Mit diesem Datensatz ist es nun möglich, mit wenigen Kennzahlen (Parametern), die Anreicherung der fossilen Formen zu erklären.

Innerhalb der *Nummuliten*, bei denen zahlreiche Gehäusemerkmale von Umweltbedingungen beeinflusst wurden, benötigt man nur zwei, nämlich die Gehäuseform und die Dichte, um das Abheben, die Transportweite und das Absinken zu berechnen. Zur Berechnung der beiden oben genannten Kennzahlen genügen zwei Abmessungen, nämlich der Gehäusedurchmesser und die Gehäusedicke.

Nach Berechnung der hydrodynamischen Parameter wurden diese mit experimentellen Werten verglichen. Da diese Korrelation extrem signifikant ist, lassen sich die hydrodynamischen Parameter für alle Formen mit nummulitiden Gehäusen berechnen. Die Transportfähigkeit der Gehäuse konnte anhand ihrer Sinkgeschwindigkeit definiert werden: man findet Foraminiferen am häufigsten in jener Wassertiefe, wo die Wasserenergie schon zu schwach ist, um die Gehäuse abzuheben. Weil die Foraminiferen, um die Photosynthese ihrer Symbionten zu ermöglichen, so viel Licht

wie möglich zu absorbieren versuchen, leben sie bevorzugt in jener kritischen Tiefe, wo einerseits das Licht noch intensiv ist, andererseits die Wasserenergie nicht zu hoch ist. Um vom Substrat nicht abgehoben zu werden, müssen die Foraminiferen Gehäuse mit bestimmten Widerstandskoeffizienten bauen.

Durch die hohe Korrelation zwischen den hydrodynamischen Gehäuseparametern und der Wasserenergie, die durch die oszillatorische Wellenbewegung am Boden wirkt, lässt sich die durchschnittliche Wassertiefe, in der die Foraminiferen lebten, ermitteln. Wichtig ist jedoch, dass nicht nur die Transportfähigkeit der Gehäuse, sondern auch die Funktion von strukturellen Gehäusemerkmalen die Tiefeverteilung der einzelnen Arten charakterisieren.

Preface:

It was probably on Thursday April 12th 2007, the day I gave my first talk to the scientific staff of the Department of Palaeontology, University of Vienna. It was the most horrible day of my career, at least, until now. I spent unsuccessfully the morning through almost all the electronics shops in Vienna to find an austrian adapter for my italian laptop and I could not practice my talk. To show my presentation I received a laptop with some kind of old-fashion slide program, which - because of common compatibility problems - produced funny slides, distorted artistically my figures and mashed together my animations. It was terrible. The public knocked on the desks as soon as I finished my presentation: I was shocked. I had never heard about such custom and usance in an academia. I have to thank Prof. Hohenegger for having explained me "in situ" the meaning of such knocking and for having calmed my fear in front of the audience's reaction. Among the many questions I got on my mashed and distorted topic, I do remember one: "Very nice work, very interesting... yes... climbing up there... but, did you consider transport into your studies?"

"Transport?"

The rest is history.

Introduction

Taphonomy is defined as the branch of science dealing with the preservation of organisms and their traces in sediments. Proposed by Efremov (1940), it literally means the laws of burial (*τάφος* = burial, *νόμος* = law). The definition of taphonomy as reported in Efremov's work reads as follows: "*the study of the transition (in all its details) of animal remains from the biosphere into the lithosphere*" (Efremov, 1940, p, 85). Consequently, it includes all the processes that may happen between the organism's death and its finding in the rock as whatever rest it has become, considering also the non-preservation condition. Thus, it deals with death, dissolution, abrasion, transport, diagenesis, and many other processes.

However, taphonomy goes beyond a mere list of different themes. It is the study of the sequence of processes, which allow the recognition of fossil forms (both body and trace fossils). The definition of the environment (or environments) that may have contained the fossil during its preservation history is a dominant part within a taphonomic study.

Taphonomy, in all its related fields (geochemistry, sedimentology, taxonomy, mathematics, tectonics etc...) plays a pivotal role in understanding the processes behind preserved or dissolved fossil. It is not only a matter of considering fossil forms (or their evidence) as autochthonous or allochthonous; but it is a matter of recognizing what was present and it is not anymore. Taphonomists should recognize the presence of fossil associations even when they are no more preserved.

From this point of view, the fossil record becomes a huge source of information about palaeocommunities and their environments; often displaced through space and time, not easy to collect, even more complicated to correlate and understand. Different time scales may be fused together at different levels: the instantaneous event may be embedded into a long time scale event; thousands or million of years may be erased in a snatch. Most of times, what we see is a poorly preserved incomplete story. However, to reconstruct the past, we should consider those missing parts not preserved or not recorded; but quite often, it is not like this.

Taphonomy, in respect to taxonomy or evolution or even biology, is a relative young and complex science and it is so strictly connected to many others disciplines that it is very difficult for scientists and taphonomists to care about all those aspects in a rigorous

way and simultaneously. Due to its variety of aspects and themes can taphonomy be studied, many scientists are approaching the topic with always more details, methods and results.

During the last decades, taphonomy became always more prominent within many studies concerning palaeontology and geology. Among all the taphonomic aspects, the preservation of the fossil organisms, strictly related to its geochemical aspects, is playing the major role. Soft tissues preservation and dissolution conditions are very common topics in recent taphonomic studies. However, as stated here, at the very beginning taphonomy goes beyond these starting issues.

The way to preservation in the fossil record is quite articulated; every single fossil has a specific story and could have been exposed to several taphonomic processes (transport, burial, diagenesis, etc.), sometimes causing its death but always acting after death. Depending on their presence and operation mode through time, there can be evidence of different taphonomic pathways.

Most of the previous taphonomic studies were based on shelly fossils and nomenclature was mainly based on such group of invertebrates (Kidwell et al., 1991). Terms as biocoenosis, thanatocoenosis, taphocoenosis and orictocoenosis are well known in the literature and scientists refer to such terms to delineate the taphonomy of an organism (Figure 1).

Thus, the main task of taphonomy is to find the way back from fossil remains to the original biocoenosis, meanwhile always considering such processes as transport, dissolution, destruction, accumulation, which might have been occurred at any time during the period of fossilization. For taphonomic analyses in marine environments, this should be a mandatory.

Concerning taphonomy, an integrated taphonomic study including sedimentology, mathematics and taxonomy, focusing on transport mechanisms of organisms in the marine systems is so far unknown. Even if shallow water environments are considered as the hot spots for biodiversity, a systematically based taphonomic study dealing with abundance of organisms and hydrodynamics is still missing.

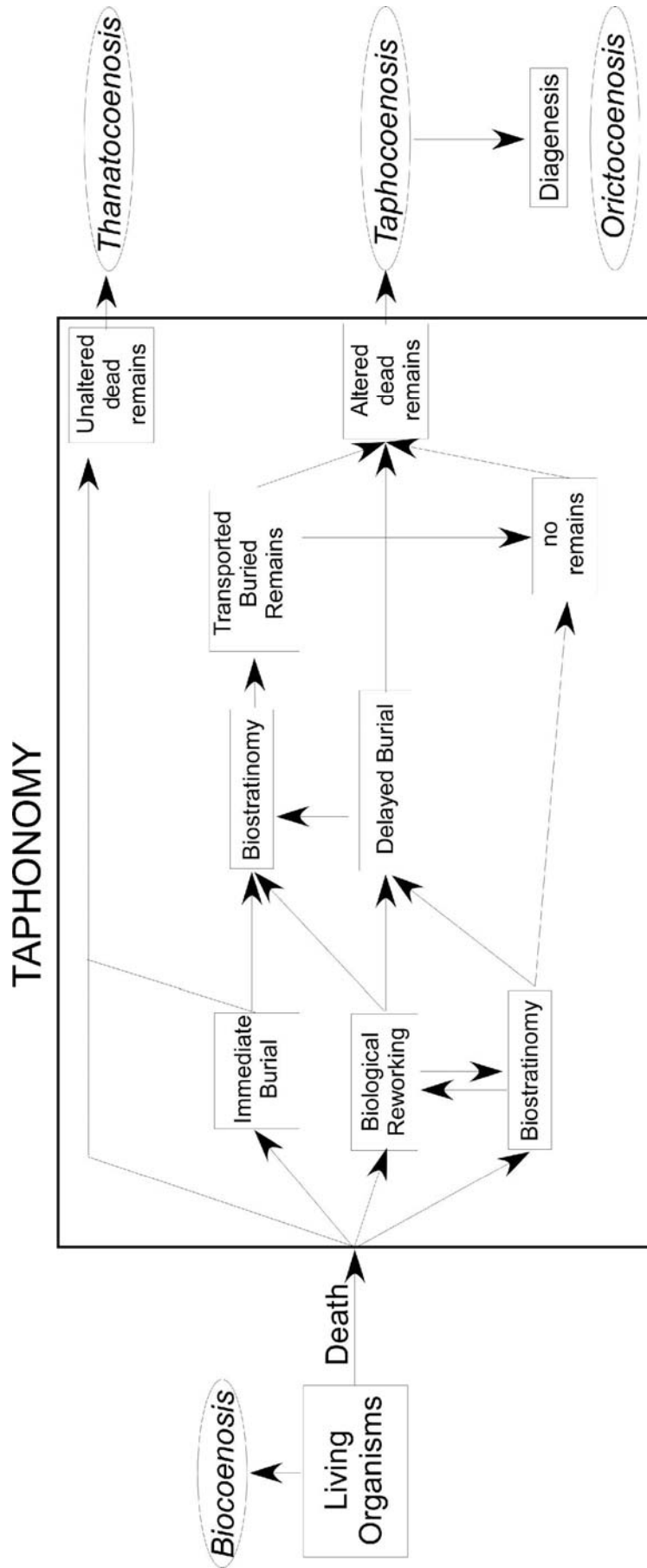


Figure 1: Taphonomic pathways.

A study on processes altering the abundance of fossils and their preservation is quite complex. The recognition and quantification of all mechanisms (physical, chemical and biological) acting on the organisms by reducing their number are still an unclear topic, even approaches by field observation, various methods and comparisons of data allows insight on the intensities of these processes. Some of these approaches require mathematical calculations with complex formulas or laboratory experiments, and are mainly avoided by many taphonomists even if the results can be very useful for palaeoenvironmental reconstructions and palaeoecological characterizations. Between the two important topics in taphonomy, transport and dissolution, the latter is the one where much was done in the past decades. By microfacies analysis and by experimental simulations some results about transport are coming out; on the contrary, a throughout quantitative analysis concerning transport and accumulation processes is still missing.

Transport and deposition are the results of energetic input on an organism remain and may occur in terrestrial, lacustrine and marine environments. Transport effects can be observed at a very large spectrum of scales. Wind generated sediments, seabed forms, sorting, grading, selection and many others are the product of energy input into a certain environment. Deposits of tsunamis, landslides, rock fall, ripples or traction carpets are examples how diverse the results of different energy input may be with different intensity and different time intervals. Such energy inputs are mainly due to gravity, solar insolation and Earth's rotation. The study of transport in an aquatic scenario is a well-known topic and the way that particles react to water input is well documented in the literature. The analysis of hydrodynamics and the hydrodynamic behaviour of particles have a long history and sedimentologists can explain seabed forms and grain sorting by quantifying shape, size and density of the particles and the energy of the transport input.

Currents, streams and deep transport may always occur with different energy from shallow waters to deeper environments; produced by different causes, such processes may lead to a high diversity of results depending on several variables. In high-energy scenarios (shallow waters, escarpment, steep slopes, etc...), transport may play the major role in forcing the spatial distribution of particles and of organisms. In low energy scenario, transport may not occur or can act only for the smallest sediment's particles.

Foraminifera, among the many groups of organisms living in high-energy scenarios, are considered as one of the most abundant and most diverse group in shallow water environments. Such group has been studied intensively since the age of d'Orbigny and Dujardin from the middle 1800. After more than two centuries, an assessed taxonomy allows clear definition and recognition of species based on morphologic variations and many taxa are considered as ecological and environmental proxies. A small group of taxa within the class Foraminiferida is characterized by larger size, extreme morphologic differentiation and by the possibility to host light dependent endosymbionts: the so-called Larger Benthic Foraminifera (LBF herein). The taphonomic analyses presented in this work are based on this informal group of foraminifera, particularly concentrated on their hydrodynamic behaviour and on the transport mechanisms they are subjected to.

Foraminifera were, in some parts of the fossil record, the organisms group most abundant and most differentiated; under convenient ecologic conditions; they could build multi kilometric monospecific assemblages still visible nowadays. Because of their benthonic life style and their photosynthetic symbionts-bearing characteristic, LBF had to survive at certain water depths where the endosymbionts could get enough light for photosynthesis. As marine organisms, the photic zone is only suited to get enough light for the symbionts. At the same time, such environments are always characterized by high energetic hydrodynamics, which may act on the seafloor keeping particles in suspension, i.e., transporting foraminifera test out of their habitat, killing or destroying them. The evidence that LBF can survive such extreme environments constantly proved by intense energy inputs, leads to hypotheses on suitable methods developed by these single celled organisms building tests capable at the same time to resist water motion and let the hosting symbionts survive.

For this reason, a taphonomic study on this organisms group focused on transport and their hydrodynamic behaviour is very important for palaeoenvironmental reconstruction; even more if considering the amazing morphological diversity, which is able to produce the same drag to transport input. In the literature, no comparative analysis between recent and fossil forms about transport intensities and processes and results exist. As experienced during this work, the study of the hydrodynamic behaviour in LBF and specifically in nummulitids allows fascinating results concerning biology, shell morphology, reproduction strategies and ecological characterization of such group

of organisms that can be assessed also in the fossil record. As the hydrodynamic rules follow physic laws of dynamics, the use of such laws in the fossil record is permitted. As already stated, LBF are an informal group within the foraminiferida possessing an extraordinary morphological diversity which led taxonomists producing a very large spectrum of characters useful for systematics and a consequently abundant number of taxa defined by morphological changes trough time. Such very high morphological diversity and complex taxonomy produced an articulated differentiation of forms, whose correlation with environmental gradient fits very well (Figure 2).

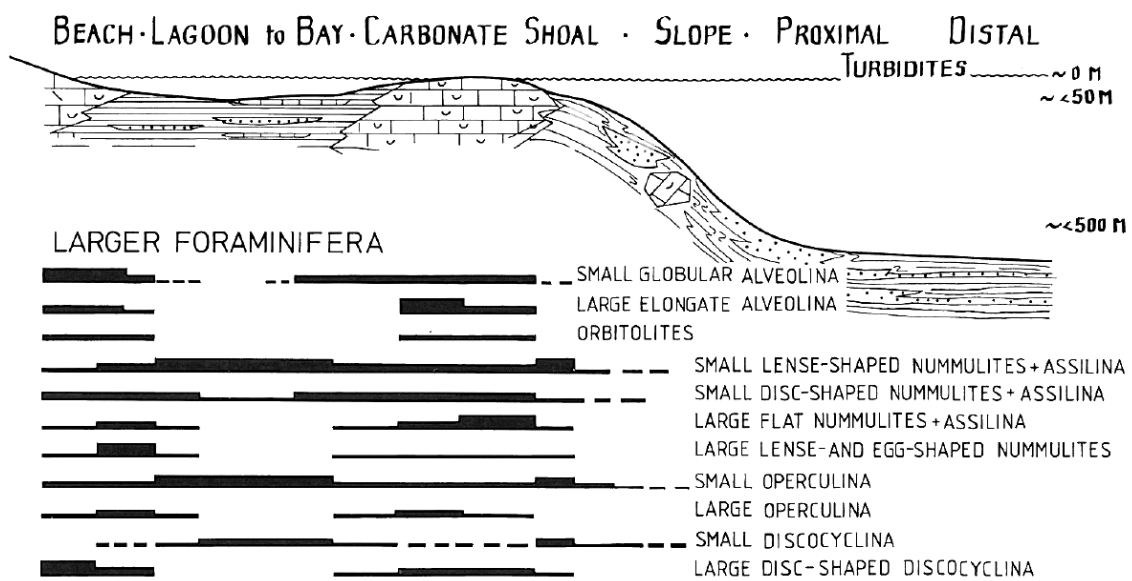


Figure 2: Palaeoecological distribution of LBF as published by Luterbacher (1984).

The definition of a *morphocoenocline*, proposed by Hohenegger (2006) and tested on the morphological diversity of larger benthic foraminifera, is based on species characteristic combination of morphological characters depending on an environmental gradient. Such feature leads larger benthic foraminifera to be one of the best-suited groups of organisms considered as a key for ecological analysis in fossil and recent environments.

This use of LBF for ecological as environmental indicators led to some considerations and questions at the beginning of this work. How is it possible that LBF are considered ecological and environmental proxies, if they live in shallow water environments with an energetic scenario very variable and intense? To survive within their habitat, they have to resist water motion, at least, until reproduction. As solution against water

motion, some species developed fixing strategies by using special anchoring systems; others hide themselves below sediment grains. However, the majority of the species do not possess any of these adaptive strategies; they must have test geometry able to resist water motion and, at the same time, large enough to host endosymbionts for photosynthesis. Thus, at the beginning of this research, the main task was the quantification of the hydrodynamic behaviour of nummulitids shape and the study of all the many hydrodynamic parameters useful for environmental and ecological reconstruction. Even if its importance has been affirmed in many studies, the hydrodynamic behaviour of nummulitids was still poorly described.

During the last decade, many theories were provided to understand the *post mortem* fate of nummulitid foraminifera and several depositional models have been proposed to understand the palaeoecology, palaeoenvironment and hydrodynamic behaviour of nummulitids. Previous studies have shown that large benthic foraminifera can be easily reworked by waves and currents (Yordanova & Hohenegger, 2007) and several authors pointed out that the hydrodynamic behaviour of *Nummulites* is an important factor controlling their distribution (Jorry *et al.*, 2006). Main factors controlling and differentiating the hydrodynamic behaviour of every object are size, density and shape. From these three parameters, many others can be calculated to get more information on particle hydrodynamics. The following hydrodynamic parameters were thus calculated: settling velocity, shear velocity and critical shear velocity, critical shear stress, shape entropy, drag coefficient and Reynolds number (Briguglio & Hohenegger, 2009a). Results were compared with those obtained using optimally preserved shells of recent nummulitids by experiments made by Yordanova & Hohenegger (2007) (Briguglio & Hohenegger, 2008). Since the results were highly comparable, it was possible – without any laboratory analysis – to reconstruct a shallow water zonation based on species-specific hydrodynamic parameters, which characterize every form and its reaction to an energy input (Briguglio, 2009). The extraordinary diversity in morphology visible and measurable on LBF, leads to an extraordinary diversity in hydrodynamic answers due to a single given input (Briguglio & Hohenegger, 2009b). Such diversity in hydrodynamic behaviour as answer to a single energy input may lead to the differentiation of ecological niches allowing occupation of several habitats in shallow water environments, or the development of hydrodynamic convenient shapes with a direct correlation shape / depth (Briguglio & Hohenegger, 2010a).

The correlation between morphological characters and water depth has been treated for long time with great results but a further step, i.e., the correlation between morphological characters and energetic scenario has not yet been investigated neither theoretically nor quantitatively. A quantitative research on how intensively foraminifera do react to water motion is still missing; the correspondence between shell morphology and water depth, well known and assessed by biological arguments, can be extended including hydrodynamic behaviour of such organisms. This is the goal of this thesis.

The first step was to understand the hydrodynamic behaviour of nummulitids by the analysis of the main parameters characterising their test: density, shape and size.

The study on sizes was possible by using shape free parameters, which, among different uses, allow the comparison between tests of different sizes (i.e., species, family). In this way, the use of a Nominal Diameter is essential (Briguglio, 2008). Once the shape free parameters have been established, the dimensionless sphere settling velocity was calculated as well as the Critical Shear Velocity (Briguglio & Hohenegger, 2009a). It has been tested that both parameters are key-values for the transport/deposition boundary definition (Briguglio, 2009).

Shape drives the equation process by reducing or increasing settling velocity: a complete set of equation has been developed and tested to calculate shape entropy produced by the shell and to evaluate the right formula to get the real settling velocity (Briguglio & Hohenegger, 2010d). The calculated shape entropies formulas are therefore diagnostic to choose the best-suited settling velocity equation. Some formulas assume the falling object as spherical, others, most accurate for flatter species (i.e., disk-like test such as *Cycloclypeus carpenteri*), take into account the ratios between the projections of the three main axes of an ellipsoid containing the test and they strongly reduce the settling velocity of a sphere. For plate-like tests or not rounded tests, the best mathematical calculation is a formula where the volume/half-surface ratio is included; such parameter significantly reduces the sinking effect and increases the accuracy of the calculation.

Elemental mapping, EDX analyses (Figures 3, 4) and micro computed tomography (CT) imaging (Figures 5, 6) have been used to identify test composition and to calculate lumina volumes in order to evaluate the density of fossilised recrystallized specimens. Density, plus size and shape dependent parameters were used to calculate the settling

velocity of every test and let the settling velocity calculation being used also for fossil tests (Briguglio & Forchielli, 2010).

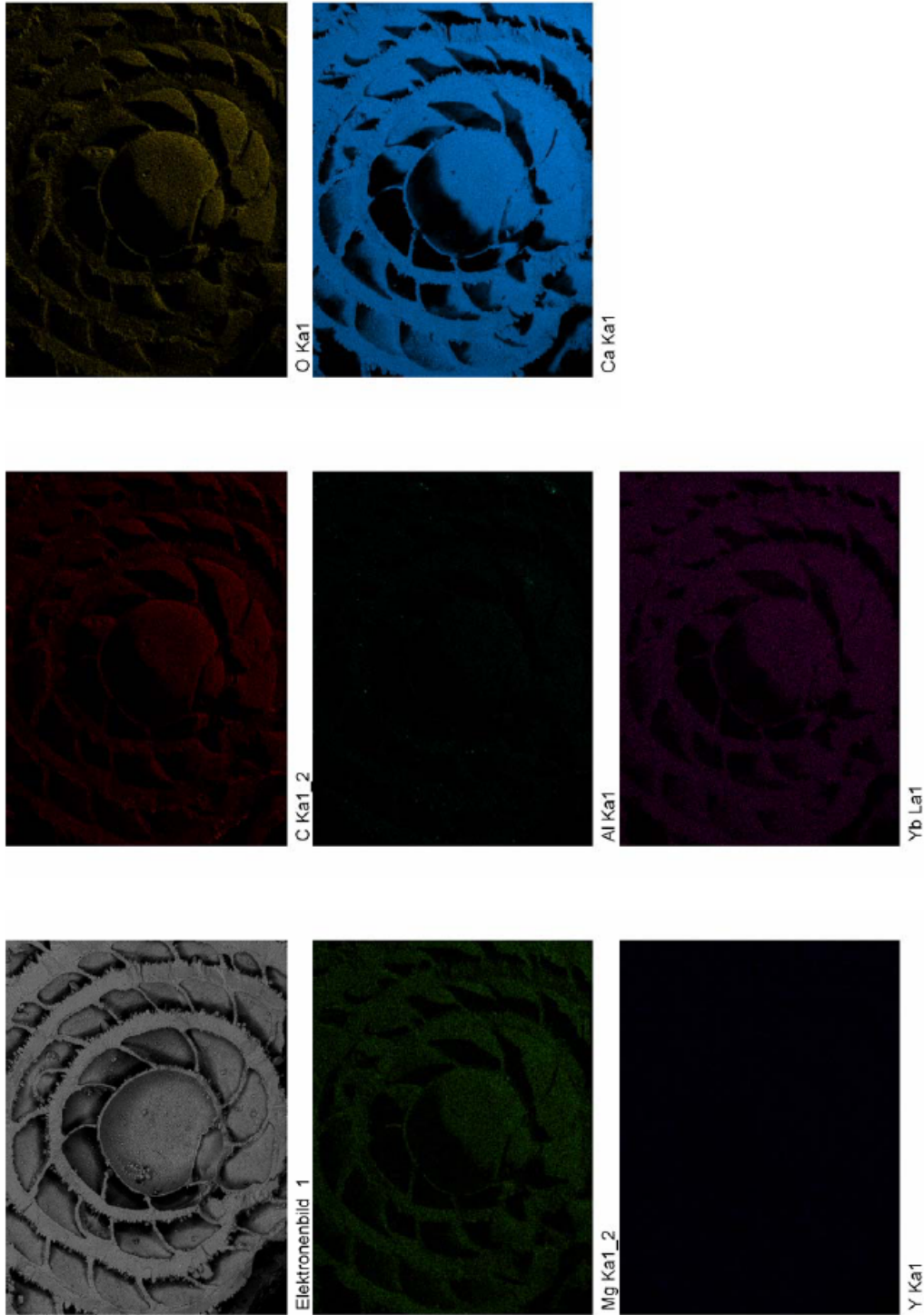


Figure 3: Element mapping of equatorial oriented section of an A-form specimens of *Nummulites perforatus*. Colors indicate the presence of the listed chemical element. The most abundant elements are Calcium (Ca), Magnesium (Mg), and Oxygen (O)

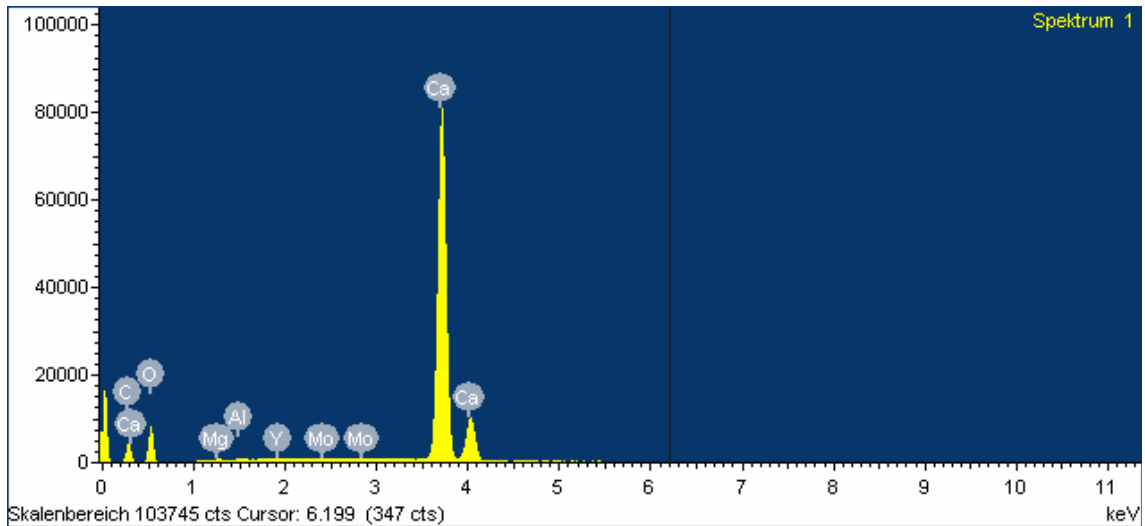
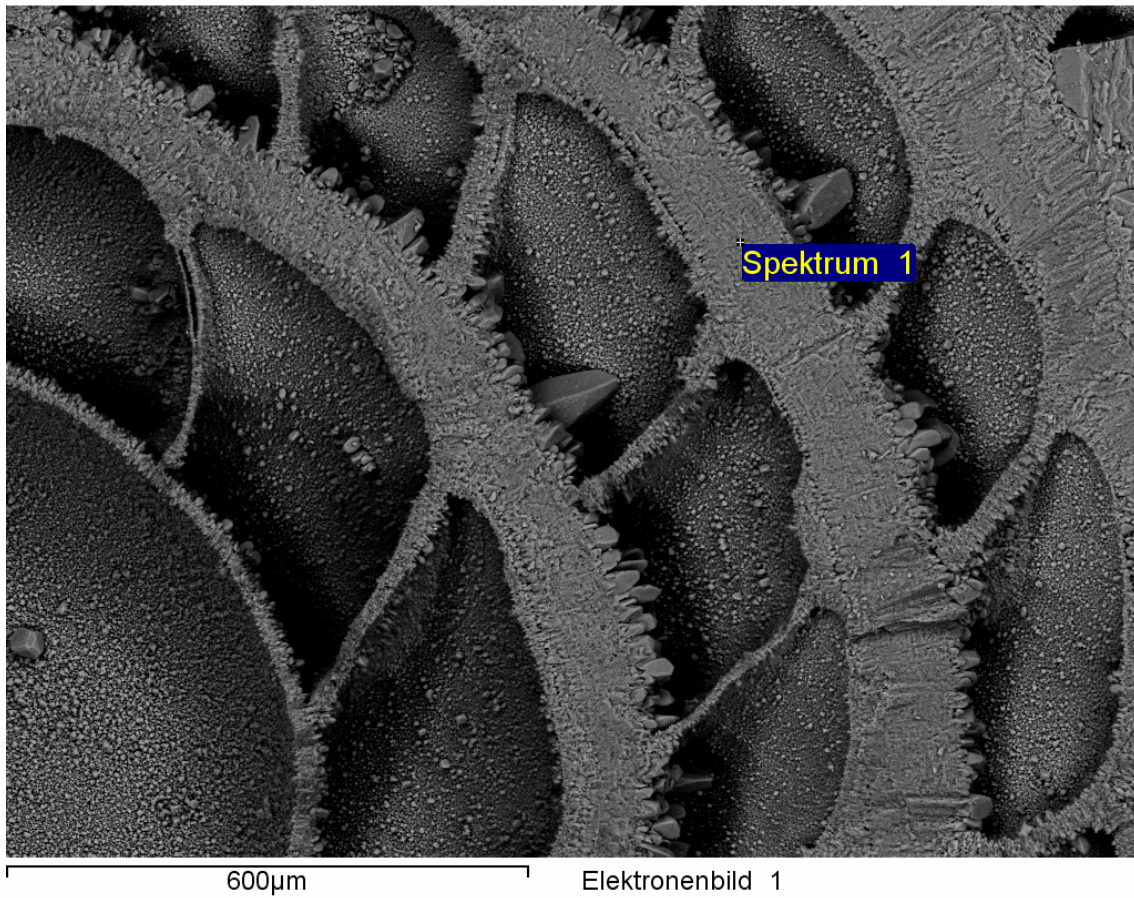


Figure 4: EDX analysis on the marginal chord of a fossil *Nummulites perforatus*. The elements abundance is revealed by the graph below.

Obtained results and future possible applications are the main part of a paper (Briguglio et al., accepted) that will be published in a volume of invited papers on LBF which represents the proceedings of the session *Tertiary Larger Foraminifera: Evolution*,

Biostratigraphy, Palaeoecology and Palaeobiogeography, which took place during the 62nd Geological Kurultai of Turkey, 13–17 April 2009, at the MTA-Ankara.

Beside the study of density, the published results concerning biometry and phylogeny by mean of computed microtomography are of great interest (Briguglio & Hohenegger, 2010b, 2010c), even if not directly connected with hydrodynamics. More work will be carried out in the future about such new technique and its application on recent and fossil forms.

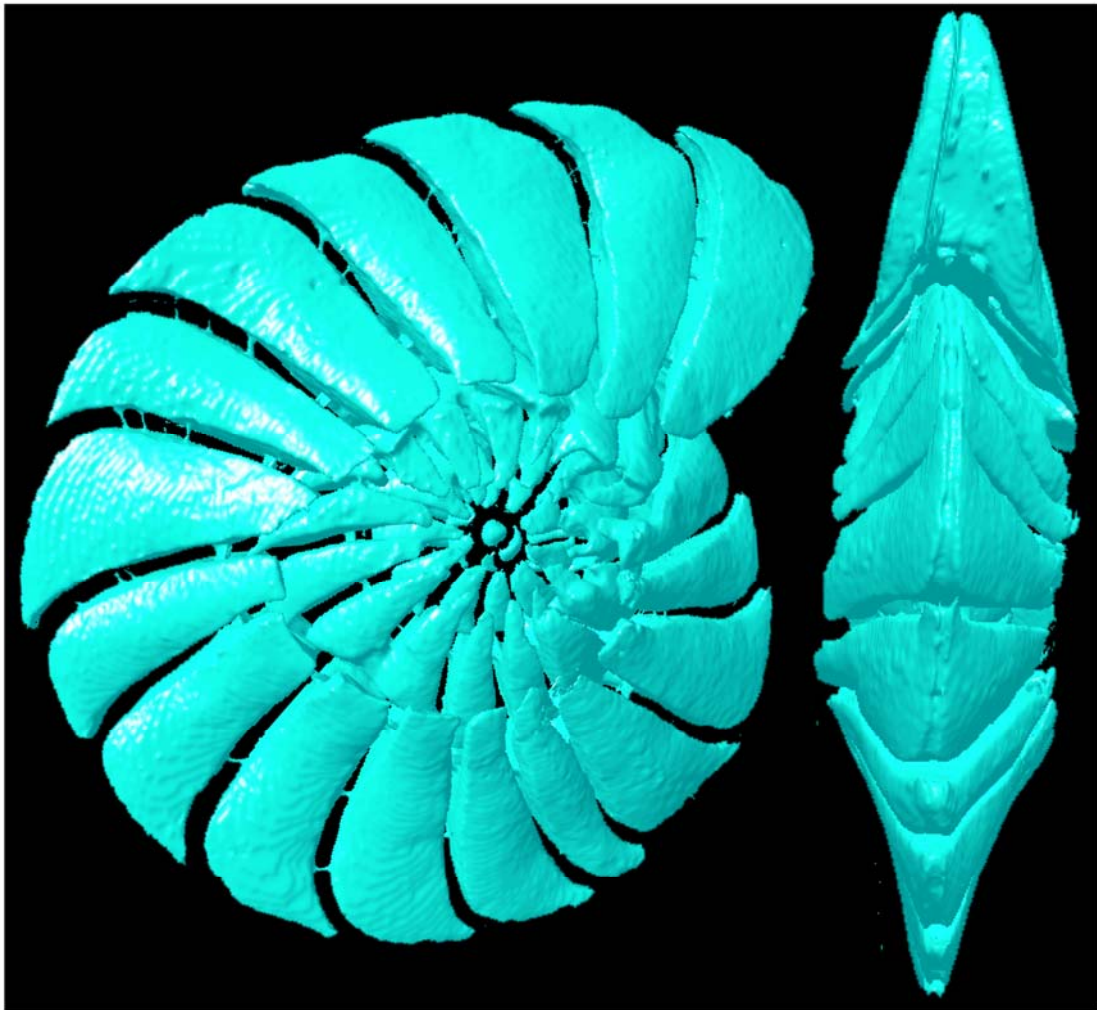


Figure 5: segmented and extracted lumina of a specimen of recent *Operculina ammonoides* by microCT imaging.

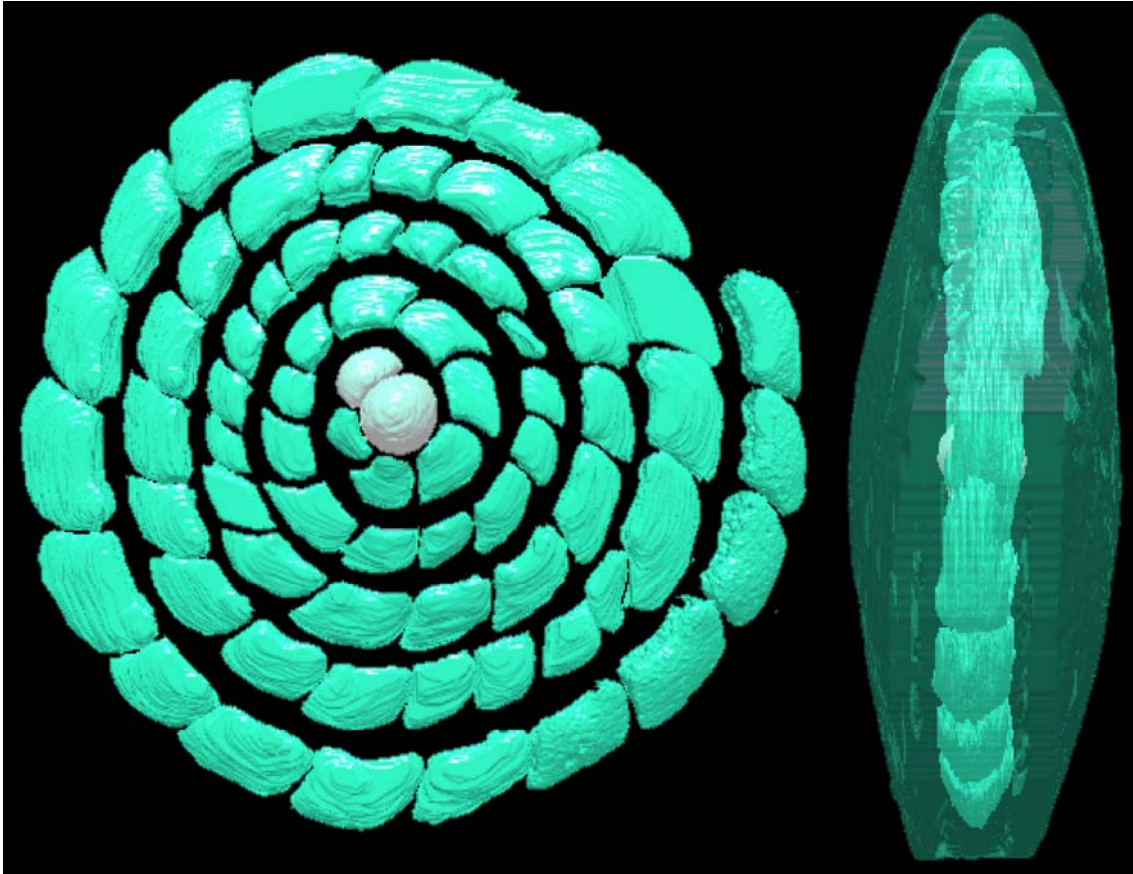


Figure 6: segmented and extracted lumina of a specimen of fossil *Nummulites fichteli* by microCT imaging.

Once the hydrodynamic parameters have been calculated and their significance was tested, the correlation between test morphology and the energy input given by water motion at the sea bottom for every depth in shallow water environments was examined in a third paper. The correlation between the high morphologic diversity (i.e., taxonomy) and the wave-induced bottom orbital velocity (BOV herein) gave exiting results (Briguglio & Hohenegger, submitted). The main part of this paper (submitted to *Marine Micropalaeontology*) deals with the correlation between water depth, species-specific settling velocity and depth-specific BOV. The results seem to be of great importance for the study of shell morphology and function. As explained in the manuscript, every species has shape entropy and settling velocity very well comparable with the energetic input acting at the water depth where the species is living and has its ecological optimum. It means that LBF build tests able to remain within their ecological optimum during lifetime at the energy condition caused by fair weather. Transported organisms are due to higher energy conditions. Some exceptions and a detailed discussion are reported in the paper.

The calculation proposed is very innovative and broadly provocative because it takes into account the near-bed orbital velocities caused by wind-generated waves: it has never been considered before.

Such velocities are mathematically calculable for every wave and for every depth and it seems that consistent velocities (able to act on low density particle and to produce transport) may happen also at water depths of several hundreds of meters. If the relation $h = \lambda/2$ defines the water depth where the orbital velocity reaches the sea floor (where h represents water depth and λ the wave length), a wave of several hundreds of meters in λ (which is not very large; in fact waves can be much larger in λ) may act to the sediment at elevated depths. Now, depending on the nature of the sediment's particles (density, shape and size), such wave-induced orbital velocity may or may not be able to move the particle itself. Concerning wave motion and water depth, it is well known that the sea wave base during fair weather condition is located at 20 - 30 meters and during storm events the limit is located at 80 - 100 meters below the sea surface. Such depths are actually considered for standard sediment particles, mainly quartz grains, with a mean density of 2.65. LBF have a density slightly above 1.2, thus more than 50% less dense than a 'normal' sediment grain. In deeper environments, the same energy input at the sea floor cannot move a sediment grain but take in suspension foraminiferal shells. The comparison between settling velocity and BOV for every test at each depth allowed us the definition of species-specific transport/deposition boundaries (Briguglio & Hohenegger, 2010a, Briguglio et al., submitted). That is why a hydrodynamic study of shallow water environment should be always taken into account, especially for LBF studies.

The hydrodynamic characterization of an energetic scenario should take into consideration the relations between energy input and the answer given by the 'objects' located in the scenario in a kind of input/output regime. The energy input is normally given by the quantification of water movement within the water column and can be acted by currents, streams, sea waves, etc. The answer given by an object to such input is quite complicated and requires some complex mathematics. It can be quantified in many different ways depending on the kind of the input. It may be represented by its critical shear velocity if it is the case of transport by entrainment or may be expressed in term of Reynolds number if the turbulence plays an incisive role. It can be expressed as sinking velocity due to gravity resisting the vertical water input. All this parameters,

measurable in adequate laboratories requiring complicated techniques and time-consuming methods, are now mathematically calculable.

The application of the hydrodynamic behaviour of nummulitids in the fossil record and the use of the hydrodynamic equilibrium between settling velocity and BOV along a vertical geological profile was the last step. The geological and palaeontological study of a profile is a fascinating topic, which always can be expanded and the amount of information a geologist can get from outcrops is enormous. Similar to taphonomy, an outcrop can be approached by a very broad spectrum of disciplines: from lithology to biostratigraphy, from stable isotopes to magnetostratigraphy. However, the hydrodynamics of the organisms we find in rocks is a complementary approach applicable for field works and palaeoenvironmental reconstruction. A multitasking approach is definitely the one giving the most comprehensive information about an outcrop, but detailed analysis on the one topic or the other may provide extraordinary results. The many equations used to reconstruct the hydrodynamic behaviour of such organisms, were applied on samples and on sequences of samples. The concept of the dimensionless velocities or the use of shape independent parameters or linear volume size parameters allows comparison within samples and between samples with different diversities. Different species may have lived in the same environment even if they possess diverse morphology and still producing the same shape entropy or resisting water motion with the same sinking rate. Often the taxonomic definition and differentiation of LBF depending on shape parameters and comparable along certain environmental gradient, are just specific hydrodynamic answers to a single energetic input, but the species itself remains the same, it is just adapting itself to different water input, then different water depths.

There are still many equations that must be corrected and proofed for a broader range of forms and taxa; many topics need to be more specifically clarified and studied. We strongly believe, that we proposed an innovative topic, provocative within its conception and certainly of very broad interest.

References:

- Briguglio, A., 2008, *Nummulites*: ein einfaches geometrisches Verfahren zur Bestimmung hydrodynamischer Parameter: in Jahrestagung Österreichische Paläontologische Gesellschaft. Dornbirn. *Berichte der Geologischen Bundesanstalt*, 75: 8. 14.
- Briguglio, A., 2009, In vita and post mortem forams events: hydrodynamic tools for paleoenvironmental reconstructions: *Tertiary Larger Foraminifera: Evolution, Biostratigraphy, Palaeoecology and Palaeobiogeography*, 62nd Geological Kurultai of Turkey, 13–17 April 2009, MTA-Ankara, Türkiye: Abstracts volume: p. 893.
- Briguglio, A., & Forchielli, A., 2010, Transportability of Larger Benthic Foraminifera. *Third International Palaeontological Congress IPC3, London*. Abstracts volume: p. 102.
- Briguglio, A., Metscher, B., & Hohenegger, J., accepted, Growth Rate Biometric Quantification by X-ray Microtomography on Larger Benthic Foraminifera: Three-dimensional Measurements push Nummulitids into the Fourth Dimension. *Turkish Journal of Earth Science*.
- Briguglio, A., & Hohenegger, J., 2008, Hydrodynamic behaviour of nummulitids: a non-experimental approach. In: Mazzei R., Fondi R., Foresi L., Riforgiato F. & Verducci M. (eds), *Riassunti dei lavori Giornate di Paleontologia 2008*: 14.
- Briguglio, A., & Hohenegger, J., 2009a, Nummulitids hydrodynamics: an example using *Nummulites globulus* Leymerie, 1846. *Bollettino della Società Paleontologica Italiana*, 48(2), 105-111.
- Briguglio, A., & Hohenegger, J., 2009b, Reconstructing the paleoenvironment of nummulitid strata: transport, erosion and deposition. 79. *Jahrestagung der Paläontologischen Gesellschaft*, Bonn 5-7/10/2009. *Terra Nostra*, 2009/3: 24.
- Briguglio, A., & Hohenegger, J., 2010a, Biostratinomy in shallow water environments: how to tackle the larger benthic foraminifera depth distribution. *Third International Palaeontological Congress IPC3, London*. Abstracts volume: p. 102.
- Briguglio, A., & Hohenegger, J., 2010b, Functional Test Morphology of larger Benthic Foraminifera: Biometric Quantification by X-Ray Microtomography. *Third International Palaeontological Congress IPC3, London*. Abstracts volume: p. 101.

- Briguglio, A., & Hohenegger, J., 2010c, Quantifying Forams' Growth with high resolution X-Ray Computed Tomography: Ontogeny, Phylogeny, and Paleooceanographic Applications. *Forams 2010 - International Symposium on Foraminifera*, Abstracts volume: 62.
- Briguglio, A., Hohenegger, J., 2010d, The Shape entropy Parameter: a Geometric Tool to Approach Larger Foraminifera Accumulation. *Forams 2010 - International Symposium on Foraminifera*, Abstracts volume: p. 63.
- Briguglio, A., Hohenegger, J., & Yordanova, K.E., submitted: How to react to shallow water hydrodynamics: The larger benthic foraminifera solution. *Marine Micropalaeontology*
- Efremov, I.A., 1940, Taphonomy: a new branch of paleontology: *Pan American Geology*, 74, 81-93.
- Hohenegger, J., 2006, Morphocoenoclines, character combination, and environmental gradients: a case study using symbiont-bearing benthic foraminifera. *Paleobiology*, 32(1), 70-99.
- Kidwell, S.M., & Bosence, D.W.J., 1991. Taphonomy and timeaveraging of marine shelly faunas. In: *P.A. Allison and D.E.G. Briggs (Editors), Taphonomy: Releasing the Data Locked in the Fossil Record*. Plenum, New York, pp. 115-209.
- Jorry, S.J., Hasler, C.A., & Davaud, E., 2006, Hydrodynamic behaviour of *Nummulites*: implication for depositional models. *Facies*, 52, 221-235.
- Luterbacher, H.P., 1984, Paleocology of Foraminifera in the Paleogene of the Southern Pyrenees. Benthos '83, 2nd International Symposium on Benthic Foraminifera, Pau 1983, 389-392.
- Yordanova, E.K., and Hohenegger, J., 2007, Studies on settling, traction and entrainment of larger benthic foraminiferal tests: implication for accumulation in shallow marine sediments. *Sedimentology*, 54(6), 1273-1306.

Chapter 1

Briguglio A. & Hohenegger J. (2009) - Nummulitids hydrodynamics: an example using *Nummulites globulus* Leymerie, 1846. *Bollettino della Società Paleontologica Italiana*, 48(2): 105-111.

Size is not everything.

Master Joda



Nummulitids hydrodynamics: an example using *Nummulites globulus* Leymerie, 1846

Antonino BRIGUGLIO & Johann HOHENEGGER

A. Briguglio, Department of Paleontology, University of Vienna, Geozentrum, Althanstrasse 14, A-1090 Vienna, Austria; antonino.briguglio@univie.ac.at
J. Hohenegger, Department of Paleontology, University of Vienna, Geozentrum, Althanstrasse 14, A-1090 Vienna, Austria; johann.hohenegger@univie.ac.at

KEY WORDS - Larger foraminifera, Hydrodynamic behaviour, Settling velocity, Nummulitids, Transport.

ABSTRACT - The main physical variables influencing the hydrodynamic behaviour of nummulitid tests are size, density and shape. After measuring these variables, further parameters must be calculated to obtain an approximation to the hydrodynamic behaviour of the test. These parameters are volume, nominal diameter, critical shear velocity, critical shear stress, shape entropy, shape-independent settling velocity, settling velocity of a non spherical form, Reynolds number, and drag coefficient. Some of these data were calculated by combining shell measurements with physical properties of the seawater.

The aim of this paper is to explain numerical calculations for qualifying and quantifying the hydrodynamic parameters of nummulitids. Every single step or formula is important to evaluate the hydrodynamics of a particle or test respectively, especially in shallow water environments where energy strongly varies depending on different physical factors induced by the climate and the topography of the platform. Several methods to calculate the same parameters are also presented and compared to show the best-suited one for nummulitids.

In the fossil record, the faunal composition and the distribution of tests mainly depend on the two groups of cause-event effects: in vita and post mortem. Inferences about a fossil shallow benthic fauna must consider beside biological and ecological features further physical parameters like transport and deposition leading to distinct distribution patterns.

RIASSUNTO - [Idrodinamica dei nummulitidi: l'esempio di *Nummulites globulus* Leymerie, 1846] - Lo scopo dell'articolo è di illustrare il procedimento matematico che porta ad ottenere i parametri idrodinamici che servono a valutare la risposta dei gusci, sia in vita che post mortem, ad un input energetico che ne può causare il trasporto. La quantificazione del trasporto e la sua qualificazione avviene tramite il calcolo matematico dei parametri idrodinamici del materiale trasportato: in questo caso i nummulitidi. I parametri calcolati sono, volume, diametro nominale, velocità critica tangenziale, stress critico, entropia del guscio, velocità di affondamento adimensionale, velocità di affondamento reale, numero di Reynolds e coefficiente di penetrazione. Le principali variabili fisiche che influenzano il comportamento idrodinamico di questi gusci sono la taglia, la densità e la forma. Ottenute queste misure per ogni singolo esemplare, possono quindi essere calcolati matematicamente e statisticamente altri parametri per ottenere un quadro completo dell'idrodinamica. L'esecuzione dei calcoli e la loro interpretazione danno un'immagine quantitativa e qualitativa del trasporto possibile per un dato ambiente. Sulla base dell'analisi qui riportata, lo studio delle caratteristiche idrodinamiche dei macroforaminiferi appare importante quanto lo studio delle caratteristiche biologiche ed ecologiche in un contesto di ricostruzione paleo ambientale. Soprattutto in ambienti di acqua poco profonda, dove questi organismi hanno vissuto e vivono con particolare abbondanza, lo studio dei comportamenti idrodinamici delle associazioni diventa fondamentale sia per ricostruire le distribuzioni di facies, sia per risalire alla ricostruzione delle caratteristiche fisiche dell'ambiente deposizionale.

INTRODUCTION

The shape of particles has many applications in sedimentology, including paleoenvironmental interpretation and sediment transport studies (Le Roux, 2004). Unfortunately, most works about paleoenvironmental analyses do not include the transport effect. Sand transport plays a vital role in many aspects of applied sedimentology and engineering. Sea-sand may be moved by tidal-, wind- or wave-driven currents, by waves or often by both (Soulsby, 1997). Understanding the intensity of the processes in terms of energetic input, which occur in marine environment, and understanding in which way every particle reacts to hydrodynamic parameters is partially unclear because of the high complexity. Previous studies have shown that modern larger benthic foraminifera can be easily reworked by waves and currents (Davies, 1970; Hohenegger & Yordanova, 2001a, b; Yordanova & Hohenegger, 2007) and several authors point out that the hydrodynamic behaviour of tests is an important factor controlling their

distribution in recent environment as well as in the fossil record (e.g., Jorriy et al., 2006). So far, the calculated hydrodynamic behaviour of sand is in concordance with the observed values obtained in laboratory using several mathematical approximations. In the same way, concerning nummulitids, several geometrical approximations give the opportunity to compare their shape with the shape of sand grains. These results can be compared with those obtained by experimental analyses on optimally preserved tests of recent nummulitids. The parameters obtained by the theoretical and empirical approach are extremely coincident (Briguglio & Hohenegger, 2008). The aim of this paper is to propose a methodology to obtain these parameters and to extrapolate from mathematical analysis. The use of *N. globulus*, and the choice of selecting only A-forms, is just an example to demonstrate the calculation methods. The discussion of the obtained results concerning *N. globulus* is thus not the task of this paper; its aim is to show the importance of hydrodynamic parameters for paleoenvironmental reconstruction.

Nummulitids hydrodynamics:
an example using *Nummulites globulus* Leymerie, 1846

Nummulitids hydrodynamics

Antonino BRIGUGLIO & Johann HOHENEGGER

A. Briguglio (corresponding author). Department of Paleontology, University of Vienna, Geozentrum, Althanstrasse 14, 1090 Vienna, Austria. antonino.briguglio@univie.ac.at

J. Hohenegger. Department of Paleontology, University of Vienna, Geozentrum, Althanstrasse 14, 1090 Vienna, Austria. johann.hohenegger@univie.ac.at

Key words: Larger foraminifera, hydrodynamic behaviour, settling velocity, nummulitids, transport.

ABSTRACT

The main physical variables influencing the hydrodynamic behaviour of nummulitid tests are size, density and shape. After measuring these variables, further parameters must be calculated to obtain an approximation to the hydrodynamic behaviour of the test. These parameters are volume, nominal diameter, critical shear velocity, critical shear stress, shape entropy, shape-independent settling velocity, settling velocity of a non spherical form, Reynolds number, and drag coefficient. Some of these data were calculated by combining shell measurements with physical properties of the seawater.

The aim of this paper is to explain numerical calculations for qualifying and quantifying the hydrodynamic parameters of nummulitids. Every single step or formula is important

to evaluate the hydrodynamics of a particle or test respectively, especially in shallow water environments where energy strongly varies depending on different physical factors induced by the climate and the topography of the platform. Several methods to calculate the same parameters are also presented and compared to show the best-suited one for nummulitids.

In the fossil record, the faunal composition and the distribution of tests mainly depend on the two groups of cause-event effects: *in vita* and *post mortem*. Inferences about a fossil shallow benthic fauna must consider beside biological and ecological features further physical parameters like transport and deposition leading to distinct distribution patterns.

RIASSUNTO – [Idrodinamica dei nummulitidi: l'esempio di *Nummulites globulus* Leymerie, 1846]. Lo scopo dell'articolo è di illustrare il procedimento matematico che porta ad ottenere i parametri idrodinamici che servono a valutare la risposta dei gusci, sia *in vita* che *post mortem*, ad un input energetico che ne può causare il trasporto. La quantizzazione del trasporto e la sua qualificazione avviene tramite il calcolo matematico dei parametri idrodinamici del materiale trasportato: in questo caso i nummulitidi. I parametri calcolati sono, volume, diametro nominale, velocità critica tangenziale, stress critico, entropia del guscio, velocità di affondamento adimensionale, velocità di affondamento reale, numero di Reynolds e coefficiente di penetrazione. Le principali variabili fisiche che influenzano il comportamento idrodinamico di questi gusci sono la taglia, la densità e la forma. Ottenute queste misure per ogni singolo esemplare, possono quindi essere calcolati matematicamente e statisticamente altri parametri per ottenere un quadro completo dell'idrodinamica. L'esecuzione dei calcoli e la loro interpretazione danno un'immagine quantitativa e qualitativa del trasporto possibile per un dato ambiente. Sulla base dell'analisi qui riportata, lo studio delle caratteristiche idrodinamiche dei macroforaminiferi appare importante quanto lo studio delle caratteristiche biologiche ed ecologiche in un contesto di ricostruzione paleo ambientale. Soprattutto in ambienti di acqua poco profonda, dove questi organismi hanno vissuto e vivono con particolare abbondanza, lo studio dei comportamenti idrodinamici delle associazioni diventa fondamentale sia per ricostruire le distribuzioni di facies, sia per risalire alla ricostruzione delle caratteristiche fisiche dell'ambiente deposizionale.

INTRODUCTION

The shape of particles has many applications in sedimentology, including paleoenvironmental interpretation and sediment transport studies (Le Roux, 2004). Unfortunately, most works about paleoenvironmental analyses do not include the transport effect. Sand transport plays a vital role in many aspects of applied sedimentology and engineering. Sea-sand may be moved by tidal-, wind- or wave-driven currents, by waves or often by both (Soulsby, 1997). Understanding the intensity of the processes in terms of energetic input, which occur in marine environment, and understanding in which way every particle reacts to hydrodynamic parameters is partially unclear because of the high complexity. Previous studies have shown that modern larger benthic foraminifera can be easily reworked by waves and currents (Davies, 1970; Hohenegger & Yordanova, 2001a,b; Yordanova & Hohenegger, 2007) and several authors point out that the hydrodynamic behaviour of tests is an important factor controlling their distribution in recent environment as well as in the fossil record (e.g., Jorry *et al.*, 2006). So far, the calculated hydrodynamic behaviour of sand is in concordance with the observed values obtained in laboratory using several mathematical approximations. In the same way, concerning nummulitids, several geometrical approximations give the opportunity to compare their shape with the shape of sand grains. These results can be compared with those obtained by experimental analyses on optimally preserved tests of recent nummulitids. The parameters obtained by the theoretical and empirical approach are extremely coincident (Briguglio & Hohenegger, 2008). The aim of this paper is to propose a methodology to obtain these parameters and to extrapolate from mathematical analysis. The use of *N. globulus*, and the choice of selecting only A-forms, is just an example to demonstrate the calculation methods. The discussion of the obtained results concerning *N. globulus* is thus not the task of this paper; its aim is to show the importance of hydrodynamic parameters for paleoenvironmental reconstruction.

For the calculation of the hydrodynamic behaviour of a test, the systematic position becomes important, because the transport of a test along a slope depends on test shape, density and size, as explained above, and systematics is mainly based on morphological differences. Because of this, the distribution of objects within an environment can

sometimes be compared with a species-specific distribution. Concerning foraminifera, and specially nummulitids, this parallelism between hydrodynamic features and taxonomy is not always correct. The prominent generation dimorphism in symbiont-bearing benthic foraminifera displaces generations of the same species in different environment because of their differing hydrodynamic behaviour, while species that are different in their internal structures, which could have just a small role in term of density variation, can still have the same hydrodynamic behaviour.

MATERIALS AND METHODS

The data published in this paper were taken on 19 optimally preserved tests (*sensu* Yordanova & Hohenegger, 2002) of A forms of *Nummulites globulus* Leymerie, 1846. The material originates from the Tremp basin (southern Pyrenean, Spain). Only very well preserved tests were selected because, according to Yordanova & Hohenegger (2002), optimal preservation indicates the release of the test by the protoplasm within the last two years at least. Therefore, optimally preserved tests can be considered as members of the time-averaged biocoenosis (Yordanova & Hohenegger, 2007). According to Beavington-Penney (2004), *Palaeonnummulites venosus* - the only living *Nummulites* s.l., failed to demonstrate test damage caused through transport, which is often interpreted for fossil forms, despite simulating transport of large distance in coarse sand.

Only A-forms were used, but the calculation here proposed may be used for both the generations and for all the nummulitids-like shapes.

Every specimen was measured on photographs taken either on thin sections or on complete tests. Photos of the equatorial section, the axial section and the external surface ornamentation were also measured. The vector image analysis program CanvasX was used. Basic calculations and statistics were performed in Microsoft EXCEL, while the program package SPSS for Windows, Release 16.0.1 was used for complex statistical analyses. All measurements were taken on large *Nummulites globulus* specimens, but it would have been possible to calculate the reaction to the hydrodynamic behaviour for every growth step (see Yordanova & Hohenegger, 2007). Every discussed parameter is reported in Tab. 1, the equations have numbers for an easier citation, and one (or two) letters for a quick link to Tab. 1.

A SPECIMEN	B		C		D		E		F		G		H		I		J		K		L		M		N		O		P		Q		R		S		T		U		V		W		X		Y		Z		AA		AB	
	unit	µm	cm	µm	cm	µm	cm	µm	cm	µm	cm	µm	cm	µm ²	axial area µm ²	cm ³	V	µm ³	TND	Dd	Dn	cm	Wd	β	Uc*	cm/sec	P ₁	P ₂	P _s	Hr	Ws	cm/sec	We	cm/sec	Re	Cd	S. height cm	A	cm ²	A	cm ²	v	cm/sec											
4358	2112	0,21	1993	0,20	949	0,09	3155173	1143766	0,0017	1708342031	0,148	29,88	0,159	7,38	0,046	2,47	0,42	0,39	0,19	0,95	14,17	12,53	176	0,73	0,12	0,04	9,72																											
4362	2095	0,21	2062	0,21	880	0,09	3306383	1257483	0,0020	1985463997	0,156	29,40	0,156	7,29	0,046	2,46	0,42	0,41	0,17	0,94	14,00	12,07	179	0,79	0,11	0,04	10,21																											
4372	2225	0,22	2000	0,20	989	0,10	3322040	1374755	0,0021	2052768251	0,158	30,86	0,164	7,56	0,046	2,48	0,43	0,38	0,19	0,95	14,52	12,86	192	0,74	0,12	0,04	10,05																											
3514	2273	0,23	2142	0,21	969	0,10	3295659	1624262	0,0024	2354815126	0,165	31,59	0,168	7,69	0,046	2,49	0,42	0,40	0,18	0,95	14,77	12,85	201	0,75	0,12	0,04	10,50																											
4364	2401	0,24	2149	0,21	856	0,09	4069638	1412802	0,0024	2394421211	0,166	30,90	0,164	7,57	0,046	2,48	0,44	0,40	0,16	0,93	14,53	12,00	169	0,78	0,13	0,05	9,89																											
4336	2277	0,23	2155	0,22	952	0,10	3785594	1447322	0,0024	2406218864	0,166	31,49	0,167	7,67	0,046	2,49	0,42	0,40	0,18	0,94	14,73	12,74	201	0,76	0,12	0,04	10,54																											
3484	2345	0,23	2309	0,23	965	0,10	4043152	1400643	0,0024	2415387369	0,166	32,68	0,174	7,88	0,046	2,50	0,42	0,41	0,17	0,94	15,14	12,96	205	0,72	0,13	0,04	10,53																											
3506	2422	0,24	2198	0,22	940	0,09	4097253	1454530	0,0025	2460213317	0,167	32,22	0,171	7,80	0,046	2,49	0,44	0,40	0,17	0,94	14,98	12,71	202	0,74	0,13	0,05	10,17																											
3486	2464	0,25	2250	0,23	897	0,09	4282990	1483937	0,0026	2579566645	0,170	32,15	0,171	7,79	0,046	2,49	0,44	0,40	0,16	0,93	14,96	12,42	201	0,75	0,13	0,05	10,17																											
3512	2405	0,24	2218	0,22	1038	0,10	3874118	1655731	0,0027	2667295832	0,172	33,32	0,177	7,99	0,047	2,50	0,42	0,39	0,18	0,95	15,35	13,44	220	0,72	0,13	0,05	10,74																											
3467	2310	0,23	2117	0,21	1088	0,11	3685435	1697843	0,0027	2708283913	0,173	32,88	0,175	7,92	0,047	2,50	0,42	0,38	0,20	0,96	15,20	13,66	224	0,74	0,13	0,04	11,09																											
4360	2110	0,21	2075	0,21	1104	0,11	3475489	1681619	0,0028	2769601819	0,174	31,85	0,169	7,74	0,046	2,49	0,40	0,39	0,21	0,97	14,85	13,62	225	0,78	0,12	0,04	11,89																											
3518	2220	0,22	2104	0,21	1190	0,12	3448479	1870776	0,0029	2906349650	0,177	33,37	0,177	8,00	0,047	2,50	0,40	0,38	0,22	0,97	15,36	14,23	239	0,74	0,13	0,04	11,86																											
3494	2587	0,26	2378	0,24	1029	0,10	4751735	1841919	0,0034	3383343277	0,186	34,84	0,185	8,25	0,047	2,52	0,43	0,40	0,17	0,94	15,84	13,54	239	0,73	0,14	0,05	11,20																											
3474	2405	0,24	2234	0,22	1162	0,12	4141930	1964345	0,0034	3383361433	0,186	34,68	0,184	8,22	0,047	2,52	0,41	0,39	0,20	0,96	15,79	14,27	252	0,74	0,13	0,05	11,91																											
3496	2529	0,25	2450	0,24	1067	0,11	4927773	1774021	0,0035	3456452407	0,188	35,35	0,188	8,34	0,047	2,52	0,42	0,41	0,18	0,94	16,01	13,84	246	0,72	0,14	0,05	11,63																											
3400	2245	0,22	2028	0,20	1430	0,14	3300124	2414044	0,0035	3549069524	0,189	35,17	0,187	8,31	0,047	2,52	0,39	0,36	0,25	0,98	15,95	15,35	276	0,74	0,13	0,04	12,86																											
3502	2475	0,25	2456	0,25	1190	0,12	4646483	2113011	0,0040	3966368700	0,196	36,43	0,193	8,51	0,047	2,53	0,40	0,40	0,19	0,96	16,35	14,65	273	0,73	0,14	0,05	12,63																											
3394	2484	0,25	2346	0,23	1267	0,13	4643243	2323379	0,0043	4342756315	0,202	36,67	0,195	8,55	0,047	2,54	0,41	0,38	0,21	0,96	16,43	15,03	289	0,74	0,14	0,05	12,99																											

TABLE 1: Geometric measurements and hydrodynamic parameters calculated on optimally preserved specimens of *Nummulites globulus* Leymerie 1846.

PARAMETER CALCULATION

Size, shape and density

The parameters test length (L), width (I), height (S), and the areas of the equatorial and axial section were measured. Test length L (Tab. 1, column B) could directly be obtained on oriented thin sections or by image analysis on entire specimens immersed in water; the test width I (Tab. 1, column D) was measured perpendicularly to L crossing in the centre of the protoconch, while the test height S (Tab. 1, column F) was measured in axial section (Fig. 1).

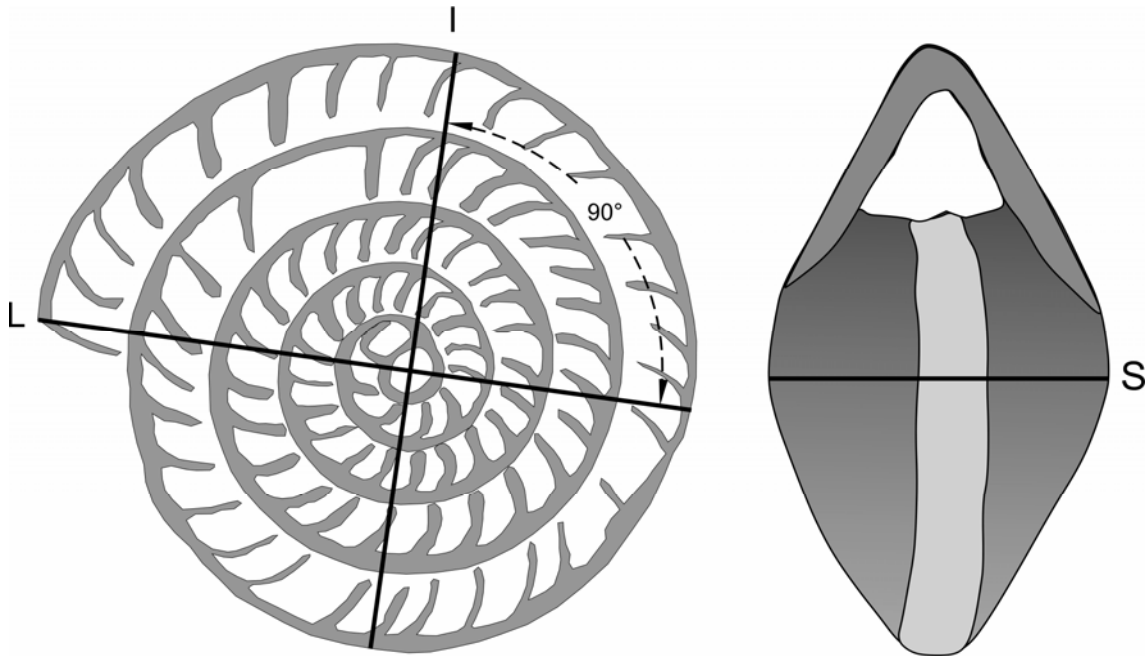


FIGURE 1: Sketches of equatorial section and axial view of a *Nummulites globulus*. L represents the highest length of the test, I must be perpendicular to L and both L and I must passing trough the protoconch. S represents the highest thickness.

Because of further analyses, L , I , and S were measured in micrometer, but transformed to cm (Tab.1, columns C, E, and G). The measurement of L was taken as the largest test diameter, thus independent from the position of the second chamber (deuteroconch), which is sometimes used by morphologists for the determination of the diameter.

Calculating the contour area of fossilized organisms is not easy. There are many computer programs for calculating the area of an object using photographs (image analyses). These methods are fast and precise; they are perfect when dealing with living organism or optimally preserved specimens, where empty chambers and pores are still

undistorted by any diagenetic process. Calculating the area of fossil forms could result in less precise values because of early diagenetic processes (Jorry, 2004; Jorry et al. 2006). Even if fossils are optimally preserved, they could be slightly distorted or be damaged by preparation, and automated computer programs could over- or underestimate the required measurements. Because of this, the areas were calculated by reconstructing by hand the original shape's profile with the image analysis computer program. Area values in μm^2 can be found in columns H and I in Tab. 1.

Using equatorial and axial areas the test volume was calculated according to Yordanova & Hohenegger (2007), using the following formula

$$\text{Volume} = \frac{\text{area}_{\text{horizontal}} \cdot \text{area}_{\text{upright}}}{\text{maximum diameter}} \quad (1) - (\text{Tab. 1, column K})$$

For the calculation of test densities in fossil forms, several authors (Jorry *et al.*, 2006; Yordanova & Hohenegger, 2007) pointed out good solutions and the values obtained show that the apparent density of *Nummulites* ranges from 1.7 to 1.9 g/cm^3 when the porous network is filled with seawater. Therefore, calculations were made on 'full-water' conditions (*sensu* Jorry et al., 2006) using an intermediate value of 1.8 g/cm^3 . This approximation is confirmed by the rather stable densities in *Palaeonummulites venosus* during growth (Yordanova & Hohenegger, 2007: Fig. 4). Data of recent nummulitids are thus comparable with this density value. Of course, for every organism and for every specimen it is possible to vary the value of this parameter in the formula to get a better approximation to the real hydrodynamic behaviour of every specimen.

Dimensionless analysis

Because of the non-linearity of the volume parameter depending on age (e.g., growth), it cannot be taken as a linear variable for calculating the interdependency of shape and hydrodynamic parameters (Yordanova & Hohenegger, 2007). Therefore, all volume values were transformed into a linear variable depending on age represented as the diameter of a sphere:

$$TND = 2 \left(\frac{3V}{4\pi} \right)^{1/3} \quad (2) - (\text{Tab. 1, column L})$$

where *TND* is the True Nominal Diameter proposed by Wadell (1932).

Such parameters, which do not take into account the original shape of an object, are called shape-independent; this peculiarity allows linear comparison within populations and to compare different populations without taking into account shapes differences; *TND* is also useful for growth analysis based on volumes as the representative parameter for age.

Thus it is always better to calculate the *TND* in cm using the correspondent volume calculated in cm³ (Tab. 1, column J).

Jorry *et al.* (2006), for further dimensionless analyses, propose to use the parameter (*D_d*) to express the size of the equivalent sphere using the equation

$$D_d = \sqrt[3]{L \cdot I \cdot S} \cdot \sqrt[3]{\rho_f g \frac{(\rho_s - \rho_f)}{\mu^2}} \quad (3) - (\text{Tab. 1, column M})$$

where ρ_f is the density of the fluid, g is the gravitational acceleration, ρ_s is the density of the fossil and μ is the dynamic viscosity of the fluid. Using (3), this diameter is higher than the one obtained by equation (2), because (3) is multiplied by densities. Nevertheless, equation (3) becomes important to calculate shear and settling velocities, and further calculations will reduce this difference.

A similar value to (2) can be obtained using the formula proposed by Le Roux (1997)

$$D_n = \sqrt[3]{L \cdot I \cdot S} \quad (4) - (\text{Tab. 1, column N})$$

For the analysis reported here, which regards lentil-shaped tests as can be found in nummulitids, the use of (4) is preferred, while for tests with irregular shape (*i.e.* calcarinids, peneroplids) the use of the *TND* must be preferred. The best solution for evaluating the volume in case of irregular tests is measuring in liquid mercury (Hg) because it is a non-wetting fluid (Jorry *et al.*, 2006).

Shear and settling velocities

It is now possible to calculate the settling velocities acting as multipliers for different scales. Le Roux (1997) and Jorry *et al.*, (2006) propose the "dimensionless sphere settling velocity" (W_d):

for $D_d < 134.9$

$$W_d = -0.375 + 0.29D_d - 0.002D_d^2 + 4.731 \times 10^{-6} D_d^3 \quad (5) - (\text{Tab. 1, column O})$$

This formula is a series expansion: a mathematical representation of a function as an infinite sum of terms calculated from the values of its derivatives at a single point. Because of the very low third coefficient, calculations of higher terms would give no improvement. Because W_d is calculated using D_d , which is mathematically size and shape independent, its results are also size and shape independent.

For $D_d > 134.9$ other solutions are proposed, but for the typical size range of symbiont-bearing benthic foraminifera, the value of 134.9 can only be found in giant B-generations of nummulitids when measured in mm.

According to Jorry *et al.* (2006), the dimensionless critical shear stress (β) is calculated in the following way

$$\beta = 0.029 + 0.003W_d - 9.935 \times 10^{-5} W_d^2 \quad \text{for } W_d > 2.5 \quad (6) - (\text{Tab. 1, column P})$$

Here, the second-degree series is precise enough to describe the nummulitid's stress behaviour with a scale independent settling velocity value higher than 2.5.

As published by Jorry *et al.* (2006), the critical shear velocity (U_c^*) becomes

$$U_c^* = 1.959 + 0.253 \sqrt{\beta g \left(\frac{\sqrt[3]{L \cdot I \cdot S}}{1.32} \right) \frac{(\rho_s - \rho_f)}{\rho_f}} \quad (7) - (\text{Tab. 1, column Q})$$

Comparing the results obtained through these set of formulas with published data (Yordanova & Hohenegger, 2007; Jorry *at al.*, 2006; Davaud & Septfontaine, 1995) shows slight incongruence, probably due to peculiar environmental factors and laboratory settings.

Settling velocity is the most important parameter characterizing the behaviour of grains in fluids. Due to gravity the settling properties of the foraminiferal test act against the energy input induced by water movement.

An input higher than its settling velocity is required to keep the test in suspension leading to transport. High settling velocities push the tests to the ground because of gravity, while low settling velocities, typical for flat nummulitids like assilinids and operculinids, can keep the test in suspension and expose it to transport.

A set of formulas was used to calculate more precise settling velocities of tests with specific morphologies deviating from a spherical or ellipsoid grain.

The settling velocity of the equivalent sphere (W_s) proposed by Le Roux (1996) was calculated using

$$W_s = \frac{W_d}{\sqrt[3]{\frac{\rho_f^2}{\mu g (\rho_s - \rho_f)}}} \quad (8) - (\text{Tab. 1, column V})$$

The next step to obtain the real settling velocity of a particle must consider the entropy of the test. In fact, the difference between the settling velocity of a sphere and a non-spherical particle with the same volume is directly related to the deviation from sphericity, where grain roundness plays a negligible role (Briguglio, 2009).

The shape entropy is an important value in hydrodynamics. Concerning nummulitids, the entropy is the most important parameter that produces differences in settling and, consequently, in transport. The best formula to calculate shape entropy is proposed by Hofmann (1994). It is based on the geometry of an ellipsoid and can be calculated with

$$H_r = -[(p_l \times \ln p_l) + (p_i \times \ln p_i) + (p_s \times \ln p_s)]/1.0986 \quad (9) - (\text{Tab. 1, column U})$$

where p_l , p_i and p_s are the proportions of the major, intermediate and minor axes of the ellipsoid

$$p_i = I/(L + I + S)$$

$$p_l = L/(L + I + S)$$

$$p_s = S/(L + I + S) \quad (10) - (\text{Tab. 1, columns R, S, and T}).$$

Knowing the entropy of a non-spherical grain, its settling velocity (W_e) can be calculated using the equation of Le Roux (1996)

$$W_e = W_s [(H_r - 0.5833)/0.4167] \quad (11) - (\text{Tab. 1, column W})$$

According to Le Roux (2004), equation (11) yields a mean accuracy of 95.7% of W_e with experimental data

Other hydrodynamic parameters

Allen (1984), studying the settling velocity of bivalve shells, discovered that a valve allowed to fall freely in a large volume of plain stagnant water at first accelerates, but finally reaches a steady terminal fall velocity given by the equation:

$$v^2 = \frac{2gV(\rho_s - \rho_f)}{C_D \rho_f A} \quad (12) - (\text{Tab. 1, column AB})$$

where C_D is the drag coefficient, A is the projected area of the shell assumed during sinking, v is the vertical component of the terminal fall velocity and V is the volume. Particles, shells and also fossil nummulitids orient their maximum projection area in the direction of settling (Komar and Reimers, 1978) and this condition reduces sinking velocity in the same way as low test densities (Yordanova & Hohenegger, 2007).

Defining the parameters A and C_D of (12) is difficult. Calculation of the area directed to the flow is complicated in nummulitids. An alternative solution, proposed by Briguglio (2008) shows good results by comparing the nummulitids test to a solid object composed by two equal cones bound by the basal area. This basal area would be the parameter A , calculated as follows

$$A = (\pi r^2 + \pi r s)/2 \quad (13) - (\text{Tab. 1, column AA})$$

where

$$s = \sqrt{r^2 + h^2} \quad (14) - (\text{Tab. 1, column Z})$$

is the slant height.

The Reynolds number and the drag coefficient C_D , according to Le Roux (1997), are given by

$$\text{Re} = \frac{\rho_f D_n W_e}{\mu_f} \quad (15) - (\text{Tab. 1, column X})$$

and

$$C_D = \frac{4D_n g(\rho_s - \rho_f)}{3\rho_f W_e^2} \quad (16) - (\text{Tab. 1, column Y}),$$

where D_n and W_e are already calculated in (2) and (11).

The relation between C_d and Re for *N. globulus* matches with the equation that relates C_d and Re of a sphere as proposed by Abraham (1970)

$$C_D = C_0 \left(1 + \frac{\delta_0}{\sqrt{\text{Re}}} \right)^2 \quad (17)$$

where

$$\delta_0 \cong 9.06 \text{ and } C_0 \delta_0^2 = 24$$

RESULTS

The resulting hydrodynamic parameters obtained by different mathematical analysis were compared with experimental data obtained on recent foraminifera and published by Yordanova & Hohenegger (2007). The comparison between *Nummulites*

venosus and *N. globulus* demonstrates good results: Reynolds number values and the relations between test length and test width and height show the same trend (Briguglio & Hohenegger, 2008). This clearly demonstrates the correctness of the calculation methods and they can now be used for the interpretation of the hydrodynamic behavior of all nummulitids independent of their size, because the calculation is based on scale- and shape-independent parameters.

They could be applied in shallow water as well as in deep-water environment.

The shape-independent diameters can be used for comparison between forms in different environments as well as within assemblages. In an energetic scenario, the distribution of forms creates assemblages with restricted settling velocities and nominal diameter values; i.e. along a slope, a variation of settling velocities vs. nominal diameters ratio can be recognized from shallower environments to deeper ones.

The entropy value is fundamental for the calculation of the settling velocity, showing how less important size is in comparison with shape or density. At the same time, shape is the most powerful variable to understand and evaluate the distribution of different tests along a slope, as demonstrated by outcrop studies (Jorry *et al.*, 2003; Racey, 2001).

The particle's Reynolds number is used to indicate whether the boundary layer around a particle is turbulent or laminar, and the drag exerted will depend on this. Understanding and quantifying the turbulence produced by a test (or even a shell) at the sea floor would probably give an advance for understanding the hydrodynamic of the huge amount of tests to evaluate their accumulation, e.g. the so called "nummulite banks", which are very abundant in the Eocene rocks in many locations of Europe and northern Africa.

The correlation found between the drag coefficient Cd and the Reynolds number Re , at the end of all this mathematic calculation, allows the use of all formula and data obtained solely by geometrical analysis without any laboratory experiment. This does not mean that the value obtained is absolutely correct, but the whole process is rigorous and the errors are only statistical and not fundamental.

More information will be obtained by further investigations, when other parameters could also be investigated. However, theoretical models and empirical correlations are affected by limits due to the large amount of environmental factors influencing hydrodynamics factors; furthermore, additional data especially from the fossil record are required to improve their accuracy and increase their ranges of applicability.

CONCLUSION:

The correlation between fossil and recent forms demonstrates the perfect coincidence of hydrodynamic parameters up to the Reynolds numbers. In this way, the distribution of different nummulitids that lived on the slope or ramp could be explained by their hydrodynamic behaviour. The ecological cause-effect scenario (abundance, biodiversity, interaction between species) is rarely fully preserved in the fossil record, and only in some exceptional preservation cases can be completely reconstructed; the *post mortem* cause-effect scenario (e.g., energy input, distribution by transport, destruction) may be recognized and calculated and it may help for a better environmental determination.

These calculations show in which way hydrodynamic parameters may be fundamental to evaluate the distribution of larger foraminifera in recent and fossil environments. On the basis of our analysis and results, the physical parameters seem to be important same as the biological and ecological factors which work as inputs in the environment, thus we consider that a calculation like the one here presented should be performed in every paleoenvironmental reconstruction, especially in shallow water environments where the hydrodynamics is a prominent tool and may be used to evaluate physical phenomena and to improve the knowledge of geometrical forms distribution along a ramp during *in vita* and *post mortem* time spans.

ACKNOWLEDGEMENTS

We thank Dr. Stefano Dominici for help with fieldwork, and Dr. Federico Falcini for help controlling the accuracy of the formulas. We are also thankful to Dr. Stéphan Jorry from IFREMER Marine Geosciences, Plouzané (FR), for his valuable comments and Dr. Cesare Andrea Papazzoni from Dipartimento di Scienze della Terra, Università di Modena e Reggio Emilia (IT), for his informative discussions and valuable suggestions.

REFERENCES

Abraham F.F. (1970). Functional dependence of Drag Coefficient of a sphere on Reynolds number. *Physics of Fluids*, 13: 2194.

- Allen J.R.L. (1984). Experiments on the settling, overturning and entrainment of bivalve shells and related models. *Sedimentology*, 31: 227–250.
- Beavington-Penney S.J. (2004). Analysis of the effects of abrasion on the test of *Palaeonummulites venosus*: implications for the origin of nummulithoclastic sediments. *Palaios*, 19: 143–155.
- Briguglio A. (2008). *Nummulites*: ein einfaches geometrisches Verfahren zur Bestimmung hydrodynamischer Parameter. *Berichte der Geologischen Bundesanstalt*, 75: 8.
- Briguglio A. (2009). In vita and post mortem forams events: hydrodynamic tools for paleoenvironmental reconstructions. *Tertiary Larger Foraminifera: Evolution, Biostratigraphy, Palaeoecology and Palaeobiogeography, 62nd Geological Kurultai of Turkey, 13–17 April 2009, MTA-Ankara, Türkiye*: 890.
- Briguglio A. & Hohenegger J. (2008). Hydrodynamic behaviour of nummulitids: a non-experimental approach. In: Mazzei R., Fondi R., Foresi L., Riforgiato F. & Verducci M. (eds), *Riassunti dei lavori Giornate di Paleontologia 2008*: 14.
- Davaud E. & Septfontaine M. (1995). Post-mortem onshore transportation of epiphytic foraminifera: recent example from the Tunisian coastline. *Journal of Sedimentary Research*, 65: 136–142.
- Davies G.R. (1970). Carbonate bank sedimentation, eastern Shark bay, Western Australia. *Memoir - American Association of Petroleum Geologists*, 13: 85-168.
- Hofmann H.J. (1994). Grain-shape indices and isometric graphs. *Journal of Sedimentary Research*, 64 (4): 916- 920.
- Hohenegger J. & Yordanova E. (2001a). Displacement of larger foraminifera at the western slope of Motobu Peninsula (Okinawa, Japan). *Palaios*, 16: 53–72.
- Hohenegger J. & Yordanova E. (2001b). Depth-transport functions and erosion-deposition diagrams as indicators of slope inclination and time – averaged traction forces: application in tropical reef environments. *Sedimentology*, 48: 1025–1046.
- Jorry S.J., Hasler C.A., Davaud E. (2006). Hydrodynamic behaviour of *Nummulites*: implication for depositional models. *Facies*, 52: 221-235.
- Komar P.D. & Reimers C.E. (1978). Grain shape effects on settling rates. *Journal of Geology*, 96: 193–209.

- Le Roux J.P. (1996). Settling velocity of ellipsoidal grains as related to shape entropy. *Sedimentary Geology*, 101 (1): 15-20.
- Le Roux J.P. (1997). An Excel program for computing the dynamic properties of particles in newtonian fluids. *Computers & Geosciences*, 23 (6): 671-675.
- Le Roux J.P. (2004). A hydrodynamic classification of grain shapes. *Journal of Sedimentary Research*, 74 (1): 135-143.
- Leymerie A. (1846). Mémoire sur le terrain à *Nummulites* (épicrotécé) des Corbières et de la Montagne Noire. *Mémoires de la Société Géologique de France*, 1 (2): 337-373.
- Soulsby R. (1997). Dynamic of marine sands. 249 pp. Thomas Telford (ed.). London.
- Wadell H. (1932). Volume, shape, and roundness of rock particles. *Journal of Geology*, 40: 443–451.
- Yordanova E. & Hohenegger J. (2002). Taphonomy of larger foraminifera: relationships between living individuals and empty tests on flat reef slopes (Sesoko Island, Japan). *Facies*, 46: 169–204.
- Yordanova E. & Hohenegger J. (2007). Studies on settling, traction and entrainment of larger benthic foraminiferal tests: implication for accumulation in shallow marine sediments. *Sedimentology*, 54 (6): 1273-1306.

APPENDIX 1. Nomenclature used in text

$L = D_f$ = large diameter (length)

$I = D_i$ = intermediate diameter (width)

$S = D_s$ = small diameter (height or thickness)

TND = True nominal diameter

V = volume

D_d = dimensionless size of the equivalent sphere

D_n = true nominal diameter according to Le Roux (1997)

W_d = dimensionless sphere settling velocity

β = critical shear stress

U_c^* = critical shear velocity

H_r = shape entropy

p_l, p_b, p_s = proportion between the axis calculated with (9)

W_e = settling velocity of a non spherical grain

W_s = settling velocity of the equivalent sphere

C_D = drag coefficient

A = area of the shell/test contrasting the water during sinking

v = vertical component of the terminal fall velocity.

Re = Reynolds number

ρ_f = density of the fluid (seawater) = 1.025 g cm^{-3}

ρ_s = density of the fossil = 1.8 g cm^{-3}

μ^2 = dynamic viscosity of the fluid (seawater) = $0,0108 \text{ g (cm} \times \text{s)}^{-1}$

g = gravity constant = $981.0327 \text{ cm sec}^{-2}$

Chapter 2

Briguglio A, Metscher B & Hohenegger J (accepted) - Growth Rate Biometric Quantification by X-ray Microtomography on Larger Benthic Foraminifera: Three-dimensional Measurements push Nummulitids into the Fourth Dimension. Turkish Journal of Earth Science.

*Concharumque genus parili ratione videmus
pingere telluris gremium, qua mollibus undis
litoris incurvi bibulam pavit aequor harenam.
quare etiam atque etiam simili ratione necessest,
natura quoniam constant neque facta manu sunt
unius ad certam formam primordia rerum,
dissimili inter se quaedam volitare figura;*

Titus Lucretius Carus: *De rerum natura*, II, 374-380.

Growth Rate Biometric Quantification by X-ray Microtomography
on Larger Benthic Foraminifera:

Three-dimensional Measurements push Nummulitids into the Fourth Dimension.

Antonino Briguglio¹, Brian Metscher² & Johann Hohenegger³

¹ Corresponding author. Email: antonino.briguglio@univie.ac.at. Department of Paleontology, University of Vienna, Geozentrum, Althanstrasse 14, 1090 Vienna, Austria Tel: +43 1 4277 53546, Fax: +43 1 4277 9535.

² Department of Theoretical Biology, University of Vienna, Althanstrasse 14, 1090 Wien, Austria. brian.metscher@univie.ac.at.

³ Department of Paleontology, University of Vienna, Geozentrum, Althanstrasse 14, 1090 Vienna, Austria. johann.hohenegger@univie.ac.at.

Abstract:

This work demonstrates the potential of three-dimensional biometric quantification using microtomography on larger benthic foraminifera. We compare traditional linear and area measures used for calculating three-dimensional characters with actual 3D measurements made from volume images obtained using X-ray microtomography (microCT).

Two specimens of recent larger benthic foraminifera, i.e., *Palaeonummulites venosus* and *Operculina ammonoides*, were imaged with a high-resolution microCT scanner. This method enables three-dimensional imaging and calculation of measurements like 3D distances, surfaces and volumes.

The quantitative high-resolution images enabled the extraction of the lumina from the proloculus to the last complete scanned chamber and of the canal system spreading into marginal chord and septa. External surfaces and volumes were calculated on the extracted parts. These measurements allowed the calculation of porosity and micro-

porosity to obtain the test density, which is the basis for many inferences about foraminifera, e.g. reconstructions of transport and deposition. Volume and surface measurements of the proloculus allow the calculation of sphericity deviation, which is useful for determining evolutionary trends in species based on individuals resulting from asexual reproduction (A forms).

The three-dimensional data presented here show the actual growth of the foraminiferal cell and the development of the test. Measurements made on an equatorial section cannot be considered representative of a three dimensional test, unless a correspondence between 2D data with 3D data shows significant correlation. Chamber height, septal distance, spiral growth and chamber area were measured on the equatorial section and correlated with the volume measurements from 3D images to determine the predictive value of the 1D and 2D measures for estimating the 3D morphological parameters.

In particular, we show that the equatorial section area of chambers correlates significantly with the chamber volume and can be used to differentiate between nummulitid genera according to their different growth patterns.

Introduction

Many earth science studies, especially in palaeontology, require examination or measurement of the internal features of specimens or rocks in three dimensions, tasks to which X-ray microtomography (microCT) is very well suited (Carlson et al. 2003). A variety of different X-ray CT instruments and techniques are now available: they can scan objects of a size range from less than one millimetre, to many decimetres and they can scan at different resolutions: from less than one micron (“nanoCT”) to one or a few microns (microCT), and up to the submillimetre-millimetre range (CT). The best-known advantage of X-ray CT is its ability to reconstruct quickly and non-destructively the interior of opaque solid objects in three dimensions when the density contrast is high enough to let the X-ray differentiate the internal features (Neues & Epple 2008, Metscher 2009). For many fossils, X-ray CT may be the only practical means of gaining information on internal materials and geometries or other features hidden from external view (e.g. Speijer et al. 2008). The digital and quantitative nature of a CT dataset facilitates computer visualization, animation, allowing the user to interact with the data

and to better understand the features and interrelationships among elements of the dataset. Finally, these digital data provide unrivalled means for archiving and exchanging information, always at high resolution with intrinsic spatial calibration.

Because 3D visualization techniques are computationally intensive, they have historically been restricted to professional workstations, preventing widespread use. However, recent advances in processing power and 3D graphics cards, along with inexpensive computer memory and hard drives, make 3D visualization of reasonably sized data sets feasible and affordable even for laboratories that face budget constraints. Although one can still usefully spend a huge amount of money on a dedicated imaging workstation, a standard modern desktop computer can now be adequate for most imaging tasks encountered in routine microscopy, and the many open source software packages available reduce the cost of the whole research effort.

Concerning larger foraminifera, the high complexity of their shells is considered the basis of their systematics down to the sub-species level. According to Hottinger (2009), quantitative morphological characters that change with time in one direction define the interpretation of phylogenetic trends in some groups of larger foraminifera. Such morphological characters are normally studied on oriented thin sections. The availability of a high-resolution three-dimensional virtual model of specimens offers key to evaluating such morphological characters within the complexity of form and shape. While the equatorial section allows the study of characters changes during growth in two spatial dimensions, this is impossible for characters represented in the 3rd dimension like chamber thickness etc. Here, the axial section shows only an incidental growth state and changes of these characters cannot be measured for each growth step. Thus, the task of a three-dimensional quantitative analysis on larger foraminifera is to test the significance of one- and two-dimensional data (like the area) in comparison with 3D measurements (like the chamber volumes). Because of the importance of all these morphological parameters for larger benthic foraminifera concerning microevolution, phylogenetic trends, paleoecology and paleoclimatology, the study of their internal structure within its complexity using microCT is even more a mandate. Speijer et al. (2008) have already discussed the potentiality of the high-resolution microCT, calculating volume and equivalent radius only.

The aim of our work is to make another step forward to show the potential of the data obtained from 3D analysis: quantifications of volumes, surfaces, distances, angles and

nearly any metrical feature of interest. Those data are still rare in many published papers concerning microCT.

We have compared the data obtained by the X-ray computed tomography with the classic way of studying biometry in nummulitids, which has a long history partially based on many parameters and some contradictions. As suggested by Schaub (1981) and widely used in many papers, the main morphological parameters describing megalospheric specimen of larger benthic foraminifera are the major and minor diameter, the morphology and number of septa per whorls and the diameter of the proloculus. Other parameters (in particular the radii of the whorls) do not seem useful to understand the growth process (Pecheux 1995). Other authors (e.g. Roveda 1970) used to determine nummulitids lineage relying mainly on the external test shape, diameter, thickness, and ornamentation. Further studies (e.g. Reiss & Hottinger 1984; Hallock & Glenn 1986; Racey 1992; Pecheux 1995) agree that these features are largely influenced by environmental parameters, such as depth, substrate, light intensity, etc; thus, they are important to obtain information about paleoecology and paleogeography of larger foraminifera. According to Hottinger (2009), the only feature that may be quantified by simple linear measurement is the diameter of the megalospheric proloculus if it is a walled sphere; but among the possible species-diagnostic characters, all require the observation of the equatorial section.

Measuring and quantifying the foraminiferal cell growth rate with a three-dimensional analysis is the first step into the fourth dimension.

Material and Methods

Two A-form specimens with excellent test preservation were investigated. The *Operculina ammonoides* (Gronovius 1781) specimen originates from muddy substrate in 18 m depth of the lagoon west off Motobu Town, Motobu Peninsula, Okinawa, Japan (Hohenegger et al. 1999). The specimen of *Palaeonummulites venosus* (Fichtel & Moll 1798) originates from 50 m depth in front of a patch reef along the investigated depth transect A between Seoko Jima and Minna Jima, Okinawa, Japan (Hohenegger et al. 1999), where the sea floor consists of middle-grained sand.

Three-dimensional analyses of more specimens or entire populations will provide much more information on volumes variability and chamber morphologies, but today these procedures are too much time consuming.

Procedure

The X-ray microtomography system used in this work is model MicroXCT from Xradia Inc., Concord, CA (www.xradia.com) in the Theoretical Biology Department at the University of Vienna, Austria. This scanner uses a Hamamatsu L9421-02 tungsten X-ray source with an anode voltage between 20 and 90 kV, power between 4 and 8 W, and a spot size of 5 to 8 μm . This scanner's configuration allows fields of view from 5 mm down to less than 500 μm . The X-ray projection image is formed on a scintillator crystal, made in-house by Xradia. The optical emissions of the scintillator is then imaged by a Nikon microscope objective lens onto a $1\text{k} \times 1\text{k}$ CCD camera (Pixis, Princeton Instruments) cooled to -55°C to reduce dark noise. The optical imaging of the scintillator allows a final magnification independent of the geometric magnification of the X-ray projection imaging, and a final image resolution that is not limited by the X-ray source spot size. Several different optical objective lenses allow selection of the final magnification, while adjustments to the source-sample and sample-detector distances can be used to change the geometric magnification of the sample image on the scintillator. Projection images are collected automatically over 180° of rotation and horizontal slices through the sample are reconstructed automatically by the supplied Xradia software. Reconstruction parameters can be adjusted and the reconstruction repeated if necessary. The scanning system's integrated control computer carries out these operations and is also used for viewing the reconstructed volumes and exporting image stacks in standard formats (e.g. TIFF).

The foram samples were scanned in small cylindrical plastic containers (a polypropylene pipette tip or a Lego® round brick 1×1),. Most plastics are relatively transparent to X-rays and so are suitable for scanning mineralised specimens. Imaging parameters for the scans reported here are summarized in Table 1.

	<i>Palaeonummulites venosus</i>	<i>Operculina ammonoides</i>
Camera binning	2x2	2x2
Camera temperature	-55°C	-55°C
Image size	510x512	504x512
Clean file size	66.3 Mb	43.3 Mb
Anode voltage kV _p	80	77
μA	46	45
Source to RA distance	40.0 mm	40.0 mm
Detector to RA distance	22.0 mm	15.0 mm
Voxel	4.258 μm	4.645 μm
Optical magnification	4.2x	4.2x
Slides	268	174

Table 1: Technical settings of the X-ray microtomography system used during the specimen scanning.

The computer used for manipulating the image stacks was equipped with an Intel®Core (TM)2 Quad CPU Q9400 at 2.66 GHz, 8 GB of RAM with a Microsoft Windows XP Professional x64 system provided by the department of Palaeontology in the University of Vienna, Austria.

In this work we used ImageJ (<http://rsbweb.nih.gov/ij/>), which is perhaps the most popular open-source imaging software in neuroscience, for measurements of 2D images and basic visualization of 3D dataset through plugins including Volume Viewer (<http://rsb.info.nih.gov/ij/plugins/volume-viewer.html>) and VolumeJ (<http://webscreen.opth.uiowa.edu/bij/vr.htm>). We used Image Surfer (another free program; <http://cismm.cs.unc.edu/>) for volume rendering, quantifications, slicing at arbitrary orientation, measurements in 2D and 3D and taking snapshots suitable for

publication. Many other 3D visualization software packages could be used for these purposes: some are commercial and quite expensive for an academic department, such as Amira (www.amiravis.com) or Analyze (www.analyzedirect.com), but others are open source and they all support conventional stereoscopic 3D display technologies.

After reading the reconstructed image stack into the measuring software and after calibrating it with the correct voxel size (three-dimensional pixel size), we could extract with the lasso tool in ImageJ every single chamber using some manual modification. In fact, because the chambers are interconnected in several locations, each chamber was artificially closed at the beginning of every connection by boundaries editing operation. If the goal of the operation is to calculate the volume of every lumen, this solution does not lead to inaccuracy of data because foramina or stolons are not part of the chamber volume itself. On the contrary, if the goal is to calculate the exact porosity the calculation of the whole canal system (septal and marginal), the stolons and the chambers connections are mandatory.

Because the foraminifera scanned are Recent, their preservation is excellent and the microCT images were able to clearly demonstrate the density contrast between the hollow chambers and the calcitic test itself. Such preservation allowed seeing the whole canal system in the marginal chord and inside every septum; stolons are also visible. Having the possibility to measure volumes of such empty space within every septum and within the marginal chord gave us the possibility to calculate the real density of the specimens. We had to take into account that the voxel size is about 4 μm : this means that 4 μm can be considered as the highest inaccuracy value in linear measurements. For areas or volumes calculated from linear measurements, the uncertainty range is propagated to the second and to the third powers.

Along with the volumes, many other values were calculated to permit the comparison of our new data with those existing in the literature. These are areas of lumina (A), chamber length (or septal distance, l), chamber height (h) and spiral distance. All these parameters were taken on the virtual equatorial section (Figure 1).

The thin section was obtained by using the slice extractor tool in Image Surfer, which allowed us to cut the specimens in every possible way; a tool like this is extremely helpful in the case of specimens that are not perfectly straight but with a curved periphery where a "mechanical thin section" is not reliable. To be rigorous in comparing the volumetric data with linear measurements or area calculations, the latter were

upgraded to the third power for becoming comparable with volumes. Only in the comparison between volume and spiral form, the volume data were downgraded to one dimension.

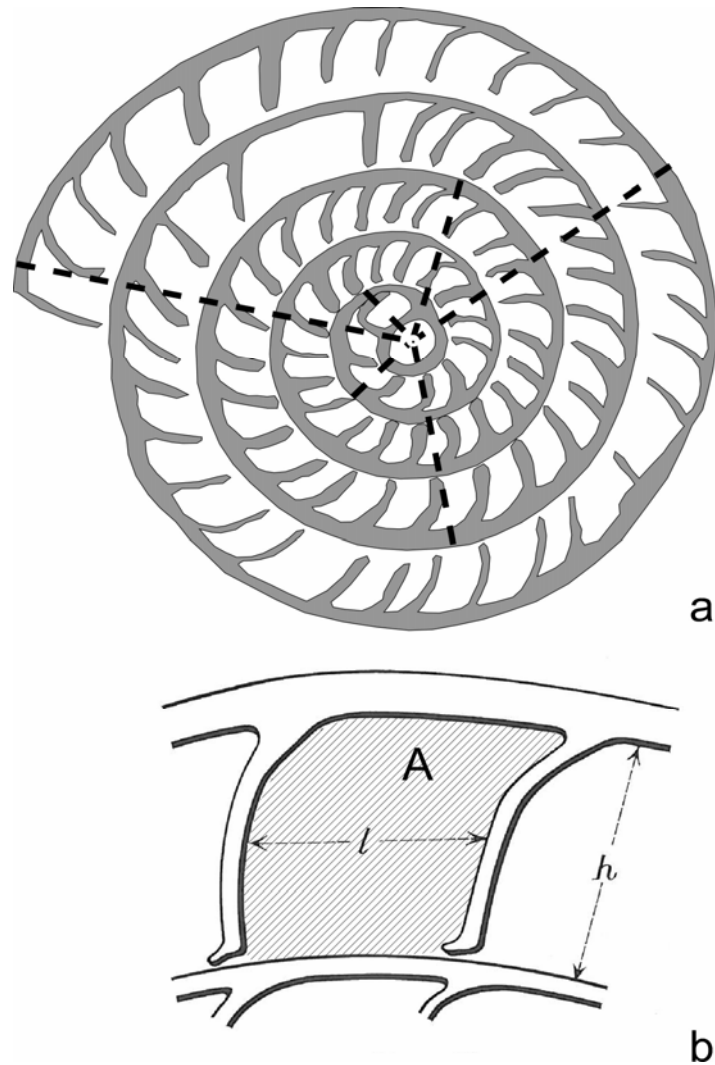


Figure 1: (a) Sketch of the equatorial section of a nummulitid, the dotted lines show how the spiral distance was measured (modified from Briguglio & Hohenegger 2009); (b) detail of the equatorial section detail with the explanation how to measure the chamber height h , septal distance l and chamber area A (modified after Blondeau 1972).

Results

Each lumen was manually extracted from the proloculus to the last completely scanned chamber, so that volume and surface could be calculated for every chamber. The extracted chambers of *O. ammonoides* and *P. venosus* are shown in Figure 2, and the measurements used in this work are reported in Table 2.

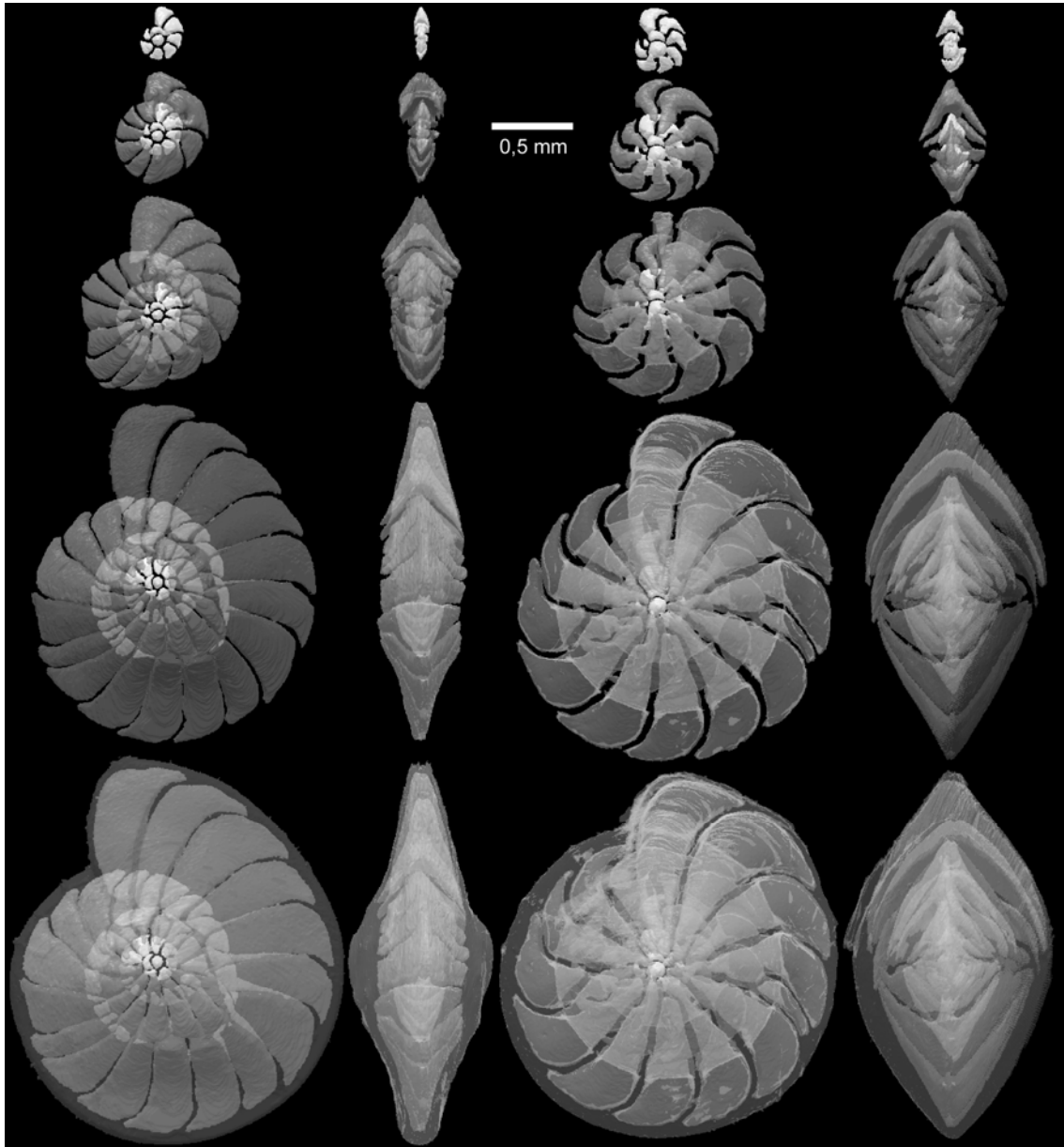


Figure 2: Three-dimensional representation of the chamber lumina, whorl after whorl, in equatorial and axial section of *O. ammonoides* (left side) and *P. venosus* (right side). The last row shows the lumina within the complete test.

A two-dimensional visualization of the three-dimensional dataset is not easy; for simplification, the extracted chamber lumina are illustrated whorl-by-whorl in equatorial and in axial view and always at the same magnification. The last row in Figure 2 shows all the extracted chambers within the test.

Chamber	Volume cubic mm		Chamber surface square mm		Chamber area square mm		Septal distance mm		Chamber height mm		Spiral distance mm	
	<i>P. venosus</i>	<i>O. ammonoides</i>	<i>P. venosus</i>	<i>O. ammonoides</i>	<i>P. venosus</i>	<i>O. ammonoides</i>	<i>P. venosus</i>	<i>O. ammonoides</i>	<i>P. venosus</i>	<i>O. ammonoides</i>	<i>P. venosus</i>	<i>O. ammonoides</i>
P	0.000409	0.00136	0.029563	0.014184	0.006961	0.00217521	0.089	0.066	0.048	0.037	0.123	0.107723
1	0.000146	0.000096	0.017026	0.01319	0.003774	0.002340357	0.03	0.032	0.034	0.045	0.113	0.11609
2	0.000021	0.000038	0.004301	0.006844	0.001106	0.001477222	0.055	0.055	0.059	0.054	0.158	0.12551
3	0.0001	0.0001	0.014205	0.013438	0.003065	0.00329745	0.061	0.058	0.064	0.064	0.155	0.1297
4	0.000195	0.000102	0.023554	0.012914	0.003763	0.0034328	0.074	0.057	0.064	0.064	0.152	0.151634
5	0.000214	0.000124	0.024848	0.015209	0.003592	0.00357764	0.068	0.064	0.058	0.08	0.172	0.1694
6	0.000186	0.000146	0.024609	0.016646	0.004721	0.00380635	0.078	0.075	0.057	0.073	0.161	0.209515
7	0.000016	0.000284	0.023671	0.027499	0.004095	0.005229585	0.082	0.075	0.057	0.073	0.231	0.23314
8	0.000228	0.000295	0.030936	0.026844	0.004491	0.006119652	0.08	0.078	0.059	0.075	0.231	0.23314
9	0.000448	0.000448	0.045938	0.035602	0.009507	0.00653568	0.086	0.086	0.091	0.089	0.259	0.259
10	0.000384	0.000391	0.04413	0.034273	0.005196	0.00562887	0.086	0.086	0.091	0.089	0.259	0.259
11	0.000705	0.000603	0.063374	0.047506	0.008954	0.006442	0.103	0.081	0.093	0.109	0.29	0.2769
12	0.000664	0.000712	0.076743	0.056689	0.007474	0.11274	0.102	0.08	0.085	0.101	0.294	0.294195
13	0.000986	0.000904	0.085652	0.062558	0.012232	0.010381	0.101	0.081	0.107	0.123	0.3	0.31219
14	0.000998	0.002675	0.083245	0.147301	0.010268	0.020123	0.106	0.216	0.087	0.137	0.324	0.292014
15	0.001744	0.001287	0.12085	0.084985	0.013121	0.014995	0.142	0.157	0.102	0.102	0.362	0.289526
16	0.001607	0.004099	0.123931	0.211189	0.012741	0.02869	0.12	0.252	0.119	0.107	0.392	0.351859
17	0.002616	0.003229	0.166694	0.16008	0.024948	0.019628	0.169	0.156	0.13	0.108	0.412	0.415904
18	0.001356	0.003414	0.10707	0.159639	0.017167	0.02002	0.1	0.135	0.129	0.152	0.446	0.469867
19	0.002662	0.0022	0.176236	0.119462	0.02694	0.01485	0.143	0.092	0.142	0.154	0.496	0.510169
20	0.004154	0.002611	0.234941	0.130729	0.024765	0.01915	0.184	0.184	0.131	0.146	0.536	0.516349
21	0.00272	0.003441	0.172897	0.1601	0.021891	0.0214	0.149	0.104	0.145	0.135	0.537	0.45108
22	0.0048	0.00376	0.296796	0.184062	0.031753	0.02178	0.186	0.124	0.148	0.127	0.526	0.484451
23	0.006095	0.004325	0.303458	0.207899	0.046577	0.02359	0.201	0.121	0.177	0.204	0.531	0.574595
24	0.007714	0.003448	0.35213	0.188593	0.052798	0.013975	0.211	0.095	0.233	0.196	0.557	0.532311
25	0.007471	0.003744	0.360852	0.218934	0.054198	0.0216	0.227	0.157	0.195	0.144	0.638	0.474102
26	0.00617	0.005087	0.307388	0.298329	0.035753	0.02175	0.185	0.199	0.199	0.127	0.676	0.4582
27	0.004618	0.003762	0.243966	0.204892	0.031476	0.016355	0.161	0.133	0.178	0.177	0.686	0.4607
28	0.011035	0.005991	0.481937	0.269852	0.051074	0.023644	0.256	0.171	0.16	0.126	0.688	0.533993
29	0.002178	0.005554	0.190077	0.282918	0.005032	0.018869	0.079	0.113	0.056	0.159	0.504	0.556742
30	0.013112	0.007306	0.591864	0.31969	0.047517	0.030308	0.192	0.137	0.182	0.18	0.709	0.592623
31	0.009868	0.006636	0.445598	0.291719	0.045313	0.035919	0.198	0.126	0.171	0.23	0.761	0.62813
32	0.011192	0.012814	0.531496	0.440857	0.048023	0.06282	0.3	0.195	0.156	0.265	0.772	0.718246
33	0.015667	0.012897	0.536248	0.411679	0.055171	0.062528	0.315	0.206	0.198	0.28	0.81	0.78219
34	0.0185	0.008269	0.723119	0.329046	0.063209	0.036789	0.3	0.129	0.229	0.298	0.817	0.824735
35	0.020688	0.010323	0.701908	0.391059	0.068671	0.061133	0.284	0.193	0.294	0.326	0.823	0.9004
36	0.022984	0.014377	0.757051	0.460644	0.071143	0.089025	0.284	0.194	0.307	0.391	0.831	0.950315
37	0.01995	0.017044	0.713578	0.523607	0.068165	0.100209	0.297	0.184	0.292	0.475	0.869	1.002945
38	0.02012	0.0169	0.734502	0.516959	0.080886	0.09345	0.308	0.182	0.305	0.46	0.941	1.030484
39	0.00461	0.015125	0.29962	0.472946	0.017296	0.02675	0.075	0.173	0.24	0.399	0.951	1.013711
40	0.020016	0.022718	0.735222	0.635489	0.067414	0.11559	0.251	0.22	0.214	0.408	0.968	0.982405
41	0.032389	0.018461	1.049335	0.588321	0.09317	0.092785	0.293	0.178	0.238	0.471	0.984	0.966269
42	0.048042	0.020728	1.287336	0.618464	0.118972	0.119296	0.37	0.211	0.312	0.487	1.002	0.912848
43	0.03685	0.018313	1.318932	0.558896	0.084064	0.091201	0.335	0.207	0.262	0.448	0.972	1.002482
44		0.022767	0.702759	0.558896	0.084064	0.120728	0.285	0.285	0.285	0.45	0.983716	0.983716
45		0.019664	0.591652	0.591652	0.1096488	0.1096488	0.208	0.208	0.482	0.482	1.044728	1.044728
46		0.02325	0.623384	0.623384	0.124131	0.124131	0.199	0.199	0.494	0.494	1.06	1.06

Table 2: Data obtained by measurements of the chambers lumen.

The canal system was isolated both along the marginal chord and within the septa; the volume of this hollow space was calculated and added to the volumes of lumina to get an exact value of the total empty space inside the test.

Subtracting porosity (chamber lumina) and micro-porosity (canal system, stolons and foramina) from the total test volume, we get the volume of the test wall. This value allows the calculation of density, which is very important for calculating different

transport effects. In *O. ammonoides* the 47 chambers lumina represent 38% of the total volume. A total of 4.5% of the test wall is empty because of the canal system (marginal chord), which increases up to 9.6% including the septa. This porosity reduces the test wall volume to 53% of the total volume and may reduce density from 1.69 g/mm³ down to 1.46 g/mm³ including micro-porosity of the pores.

For *P. venosus*, the volume of all chambers represents 28% of the entire test (i.e., the marginal chord and septa are relatively thicker than in *O. ammonoides*) and the total porosity gets 10% (against 15% in *O. ammonoides*); such values let test density drop off from 1.95 g/mm³ to 1.75 g/mm³.

The progression of lumina with test growth displays the ontogeny of the cell body. Such information can be used to detect or expect the reproduction stage in foraminifera (Hemleben et al. 1989). The embryonic apparatus was also extracted and separately compared (see Figure 3b). In the megalospheric generation of larger benthic foraminifera, the proloculus size and its connection with the deuterocoel is one of the main parameters for reconstructing phylogenetic trends (Less & Kovacs 1996; Papazzoni 1998).

The relation between growth rates of *P. venosus* and *O. ammonoides* is shown in Figure 3. The volumes of chambers lumina are presented as an overview (Figure 3a) and then whorl-by-whorl to study growth rate in detail (Figures 3c - f). Of course, the representation of the first whorl does not count proloculus and deuterolocus, but starts actually from the consecutive chamber, then the first chamber after the embryonic apparatus. All values can be represented by an exponential function. In the first whorls, the exponential rate is high, but in the very last whorl, especially in the last four chambers showing reduced increase, the adult stage seems to be reached and reproduction might be possible; the algebraic function switches from an exponential to a logistic one, very commonly indicating the adult stage in foraminifera.

Therefore, chamber volume trends appear to be comparable with other nummulitids, i.e., tending to have an inflection point at the adult stage. In Figure 3b, proloculus (P), deuterolocus (D) and first chamber (1) volumes are plotted and compared with their areas, measured on the equatorial section of the 3D image. Because of the identical slopes, the study of the embryonic stages in equatorial sections might be representative for the three-dimensional embryo.

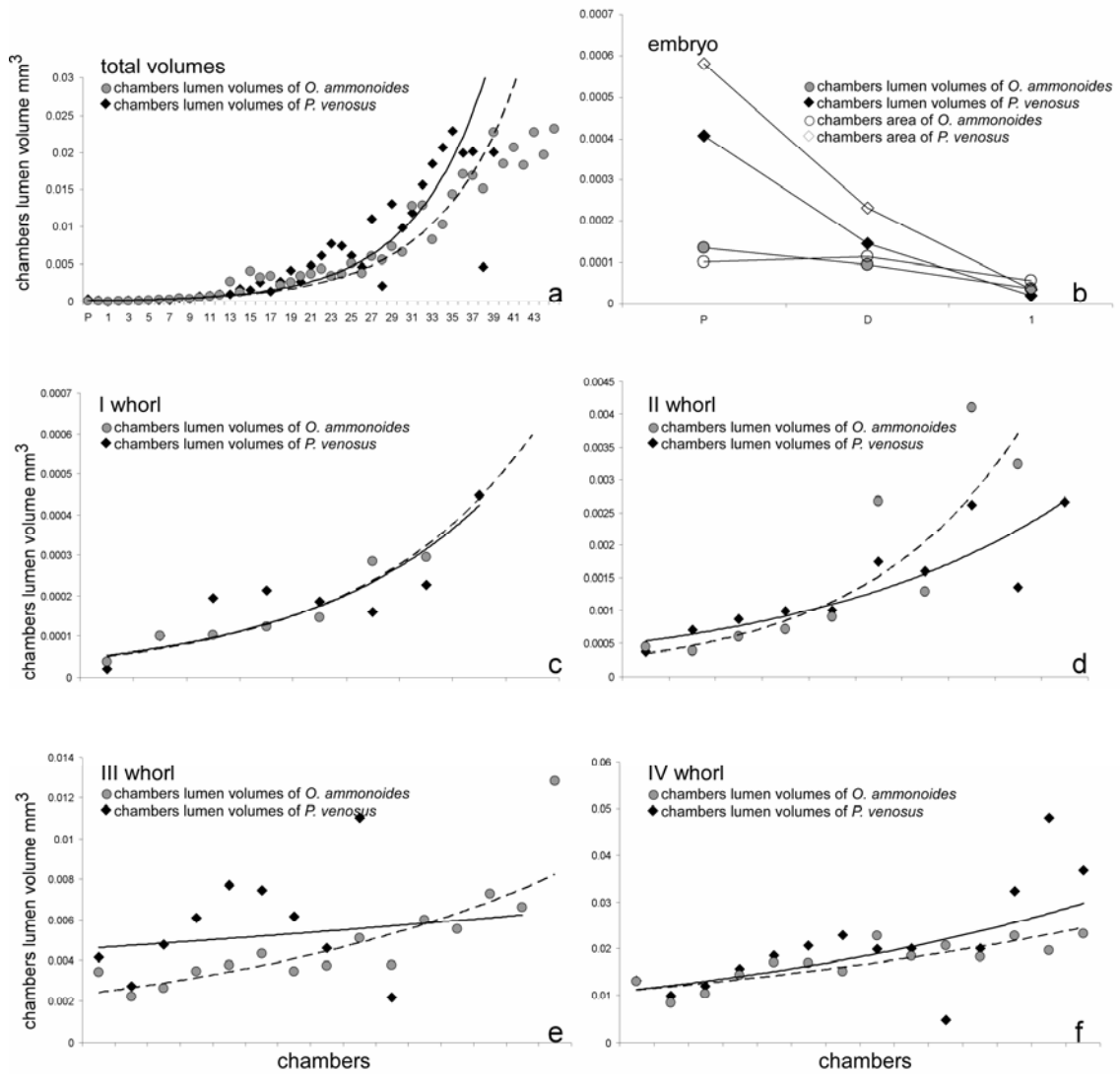


Figure 3: (a) Correspondence between chambers lumen volumes of *P. venosus* and *O. ammonoides*, the functions are calculated as exponential; (b) correspondence between chambers lumen volumes and areas of the first three chambers (P, D, 1) of the two specimens; (c) - (f) chambers lumen volumes correspondence, whorl after whorl, of the two specimens. Continuous lines are exponential functions for the *P. venosus* set of data; dashed lines are exponential functions for the *O. ammonoides* set of data. All areas were recalculated as the cubic power to make them comparable with volume.

Area calculation and its comparison with volumes also give interesting results. As shown in Figure 4, the growth trend of the area is very similar to the volume growth rate in both investigated specimens. Because of different chamber morphologies between the two specimens, the areas in *O. ammonoides* are more similar to their volumes.

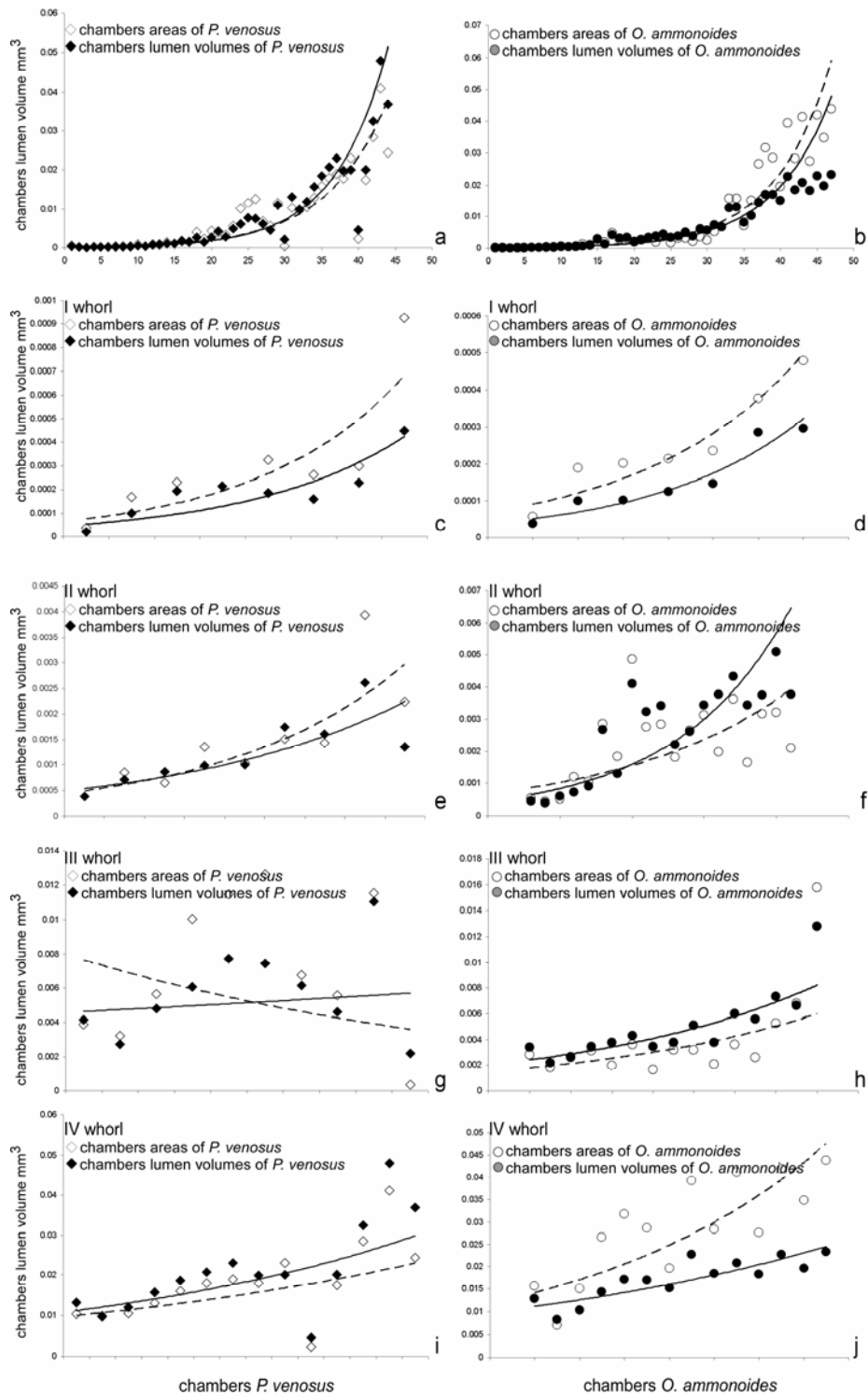


Figure 4: (a) correspondence between chambers lumen volumes of *P. venosus* and its areas; (b) correspondence between chambers lumen volumes of *O. ammonoides* and its areas; (c) & (e) & (g) & (i) correspondence between chambers lumen volumes and areas, whorl after whorl, of *P. venosus*; (d) & (f) & (h) & (j) correspondence between chambers lumen volumes and areas, whorl after whorl, of *O. ammonoides*. Continuous lines are exponential functions for the *P. venosus* set of data; dashed lines are exponential functions for the *O. ammonoides* set of data. All areas were recalculated as the cubic power of the radius to make them comparable with volume.

Because the alar prolongations of *O. ammonoides* are shorter than in *P. venosus*, area calculation by equatorial section is more representative in operculinids (sensu Hottinger

1997) than in taxa, where alar prolongations can reach the umbilical boss. In the last whorl of *O. ammonoides* the calculation of the volume based on the area

$$v_i = (\sqrt{a_i})^3$$

tends to overestimate the real volumes because of the elevated chamber heights (see Figure 4 j).

In thin sections, we might have the impression that operculinids should possess higher growth rates than nummulitids, but the data obtained here seem to show a different trend: the growth rate measured by volumes does not have the same behaviour as chamber height (Fig. 5 & 6). As discussed later, the chamber height, which grows faster in operculinids than in other nummulitids, produces such effects in thin section.

Comparing the growth of chamber length and height (Figs 5 & 6) with volumes, differences in chamber morphology becomes distinct. An estimation of the main ontogenetic trend is given for the first two whorls. In the last whorls, the chamber length is not significant for *P. venosus* and is underestimated (bigger whorl after whorl, Figures 5f, h, j) for *O. ammonoides*. Concerning the growth rate in chamber height (Figure 6), it is consistent with the volume growth in *P. venosus*, but definitely overestimated in *O. ammonoides* (Fig. 6j).

The relation between spiral and volumes growth rates is shown in Figure 7. The data were recalculated to be comparable, i.e., volumes data were transformed to linear data by cubic root to compare this trend with spiral growth, and these functions were calculated as linear and forced to intersect the origin (Fig. 7a & b). This comparison gives us information about growth relating the biological need (volume for protoplasm growth) to chamber geometry. For both *P. venosus* and *O. ammonoides* the spiral has a higher growth rate than the linearized volume. The different chamber morphology of the two specimens does affect the spiral growth, which is in fact very similar, whorl-by-whorl, in both taxa. No inflection points are observed in spiral growth, as is expected close to the proposed reproduction status in volume growth.

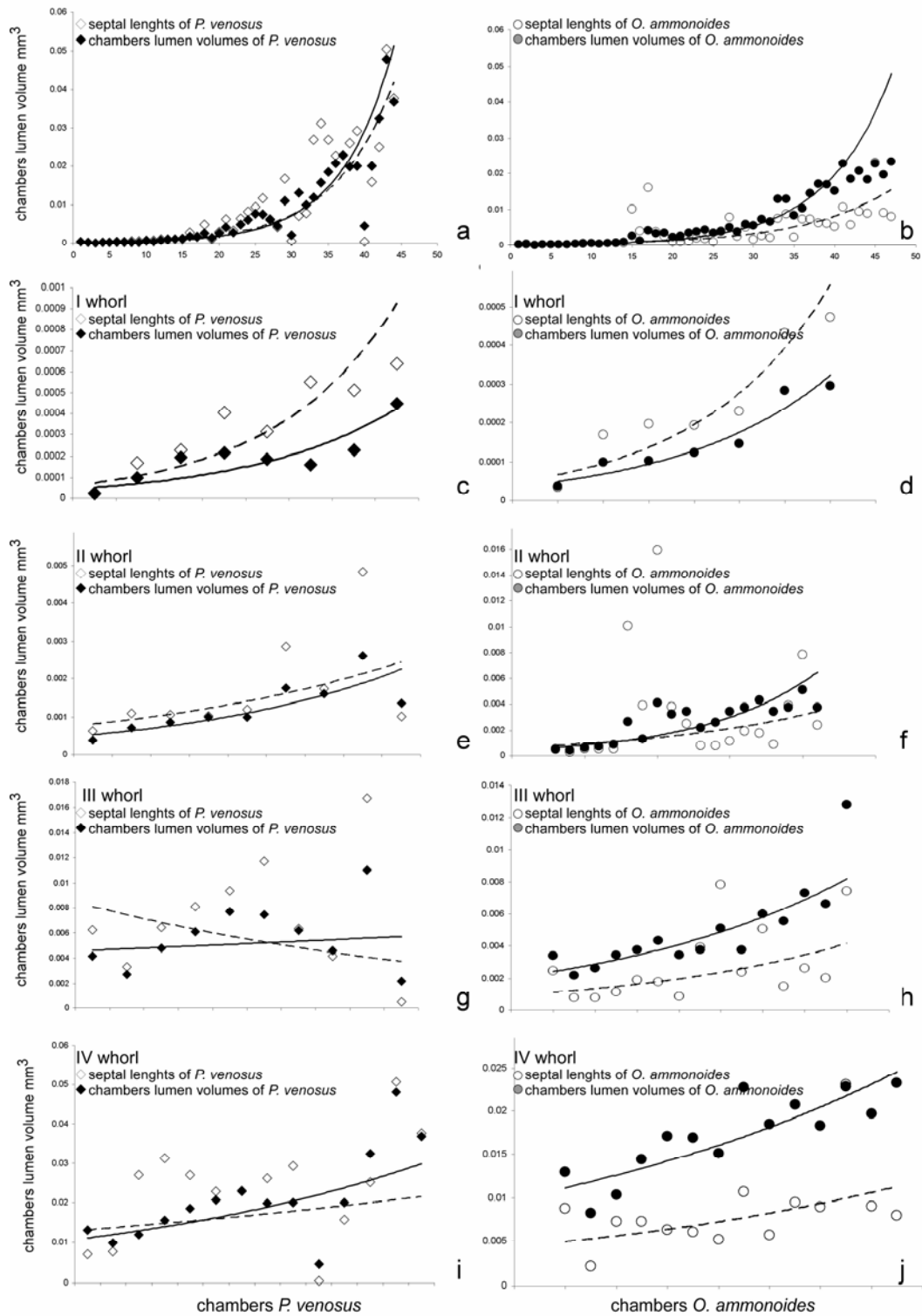


Figure 5: (a) Correspondence between chambers lumen volumes of *P. venosus* and septal lengths; (b) correspondence between chambers lumen volumes of *O. ammonoides* and septal lengths; (c) & (e) & (g) & (i) correspondence between chambers lumen volumes and septal lengths, whorl after whorl, of *P. venosus*; (d) & (f) & (h) & (j) correspondence between chambers lumen volumes and septal lengths, whorl after whorl, of *O. ammonoides*. Continuous lines are exponential functions for *P. venosus*; dashed lines are exponential functions for the *O. ammonoides*. All septal lengths were recalculated as the cubic power to make them comparable with volume.

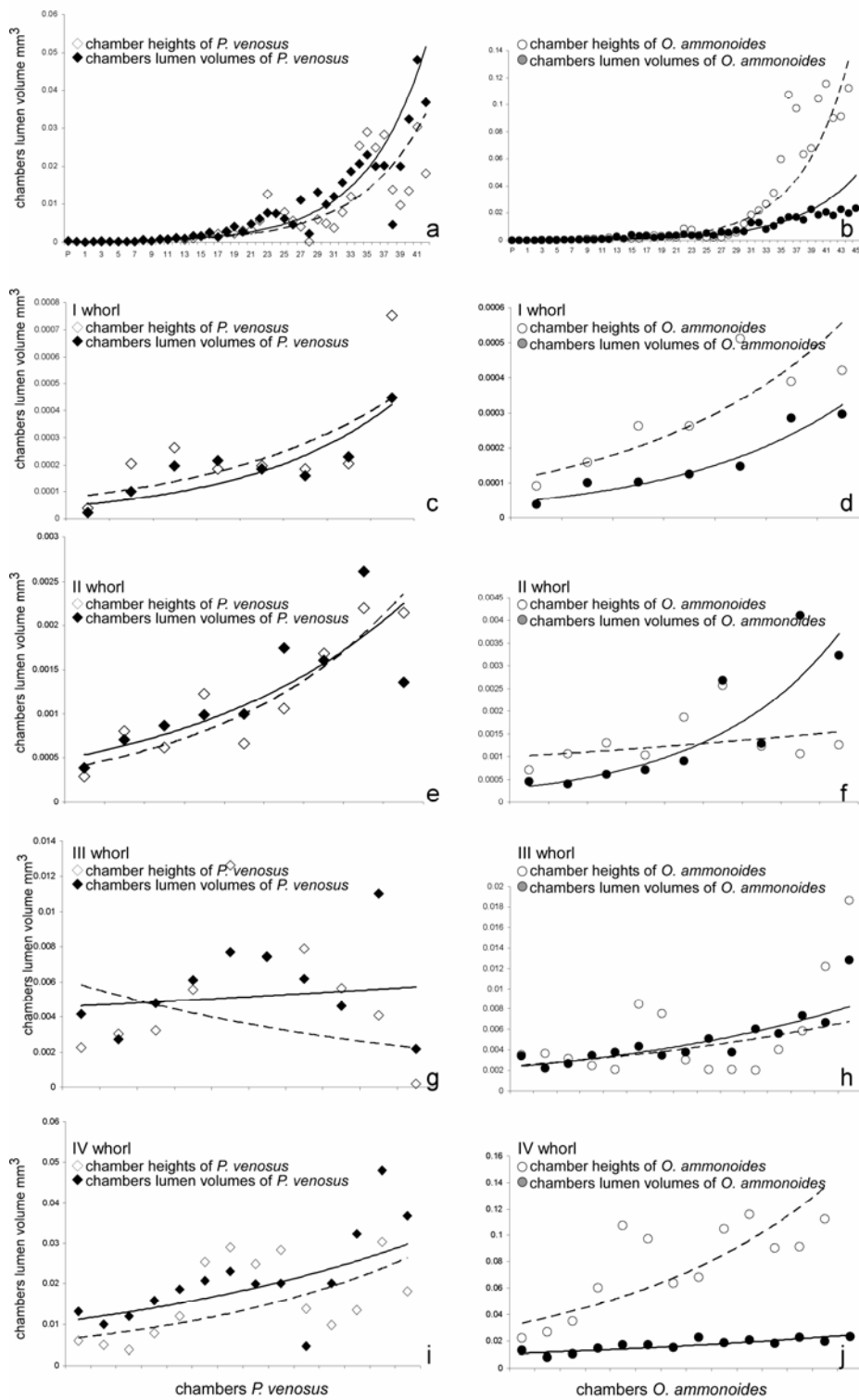


Figure 6: (a) correspondence between chambers lumen volumes of *P. venosus* and chamber heights; (b) correspondence between chambers lumen volumes of *O. ammonoides* and chamber heights; (c) & (e) & (g) & (i) correspondence between chambers lumen volumes and chamber heights, whorl after whorl, of *P. venosus*; (d) & (f) & (h) & (j) correlation between chambers lumen volumes and chamber heights, whorl after whorl, of *O. ammonoides*. Continuous lines are exponential functions for *P. venosus*; dashed lines are exponential functions for *O. ammonoides*. All chamber heights were recalculated at the cubic power to make them comparable with volume.

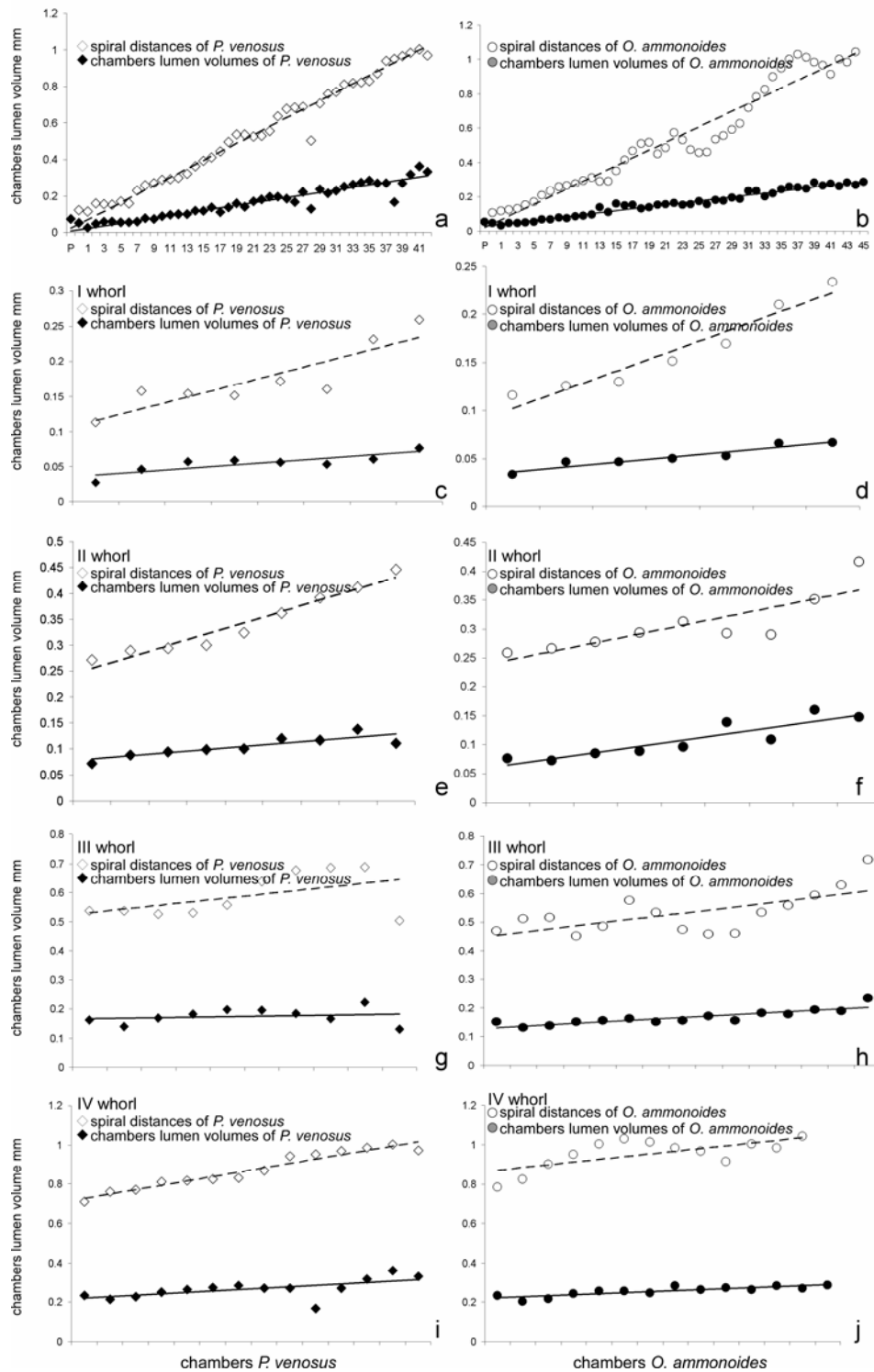


Figure 7: (a) Correspondence between chambers lumen volumes of *P. venosus* and its spiral distances; (b) correspondence between chambers lumen volumes of *O. ammonoides* and its spiral distances; (c) & (e) & (g) & (i) correspondence between chambers lumen volumes and spiral distances, whorl after whorl, of *P. venosus*; (d) & (f) & (h) & (j) correspondence between chambers lumen volumes and spiral distances, whorl after whorl, of *O. ammonoides*. Continuous lines are linear functions for *P. venosus*; dashed lines are linear functions for *O. ammonoides*. All chambers lumen volumes were recalculated at the cubic root to make them comparable with spiral distances data.

The deviation from sphericity is illustrated in Figure 8. The correspondence between volume surface ratio and linear volume is reported for both specimens (see Fig. 8 a), but nothing seem to differentiate the two linear growths. More successful is the use of the calculation proposed by Wadell (1932) with the following equation:

$$\psi = \frac{\pi^{\frac{1}{3}}(6V)^{\frac{2}{3}}}{S}$$

where, in this case, V and S are the chamber volume and the chamber surface respectively. Using this formula, the range limits are given by 0 (e.g., surface without volume) and 1 (e.g., perfect sphere).

In both the specimens the proloculi have a value slightly higher than 0.9 and can be considered as spheres, but after the first two whorls showing a decrease, sphericity seems to reach stable values close to 0.5 for *P. venosus* and 0.6 for *O. ammonoides*.

Because of the good correspondence between volumes and areas, regressions were calculated for *P. venosus* and *O. ammonoides* to see the power of statistical correlations. As shown in figure 9 the best fitting for *O. ammonoides* is represented by a linear regression (forced through the origin) which is not the best solution for *P. venosus*. In this case, the best fitting is represented by a power regression with an exponent > 1 .

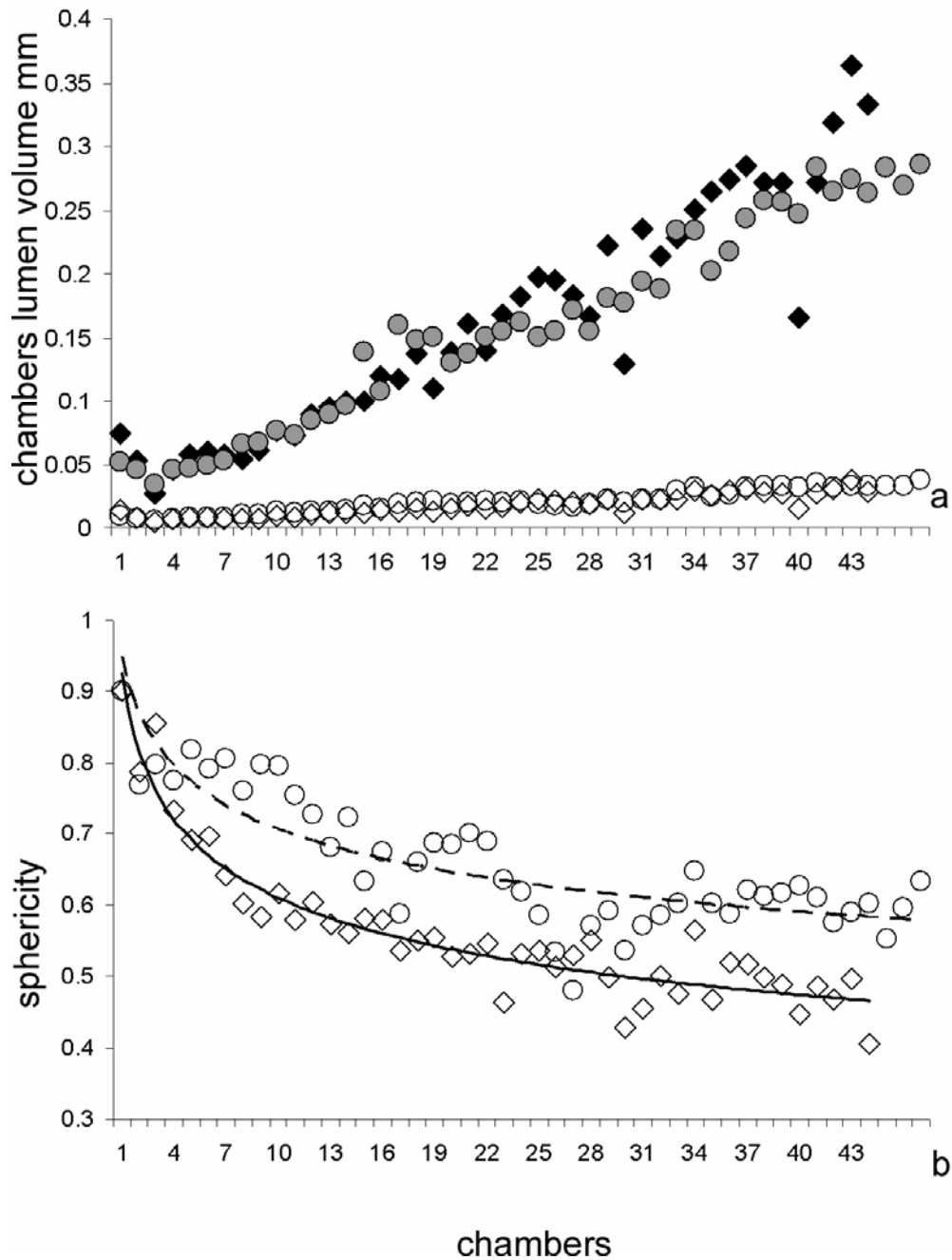


Figure 8: Deviations from sphericity. (a) correspondence between cubic root chamber lumen volumes and volume surface ratio. *P. venosus* chambers lumen volumes and volume surface ratios are represented by full and empty rhombuses; *O. ammonoides* chambers lumen volumes and volume surface ratios are represented by full and empty circles; (b) correspondence between sphericity deviation of *P. venosus* and *O. ammonoides* using the Wadell equation. Continuous line is the power function for *P. venosus*; dashed line is the power function for *O. ammonoides*.

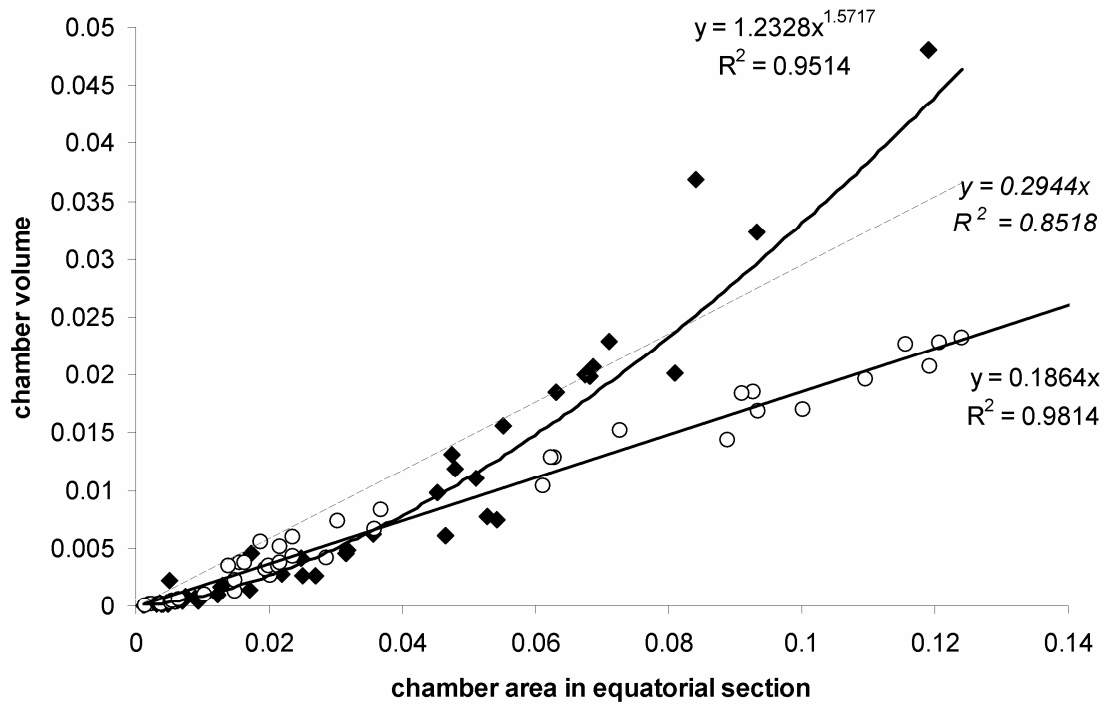


Figure 9: Regression of chamber volume on the equatorial section area in *P. venosus* (full rhombuses) and *O. ammonoides* (empty circles). The regression functions are calculated as linear and power regression for *P. venosus* and as linear regression for *O. ammonoides*. Equations and coefficients of determination (R^2) are given.

Discussion

The calculation from 3D images of chamber volumes and shapes and their changes during ontogeny gives a huge amount of information quite impossible to obtain by the traditional two-dimensional methodology of the oriented thin section. The volume measure gives no information about shell geometry but indicates the influence of temporal changes during the foraminiferal growth.

Mathematically, the construction of a chamber possessing a specific volume has an infinite number of solutions; but the evolved morphogenetic solutions are strictly limited by developmental genes and their interactions with the physico-chemical properties of the developing tissues (Newman & Müller 2000), in a case of single celled foraminifera the mineralised test. In nummulitids the form of the outer margin can be modelled by equation

$$r = b_0(b_1 + b_2\theta)^\theta$$

considering the length of the initial spiral (b_0), the expansion rate (b_1) and the acceleration rate (b_2) as constants (Hohenegger 2010). The parameter values are fixed for each individual, presumably as an inflexible part of their developmental genetics. Deviations from these fixed structures are caused by short but major environmental stress (like extreme temperature or attack by a predator fish). Thickness, the second important character describing test and chamber shape, is also fixed, on the one hand by the connection with the radius, and on the other by parameters of the equation

$$th = b_0 r \exp b_1$$

where b_0 represents the thickness constant and b_1 the allometric constant (Hohenegger, 2010).

Every environmental stress can lead to a variation in volume growth rate. The chamber lumina, fixed by height (marginal radius) and thickness determined by genetic factors, can only react to stress by varying the septal distance during building the new wall.

Therefore, the mathematically infinite combinations of morphological solutions in building chambers with identical volumes are restricted by the verification limits of the character (e.g., negative numbers for test-wall thickness are impossible), degrees of freedom (e.g. dependence of septal distances from fixed marginal radius and thickness) and by the intensity and form of inter-correlations between characters based on gene and other regulatory interactions during development.

The study of the volume by 3D analysis gives a more complete idea of the specimen's growth than do equatorially oriented thin sections. In thin sections, the chamber size in the operculinids seems to be generally bigger than in nummulitids; i.e., the chambers of operculinids are higher and the septal distance is bigger than in other nummulitids. In contrast, volume analysis shows that chambers of *P. venosus* reach the same size as *O. ammonoides* because the former is not as evolute as the latter. On Figure 3 some graphs are plotted showing the volume differences between the two specimens. The growth trend is comparable, and it is exponential at least for the first and the second whorl (Fig. 3c, d). The last two whorls are not increasing so fast as the first ones and the very last chambers are not increasing at all. Such trends, already shown three dimensionally by Speijer et al. (2008), reflect the achievement of reproduction in the adult stage. It is interesting that the chamber morphology is different in these two genera, but the chamber volumes are very similar. These differences at the genus level, and above it,

are not caused by ecological factors like decreasing light intensities. The specimens studied here, belonging to two different genera and have similar thicknesses of shell, despite living at different water depth, hinting at the underlying historical-phylogenetic background that is reflected in their inherited morphogenetic pathways.

In *O. ammonoides*, the chamber volume is reached by extending the chamber height and by reducing alar prolongations; in contrast, the same volume is reached in *P. venosus* by reducing the chamber height and by extending alar prolongations until the umbilical boss is reached. Thus, a similar biological need has been satisfied through two different developmental genetic solutions.

The three dimensional study of the embryo is also presented for these two species. The dimension of the proloculus is one of the main parameter in taxonomy and systematics of larger foraminifera, and its dimension and position with respect to the deuterolocus is characteristic for recognising phylogenetic trends (Drooger 1993; Less et al. 2008). The deviation from sphericity in both proloculi is very low (close to 0.9) and they can be approximated as spheres. For these reasons, the traditional methodology of calculating only the largest diameter of the proloculus is representative for its volume.

The equatorial section can generally be considered as suitable to study the ontogenesis in larger foraminifera, but according to our comparisons, the equatorial section character most consistent with the volume growth rate is the area. From the first whorl to the last one, the area growth rate gradually follows the volume data. As shown in Figure 9, the equatorial section area can be considered as well-suited to evaluate ontogeny in larger benthic foraminifera. The difference between evolute and involute forms is reflected in this figure.

In the involute *P. venosus* the equatorial section area of a chamber underestimates its actual volume. This underestimation increases with chamber growth and is caused by neglecting the alar prolongations, which are not visible in the equatorial section. In contrast, the constant evolute coiling of *O. ammonoides*, gives an accurate estimation of volume from the area by a constant multiplication factor.

Chamber length and height are only partially representative of the ontogenesis of the cell, mainly in the first two whorls.

Density calculation gives good results, although it is time consuming for the extraction of all the hollow space within the marginal chord and septa, and requires very high image resolution. Nevertheless, such evaluation is useful to test the calculation of

density by mathematical formula (Yordanova & Hohenegger 2007). Concerning Nummulitidae, density values adopted in recent studies about hydrodynamics (Briguglio & Hohenegger 2009) or about paleogeographic reconstruction (Jorry et al. 2006) are between 1.5 and 1.8 g/mm³. The values obtained with this method also show significant differences between the two genera, and such difference can explain partially the different depositional environment they belong.

Conclusion

The detailed morphological and volumetric data obtained with 3D analysis indicate that the use of X-ray microtomography can be very useful for biometric research on foraminifera. Not only can intraspecific variation and evolutionary lineages be assessed or confirmed based on the 3D shapes and sizes (Speijer et al. 2008), but such methodology can be particularly advantageous for nummulitids where the growth rate and chamber geometry are the most important parameters for taxonomy, systematics and paleobiology.

The calculation of volumes is important to study the ontogenesis of the cell and can predict the reproduction stage or give details on the cell response to environmental changes through time (e.g. seasonality). The calculation of density can be used for prediction and evaluation of the hydrodynamic behaviour of nummulitids in fossil record (Briguglio & Hohenegger 2009).

Any further use of a microCT scan on larger benthic foraminifera is welcome because of the huge diversity of the group and because many hypotheses on evolution and phylogeny are based on classic 2D analysis and it would be interesting to test them on a three-dimensional scale.

Three-dimensional analyses of populations will also give much more information on volumes variability and chamber morphologies, but today these procedures are too much time consuming.

However, we believe that the quantitative calculation of lumina concerning their shape, volume and growth rate may give a huge amount of information on ontogenesis, paleobiology, phylogeny, microevolution and taxonomy of larger benthic foraminifera.

All the correspondences considered in this work indicate that not all the possible linear measurements on the equatorial section of a nummulitids are useful, at least for the last

whorls in the adult stage. The calculation of the area, fast and precisely calculable with many computer programs, is more similar to the volume trend in every whorl and in the specimens here exposed. Thus, area calculation might be considered especially useful for growth rate studies in thin section.

Acknowledgements

Thanks are due to the reviewers Prof. Robert Speijer (Lueven, Belgium) and Prof. Jarosław Tyszka, (Cracow, Poland), which corrected the manuscript and gave many comments and hints. From the University of Vienna, we thank Prof. Gerd Müller (Department of Theoretical Biology) for the possibility to use the MicroCT, Mag. Martin Dockner (Department of Anthropology) and Kai Uwe Hochhauser (Department of Paleontology) for the IT support.

References

- BLONDEAU, A., 1972 - Les Nummulites, Vuibert, Paris.
- BRIGUGLIO, A. & HOHENEGGER J., 2009. Nummulitids hydrodynamics: an example using *Nummulites globulus* Leymerie, 1846. *Bollettino della Società Paleontologica Italiana* **48**, 105-111.
- CARLSON, W.D., ROWE, T., KETCHAM, R.A. & COLBERT, M.W. 2003. Application of high-resolution X-ray computed tomography in petrology, meteoritics and palaeontology. In: MEES F., SWENNEN R., VAN GEET M. & JACOBS P. (eds.), *Applications of X-ray Computed Tomography in the Geosciences*. Geological Society, London, Special Publication **215**, 7-22.
- DROOGER, C.W. 1993. Radial foraminifera: Morphometrics and evolution. *Proceedings of the Koninklijke Nederlandse Akademie van Wetenschappen Series afd. Physics, eerste reeks* **41**.
- FICHEL, L. & MOLL, J.P.C. 1798. Testacea microscopica aliaque minuta ex generibus *Argonauta* et *Nautilus* ad naturam picta et descripta. In RÖGL, F. & HANSEN H.J. 1984. Foraminifera described by Fichtel & Moll in 1798, A revision of Testacea Microscopica. *Neue Denkschriften des Naturhistorischen Museums in Wien*, v.3, p.1-143.

- GRONOVIVS, L.T. 1781. *Zoolphylacii Gronoviani. Exhibens vermes, Mollusca, Testacea et Zoophyta*. Theodorus Haak et Soc .Leyden 241-380.
- HALLOCK, P. & GLENN, E.C. 1986. Larger Foraminifera: a tool for paleoenvironmental analysis of Cenozoic carbonate depositional facies. *Palaios* **1**, 55–64.
- HEMBLEBEN, C., SPINDLER, M. & ANDERSON, O.R. 1989. *Modern planktonic foraminifera*. Springer, New York.
- HOHENEGGER, J., YORDANOVA, E., NAKANO, Y., & TATZREITER, F. 1999. Habitats of larger foraminifera on the upper reef slope of Sesoko Island, Okinawa, Japan. *Marine Micropaleontology* **36**, 109–168.
- HOHENEGGER, J. 2010 (submitted). Growth invariant meristic characters. Tools to reveal phylogenetic relationships in fossil Nummulitidae. *Turkish Journal of Earth Sciences*.
- HOTTINGER, L., 1977. Foraminiferes Operculiniformes. *Mémoires du Muséum National d'Histoire Naturelle*. Série C, Science del la terre, Tome XL.
- HOTTINGER, L. 2009. The Paleocene and earliest Eocene foraminiferal Family Miscellaneidae: neither nummulitids nor rotaliids. *Carnet de Géologie / Notebooks on Geology*, Brest, Article 2006/06 (CG2009_A06).
- JORRY, S., HASLER, C.A. & DAVAUD, E. 2006. Hydrodynamic behaviour of *Nummulites*: implications for depositional models. *Facies* **52**, 221-235.
- LESS, G. & KOVACS, L. 1996. Age-estimates by European Paleogene Orthophragminae using numerical evolutionary correlation. *Geobios* **29**, 261-285.
- LESS, G., ÖZCAN, E., PAPAZZONI, C.A. & STÖCKAR, R. 2008. The middle to late Eocene evolution of nummulitid foraminifer *Heterostegina* in the Western Tethys. *Acta Palaeontologica Polonica* **53**, 317–350.
- METSCHER, B.D. 2009. MicroCT for comparative morphology: simple staining methods allow high-contrast 3D imaging of diverse non-mineralized tissues. *BMC Physiology* **9**: 11.
- NEUES, F. & EPPLE, M. 2008. X-ray Microcomputer Tomography for the Study of Biomineralized Endo- and Exoskeletons of Animals. *Chem Rev* **108**(11): 4734-4741.
- NEWMAN, S. A. & MÜLLER, G. B. 2000. Epigenetic Mechanisms of Character Origination. *J. Exp. Zool. (Mol. Dev. Evol.)* 288:304–317.

- PAPAZZONI, C.A. 1998. Biometric analyses of *Nummulites "ptukhiani"* Z.D. Kacharava, 1969 and *Nummulites fabianii* (Prever in fabiani, 1905). *Journal of Foraminiferal Research* **28**, 161-176.
- PECHEUX, M.J.F. 1995. Ecomorphology of a recent large foraminifer, *Operculina ammonoides*. *Geobios* **28**, 529-566.
- RACEY, A. 1992. The relative taxonomic value of morphological characters in the genus *Nummulites* (Foraminiferida). *Journal of Micropalaeontology* **11**, 197-209.
- REISS, Z. & HOTTINGER, L. 1984. The Gulf of Aqaba. Ecological Micropaleontology. Springer-Verlag, Berlin.
- ROVEDA, V. 1970. Revision of the *Nummulites* (Foraminiferida) of the *N. fabianii-fichteli* group. *Rivista italiana di Paleontologia* **76**, 235-324.
- SCHAUB, H. 1981. *Nummulites* et *Assilines* de la Téthys paléogène. Taxinomie, phylogénese et biostratigraphie. *Schweizerische Paläontologische Abhandlungen* **104-106**.
- SPEIJER, R.P., VAN LOO, D., MASSCHAELE, B., VLASSEN BROECK, J., CNUUDE, V. & JACOBS, P. 2008. Quantifying foraminiferal growth with high-resolution X-ray computed tomography: New opportunities in foraminiferal ontogeny, phylogeny, and paleoceanography applications. *Geosphere* **4**, 760-763.
- WADELL, H. 1932. Volume, shape and roundness of rock particles. *Journal of Geology* **40**, 443-451.
- YORDANOVA, E. & HOHENEGGER, J. 2007. Studies on settling, traction and entrainment of larger benthic foraminiferal tests: implication for accumulation in shallow marine sediments. *Sedimentology* **54**, 1273-1306.

Chapter 3

Briguglio A., Hohenegger J. & Yordanova K.E., (submitted): How to react to shallow water hydrodynamics: The larger benthic foraminifera solution. *Marine Micropalaeontology*

*Nam per aquas quae cumque cadunt atque aera rarum,
haec pro ponderibus casus celerare necessest
propterea quia corpus aquae naturaque tenvis
aeris haud possunt aequae rem quamque morari,
sed citius cedunt gravioribus exsuperata.*

Titus Lucretius Carus: *De rerum natura*; II, 230-234.

**HOW TO REACT TO SHALLOW WATER HYDRODYNAMICS:
THE LARGER BENTHIC FORAMINIFERA SOLUTION**

ANTONINO BRIGUGLIO^{1*}, JOHANN HOHENEGGER¹, and ELZA K.
YORDANOVA²

¹*Universität Wien, Geozentrum, Institut für Paläontologie, Vienna, Austria;*

²*Geologische Bundesanstalt (GBA), Vienna, Austria.*

e-mail: antonino.briguglio@univie.ac.at

fax: +43142779535

*Corresponding author

Keywords: shell morphology, transport, tests distribution, settling velocity, shape
entropy

ABSTRACT:

Larger benthic foraminifera are entrained and transported in shallow water depending on fixing mechanisms in living individuals together with the hydrodynamic parameters of the shell and on the energy at the water sediment interface. The use of mathematic equations to calculate hydrodynamic parameters of a test is a method to quantify its answer to the energy input given by water motion at the sea bottom. Measuring density, size and shape of every test, combined with experimental values obtained in the laboratory, helps to define the best mathematical approach for obtaining the settling velocity and Reynolds number of every shell. The comparison between water motion at the sediment-water interface and the species-specific settling velocity helps to calculate the water depth at which deposition for a certain test type may occur and at which tests may accumulate. Based on these correlations, paleodepths can be estimated using the foraminiferal distribution in the fossil environment according to size-independent parameters. Calculating the hydrodynamic parameters of tests has clear potential for estimating the transportability of larger foraminifera, i.e., the capability of a

certain test to be kept in suspension by an energy input at specific water depths, and thus to be transported within selected hydrodynamic boundaries.

1. Introduction

Habitats of larger benthic foraminifera (LBF) are determined by a set of environmental gradients. The main factors influencing the distribution of LBF are temperature, light intensity, water movement, substrate, and food (Hallock et al., 1991; Hohenegger, 2004). Distribution, abundance and bauplan diversity (*sensu* Hohenegger, 2009) of living foraminifera reflect the variation and concurrence of these environmental factors. Accordingly, changes in ecological factors, such as global warming, ocean acidification, or sea level changes, are reflected and recorded in the fossil distribution of larger foraminifera (Pecheux, 1995; Hohenegger, 1996). Haynes (1965) proposed that shape might be a compromise between hydrodynamic factors, light and metabolic requirements associated with algal symbiosis. This would make LBF powerful paleoenvironmental indicators, particularly in estimating paleodepth, because water motion and light both decline exponentially with depth (Hallock, 1979). Gathering enough light for endosymbionts under differing hydrodynamic conditions is the main functional demand of symbiont-bearing benthic foraminifera (Hohenegger, 2009). Shell morphology becomes thus the compromise between optimal functionality for hosting symbionts and for contrasting hydrodynamic forces.

Because LBF inhabit shallow waters, the hydrodynamic conditions are very strong and water motion can keep them in suspension and transport them to any direction. Thus, under weak hydrodynamic conditions the best hydrodynamically adapted tests are characterized by a large surface/volume-ratio (e.g., *Cycloclypeus*), whereas under strong hydrodynamic conditions the simplest way to resist transport in movable substrates like gravel and coarse sand is to develop high density or thick lenticular tests (e.g., *Archaias*, *Nummulites*) (Hohenegger et al., 1999). Such shape differentiation fits also symbiont's requirements: i.e., larger disk-shaped tests (with broader light-exposed surface) may live in deeper water with low light penetration, while shallower specimens, with higher light availability, may need a less light-exposed surface (Hallock et al., 1991).

This allows the depth distribution boundaries of living LBF to be calculated based on the light dependence of their symbionts, and their capability to contrast water motion by

hydrodynamic convenient test shape or anchoring mechanisms. Post mortem distribution, however, follows completely different rules. After reproduction or death, all tests may be at the mercy of water motion; if they were anchored, they can be easily detached from the substrate and thus redistributed. If the test possesses a hydrodynamic convenient shape for the depth it lived at, than it may resist transport under the same energy condition.

Transport evidences are often combined with test preservation; i.e., abrasion, destruction, or huge accumulations are considered as evidence for transport, deposition and accumulation processes. Concerning test abrasion, Beavington-Penney (2004) used recent LBF to demonstrate that mechanical test destruction is rare even during long-distance transport. Thus, mechanical abrasion or break-off of tests represent transport records only in very restricted conditions and may reflect high-energy events (e.g., tsunamis, long-time rewashing or entrainment by strong currents). Consequently, optimally preserved tests (*sensu* Yordanova and Hohenegger, 2002) may also have been affected by transport and cannot *a priori* be considered as *in situ* material.

Although transport and deposition of both living and dead tests significantly influence the distribution of LBF tests, very few studies have considered the importance of such modifications, particularly by a hydrodynamics point of view.

Some authors, mainly sedimentologists, provided mathematical solutions to approximate the hydrodynamic behaviour of sand particles moved by waves and currents. Some of these equations are well known (Soulsby, 1997; Wiberg and Sherwood, 2008). Other authors studied the distribution of living foraminifera using various approaches: morphocoenoclines (Hohenegger, 2004), character combination (Hohenegger, 2006) and presence/absence data (Pecheux, 1995; Renema 2002; Hohenegger, 2005; Rasser et al., 2005). The first study on nummulitids hydrodynamics was published by Jorry et al. (2006), then expanded by Yordanova & Hohenegger (2007) to other LBF using an enhanced statistic approach. The high diversity of LBF test shape leads to different hydrodynamic answers (Jorry et al., 2006) within the same energetic scenario, and the different hydrodynamic behaviours are calculable for every test. As proposed by Beavington-Penney et al. (2005), a good parameter to calculate LBF variations along the paleoenvironmental gradient is the diameter/thickness ratio. Such calculations, broadly used in recent publications (e.g., Adabi et al., 2008), gives some generic results but approximate too vaguely shape and do not take LBF size and

density into account, which are the most important parameters to evaluate the test distribution. In nummulitids, density may vary within the same genus (Jorry et al., 2006) and within the same species due to different growth stages (Yordanova and Hohenegger, 2007). More accurate calculations (Jorry et al., 2006; Yordanova and Hohenegger, 2007; Briguglio and Hohenegger, 2009), which consider shape entropy, nominal diameter and many other shape- or size-independent parameters, allow comparison between different environments and give much better results, without being much time consuming or depending on complex mathematics algorithms.

The present study calculates these parameters to yield precise values on foraminifera transportability, focusing on transport in suspension, thus considering the differences between living specimens and optimally preserved tests depth distribution. Such correlations, once measured and tested in recent environments, can be most useful for the fossil record. This paper explains how a single test reacts to the hydrodynamic input, at what depth the test starts to react, until what depth does it react under the same input, and how important the taxonomically significant geometric differences of LBF in this energy scenario are.

All the geometrical and structural characters, most useful in paleontology for taxonomy and ecology, are now the basics to quantify the response to hydrodynamics. Physically, these are the same processes affecting sand particles. Thus, the displacement of tests in the fossil record is merely the product of the species-specific biological distribution (habitat) modified due to classical sorting produced by water motion.

1.1 *Transportability and the role of Bottom Orbital Velocity*

Wind-generated waves induce – in sufficiently shallow water (*sensu* Soulsby, 1997) – orbital motion within the water column to a depth roughly equal to half the wavelength of the source waves. When water depth is less than half the wavelength, this wave-induced orbital motion affects particles lying on the seabed. Depending on the material (i.e., density) and on the form (i.e., size and shape) of such particles, they can be entrained, moved or kept in suspension. Wave-generated water motion interacts with the bed to influence surface waves through frictional dissipation of wave energy. This influences the bed through mobilization of bed sediment by wave-motion-induced bed shear stresses (Wiberg and Sherwood, 2008). Theoretical relationships between low-

amplitude monochromatic waves and near-bed water motion were derived during the late 1960s and then extended and improved to encompass an ever broader wave spectrum and environmental conditions. Many coastal problems require the calculation of wave-generated oscillatory (orbital) velocities at the sea-bed for applications such as sediment transport, suspension and mobility and many websites share java applets to easily calculate bottom velocities (and many others values) by surface wave parameters (e.g., <http://www.coastal.udel.edu/faculty/rad/>; http://woodshole.er.usgs.gov/staffpages/csherwood/sedx_equations/sedxinfo.html).

During the last decade the bottom orbital velocity periodic function and the near-bed wave orbital velocity got more and more attention by marine scientists, as well as coastal and marine engineers (e.g., Cookman and Flemings, 2001; Li and Amos, 2001; Schutten et al., 2004).

Sediment suspension and subsequent transport occur only if two conditions are contemporarily satisfied: the bottom orbital velocity (BOV) is greater than or equal to the particle settling velocity, and a secondary force, once the particle is kept in suspension, moves it horizontally to any direction. Such a combination of forces leads to particle suspension and transport, mostly avoiding test break-off or destruction. BOV put tests in suspension and move them vertically; without any other energy input, the particle will remain in the same environment or at the same depth. Once a secondary, orthogonal (i.e., on the horizontal plane) energy input is available (e.g., currents), the particle, if already kept in suspension, can be moved in the flow direction. When directional flow is present and orbital velocity is too weak to keep particles in suspension (e.g., in deeper water), transport may occur as traction or saltation depending on turbulence effects and near-bed friction laws. In the case of LBF, such mechanical effects may damage tests. The transportability of LBF shells only expresses its capability to be kept in suspension and is thus independent from transport intensity and direction.

As already stated, shell morphology is a compromise between light exposition and resistance to water motion. Under a functional morphologic view LBF must build non-transportable tests, at least during lifetime. Thus for LBF transportability is defined as the water depth range at which the test can be suspended by water motion, then potentially subject to secondary inputs. The equilibrium between orbital bottom velocity and test settling velocity is reached at the deepest point of this depth range. For LBFs

without special attachment mechanisms (e.g., spines in calcarinids) this point represents the best environmental condition, in term of depth, that must be satisfied to get sufficient light for symbionts of the foraminifer without being transportable anymore.

However, the mathematical quantification of orthogonal secondary water inputs (i.e., currents or streams) becomes thus unimportant for transportability. Accordingly, current parameters are not considered in the equations presented here, although they primarily are responsible for transport's width and direction.

The transportability of LBF is given by the combination of many parameters, including test density, size and shape and – concerning the energy scenario – sea bottom morphology, sedimentology and wave-induced orbital bottom velocity. The major factor within the following calculation is the bottom orbital velocity vs. settling velocity ratio, which delimits the transport - deposition boundary.

BOV can be calculated from surface-wave parameters using different equations. Water movement and, therefore, the resulting forces can be resolved at each point into vertical and horizontal components. Depending on the application and due to the vector character of velocity, all possible near bed velocities may be calculated to any direction and according to the linear wave theory know as the Airy wave theory (Airy, 1828) both in horizontal and in vertical direction as follow:

$$u=(\pi H/T) \{ \cosh[k(z_0+h)]/\sinh(kh) \} \cos(kx-\omega t) \quad (1)$$

for the horizontal orbital velocity, and

$$w=(\pi H/T) \{ \sinh[k(z_0+h)]/\sinh(kh) \} \sin(kx-\omega t) \quad (2)$$

for the vertical orbital velocity, where H is wave height, T is wave period, h is water depth, k is wave number, \sinh and \cosh are the hyperbolic sine and cosine, z_0 is the depth where the orbital velocity must be calculated, ω is the radian frequency $2\pi/t$, x is the coordinate in the direction of wave propagation, and t is the time (Fig. 1).

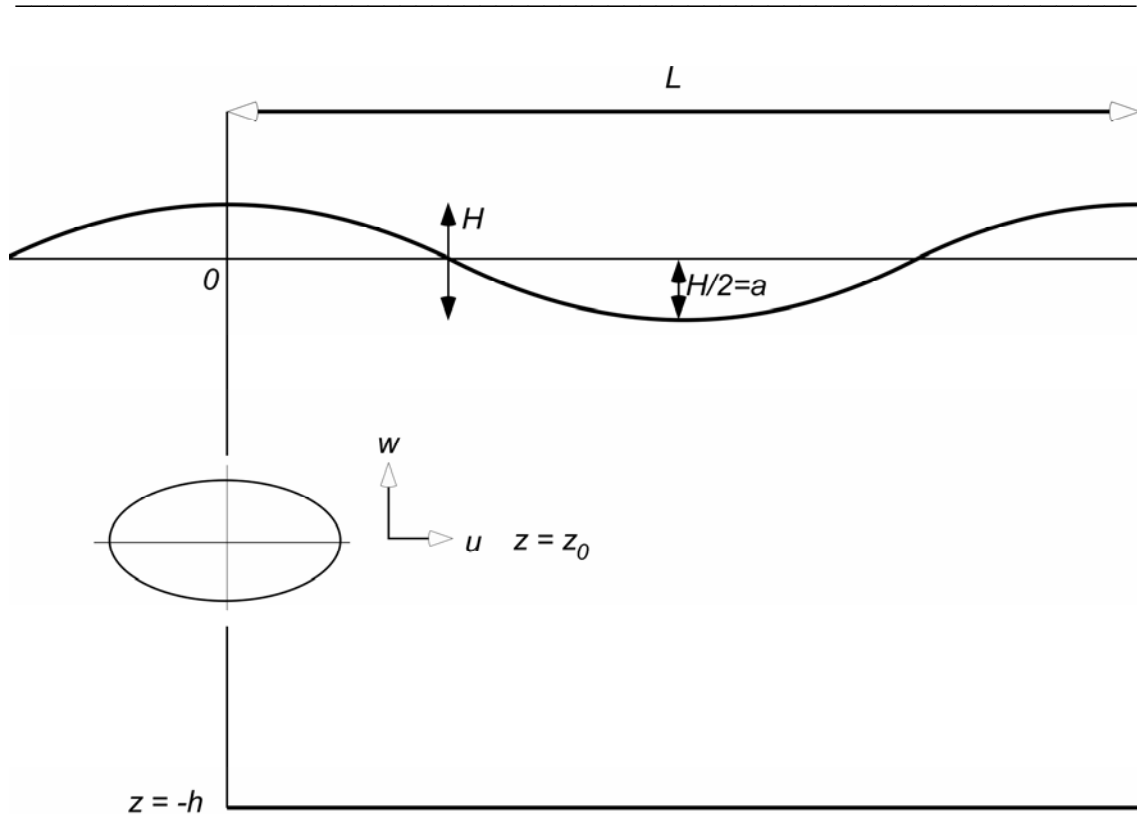


FIGURE 1 – Wave generated orbital velocity geometry and parameters (modified after Komar 1997).

Because the highest values are reached for horizontal and vertical velocity, in both cases the periodic functions sine and cosine are equal to one. In fact the horizontal component of orbital velocity reaches its maximum when $\cos(kx - \omega t) = 1$ and, vertically, (i.e., $\pi/2$), the vertical component reaches its maximum when $\sin(kx - \omega t) = 1$.

Considering orbital velocity at the sea bottom, it induces the condition $z_0 = -h$ in both equations (1, 2).

In equation (2), at the given condition, $\cosh[k(z_0 + h)] = 1$. In equation (3), at the same condition $z_0 = -h$, the value $\sinh[k(z_0 + h)] = 0$. This means that at the sea bottom, the horizontal velocity is always calculable but the vertical component goes to zero. However, it increases rapidly from the condition $z_0 + h > 0$ because of the divergent (i.e., non-periodic) character of the $\sinh(r)$ function.

Because of this inconvenience, several solutions have been proposed to quantify the vertical component of the orbital velocity at near-bed depth.

In linear wave theory, the equations for calculating the two components of bottom velocity differ for deep and shallow water because, friction with the bottom sediment plays a significant role in shallow water. According to several authors (Komar, 1998; Schutten et al., 2004), the formula for the deep-water approximation may be used for near bed vertical velocity providing good fitting with field observations. The vertical component of the orbital velocity for deep-water waves is:

$$w = (\pi H/t) \exp(kz) \sin(kx - \omega t) \quad (3).$$

For common waves of height less than 1.5 meters and of short period (i.e., $5 < T < 10$ sec) there is almost no difference between horizontal and vertical component. Below 30 meters water depth, they act, quantitatively, very similarly to the sediment (Fig. 2).

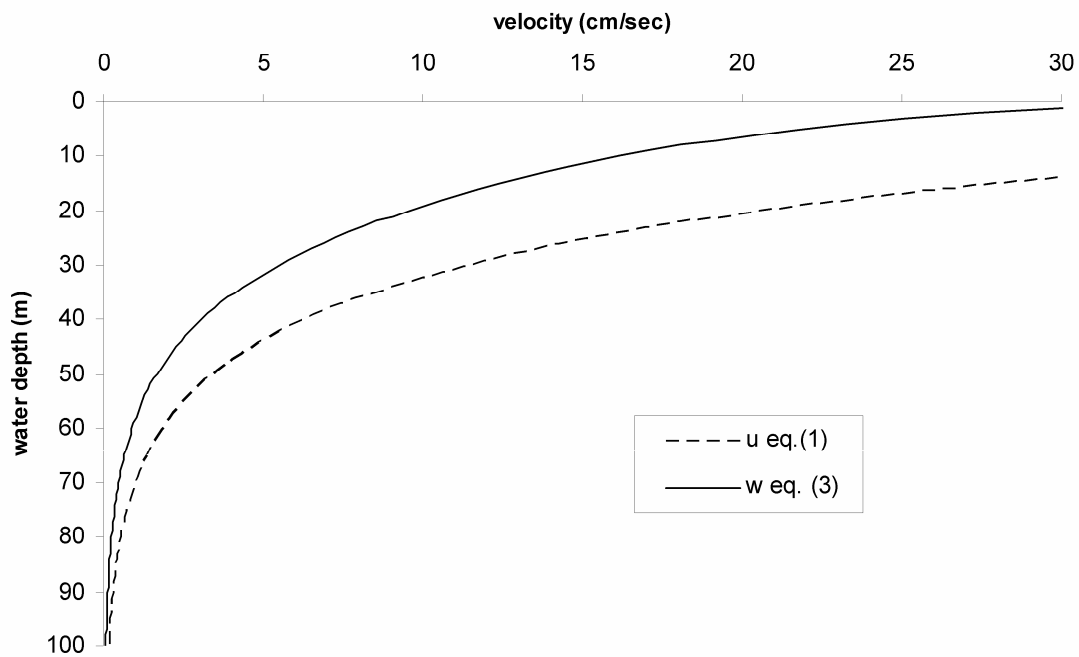


FIGURE 2 – Horizontal (u) and vertical (w) orbital bottom velocities calculated with equation 1 and 3, respectively.

That is why in many studies (see websites linked above) on near bed orbital velocity only equation (1) is used (Soulsby, 1997; Cookman and Flemings, 2001; Wiberg and Sherwood, 2008) to quantify the energy input at the sea-floor; the use of the mere vertical component for near bed orbital velocity is thus no further suggested.

However, in this work, the near bed orbital velocity was calculated using equation (1) modified after applying the conditions $z_0 = -h$ and $\cos(kx - \omega t) = 1$. The used equation results:

$$U_w = H\pi / T \sinh(kh) \quad (4)$$

This formula is the best-suited one for small-amplitude wave theory, which assumes the bed to be frictionless (Soulsby, 1997; Wiberg and Sherwood 2008). Orbital velocities calculated using this theory agree well with observed oscillatory flows under monochromatic waves. Note, however, that wind-generated waves are not monochromatic, and bed friction must be considered for the transport of sediment particles lying on the bottom. Nevertheless, for small-amplitude wind-generated waves, the approximation using H is still very accurate (Wiberg and Sherwood 2008) and the calculation of bed friction can be omitted when studying long-distance transport of optimally preserved specimens (i.e., considering neither rolling nor saltation). Figure 3 shows how deep such velocities affect the sea bottom depending on surface wave parameters.

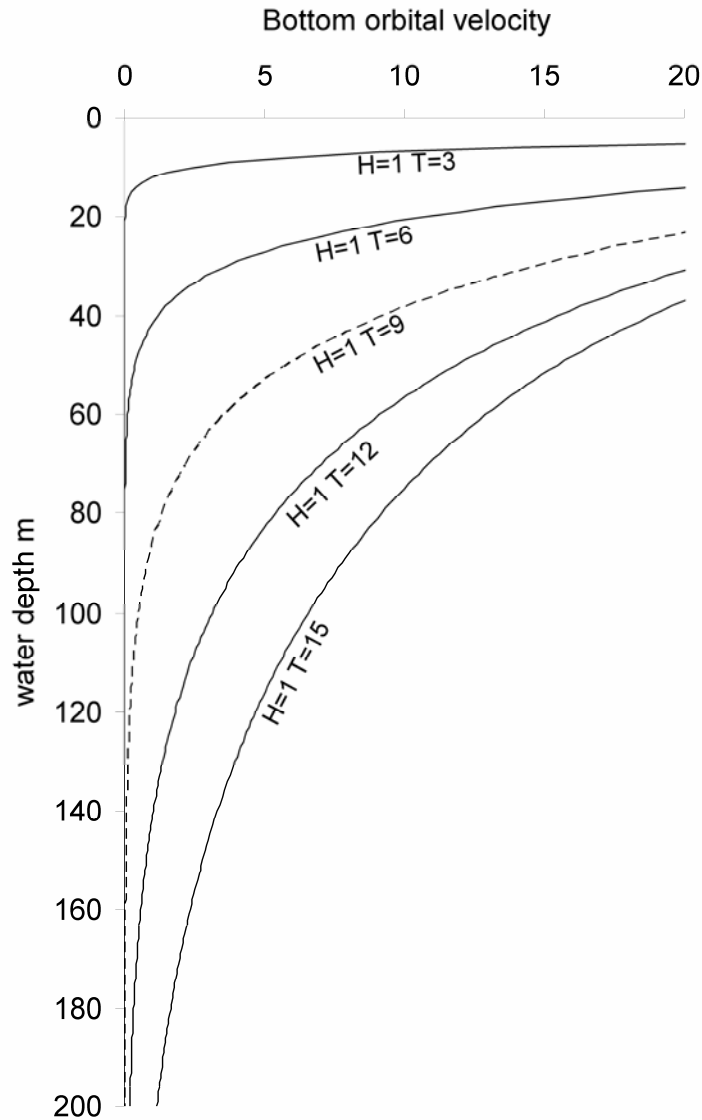


FIGURE 3 – Bottom orbital velocity calculated with equation (4) at different T and H conditions. The dotted line represents the energy condition used in the present work.

Using this formula from surface-wave parameters is not as immediate as it seems. Surface-wave parameters are normally considered as H , T and h (because they are depending each other). The calculation of k is more complicated. The wave number k represents the number of oscillations made by a given wave within its distance unit and it is proportional to the reciprocal of the wavelength (L). The procedure presented here to calculate L is the main procedure used in the Java applets linked above and published by Hunt (1979) (therefore called as "Hunt's Method"), then in the following years widely corrected and improved (Soulsby et al., 1987, Soulsby, 1997; Komar, 1998; Wiberg and Sherwood 2008).

The radian frequency is given by:

$$\omega = 2\pi/T \quad (5).$$

The two dimensionless variables, calculated from the dispersion equation

$$\omega^2 = gk \tanh(kh) \quad (6),$$

are expressed as $x = \omega^2 h/g$ and $y = kh$.

The Hunt's formula, used as follows, is an approximation for $y(x)$:

$y = (x^2 + Bx)^{1/2}$ where B is a constant calculated as:

$$B = 1/(1+x(0.66667+x(0.16084+x(0.02174+x(0.00654+x(0.00171+x(0.00039+x(0.00011))))))) \quad (7)$$

This is computationally fast because it avoids calculations of $\tanh(y)$ (6). The relative error in y is less than 10^{-5} for all x . The relative error in U_w is $<0.02\%$ for all x .

The calculation of the wave number is therefore given by:

$$k = y/h \quad (8),$$

following the wavelength as

$$L = 2\pi/k \quad (9).$$

To keep a particle in suspension and make it transportable, the water energy input must exceed the energy that pushes the particle to the bottom due to gravity. Such energy can be calculated as settling or sinking velocity. Some sedimentologists and paleontologists have already recognized the importance of settling velocity for the study of particle transport and distribution on slopes and ramps. In recent years, mathematical equations allowed the calculation of settling velocities without empirical measurements. Concerning LBF, calculated settling velocities as well as experimental data are already published. Their importance as a powerful tool in understanding the distribution of tests in shallow water environments has been already demonstrated (e.g., Beavington Penney

et al., 2005; Jorry et al., 2006; Yordanova and Hohenegger, 2007; Briguglio and Hohenegger, 2009). However, the quantitative equation between water motion and LBF distribution remains, so far, unknown.

Mathematically, for a given wave, every depth is characterized by one calculated orbital velocity and, at this water depth, only particles with settling velocities higher than the energy input can be deposited.

Concerning LBF, high diversity in test geometry and bauplan (reflected in the high number of taxa, then duplicated due to the generation's dimorphism) may lead to the same high diversity in hydrodynamic behaviours. At the species level, the intraspecific variability - within the same generation of LBF (e.g., agamonts) leads to a spectrum of settling velocities which may differ significantly from species to species (Yordanova and Hohenegger 2007, fig. 5). Such differences are reflected in the response of every taxon to hydrodynamics.

To occupy and flourish in a niche, a species must be adapted to the range of physical conditions in the environment and must be able to accumulate the trophic resources necessary to produce new generations at least as fast as predators, disease and physical factors reduce their numbers (Hallock et al., 1991). Concerning symbiont bearing LBF, morphology is the basic adaptive characteristic. Foraminifera have to provide enough light to the symbionts and to resist hydrodynamic inputs at the same time; it let them build very complicated but adaptive test morphologies and bauplans (Hohenegger, 2009). Below nutrient availability, the presence of competitors and other inconvenient environmental characteristics, the ecological optimum for LBF will occur at that water depth where light intensity satisfies the symbiont's demand and where the foraminiferal shell resist entrainment due to weight or attachment mechanisms.

Correlating water depth with test's settling velocity and orbital velocity (Fig. 4), transport will occur only below the calculated function (equation 4) and deposition will occur only above.

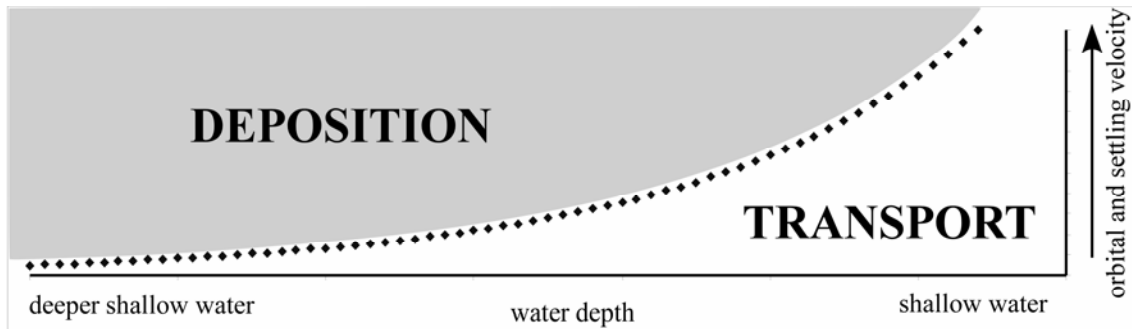


FIGURE 4 – Settling and/or orbital velocity versus water depth. The dotted line represents the orbital velocity function as related to the water depth. Depending on the orbital velocity function, particles with low settling velocity in shallow water would be transported, whereas particles with higher settling velocity in deeper water would be deposited.

If particle's settling velocity is lower than the orbital velocity, then this particle will be kept in suspension and, if a secondary force is present, will be transported. Consequently, the same particle will be unaffected in deeper water, where its settling velocity exceeds bottom velocity. Concerning a single LBF specimen, its settling velocity value indicates the water depth where under normal weather conditions the shell is not transportable anymore and where maximum light intensity is available for its symbionts. Without special fixing mechanisms as in nummulitids, such depth may represent the ecological optimum for that test shape.

Considering not a single individual but the complete morphological diversity within the same species (and within the same generation), deposition of tests starts occurring at the water depth where the bottom velocity function (at the given condition k , T , H) intersects the highest settling velocity value within all values calculated for the species.

At water depths where the bottom velocity function matches the minimum value of settling velocities within all specimens of the same species, the water energy cannot keep any of the particles (all the species' tests) in suspension. This second hydrodynamic boundary defines the water depth at which tests of that species with the slowest settling velocity remain unaffected; it may predict accumulation.

The definition of such transport and deposition areas is reliable only if particles (or tests) are present and available at every water depth. In such conditions, certain tests will be transported (i.e., from shallower areas) and certain others (i.e., in deeper or calmer areas) not. LBF live in restricted habitats determined by a set of environmental gradients, which may occur in the transport and/or in the deposition zone.

Therefore, transport occurs hydrodynamically only if specimens are in the transport zone (below the function in fig. 4): e.g., disk-like tests with low settling velocity in high-energy scenario. Besides the specific behaviour of foraminiferal tests in fluids, slope morphology represents another important factor influencing transport: the steeper the slope, the more intensive the depth transport of larger tests (Hohenegger and Yordanova, 2001b).

2. Material and methods

Specimens were collected from the slope west off Sesoko Jima, a small island west of Motobu-Peninsula, Okinawa, Japan. Two transects were chosen northwest off Sesoko Jima, one in the northern part of the slope and one in the southern part. Sampling was conducted during June and July 1996, and completed before the first typhoon occurrence. Thus, samples are composed of non-transported living foraminifers. Additional data about these two transects are reported in Hohenegger et al. (1999).

The distribution of living specimens along the transects is published in Hohenegger (2000), whereas the empty test distribution is reported in Yordanova and Hohenegger (2002). In the latter, the empty specimens were studied and sorted based on their preservation grade into optimally, well and poorly preserved tests.

The present study considers the distributions of living specimens and the distribution of optimally preserved empty tests. The distribution of the former represents the depth limits of the habitat and the distribution of the latter, optimally preserved, can be regarded as the distribution of members of the time-averaged biocoenosis. Their depth distribution mirrors displacement under differing weather conditions within a time interval of a few years (Yordanova and Hohenegger, 2002), which may actually reach kiloyears (Resig, 2004) including well-preserved tests. The former may have lived both under quite normal weather conditions and under sporadic high-energy water inputs (typhoons).

Several geometric and physic variables were measured (i.e., largest, intermediate and shortest diameter, equatorial surface, axial surface and density), and the list of equations published by Briguglio and Hohenegger (2009) was applied to calculate the theoretical hydrodynamic behaviour of nummulitids tests. Such mathematically obtained results

were compared with experimental results using a settling tube (Yordanova & Hohenegger, 2007) (Fig. 5).

Because the mathematical calculation of hydrodynamic parameters of a shell is always realizable (once the diameters, the surfaces and densities are measured), all collected specimens can be used for scientific purposes.

Four different formulas were used to predict particle settling velocity depending on particle shape.

The first formula calculated settling velocity, termed "settling velocity of an equivalent sphere" (*sensu* Le Roux, 1997a)

$$W_s = W_d / (\rho_f^2 / (\mu g (\rho_s - \rho_f)))^{1/3} \quad (10)$$

where W_d is the dimensionless sphere settling velocity (calculated as in Briguglio and Hohenegger, 2009), ρ_f is the density of the fluid (seawater), ρ_s is the density of the test, μ is the dynamic viscosity of the fluid (seawater) and g is the gravity constant. This parameter is a shape-independent value and can be correctly used for comparisons involving other foraminifera having the same volume.

The second formula calculates settling velocity by considering the shape entropy, thus reducing the former formula values significantly.

$$W_e = W_s [(H_r - 0.5833) / 0.4167] \quad (11)$$

The deviation from sphericity H_r was calculated with the equation proposed by Hofmann (1994), widely used for ellipsoidal grains (Le Roux, 1997a, 2005), then for nummulitids (Jorry et al., 2006; Briguglio and Hohenegger, 2009).

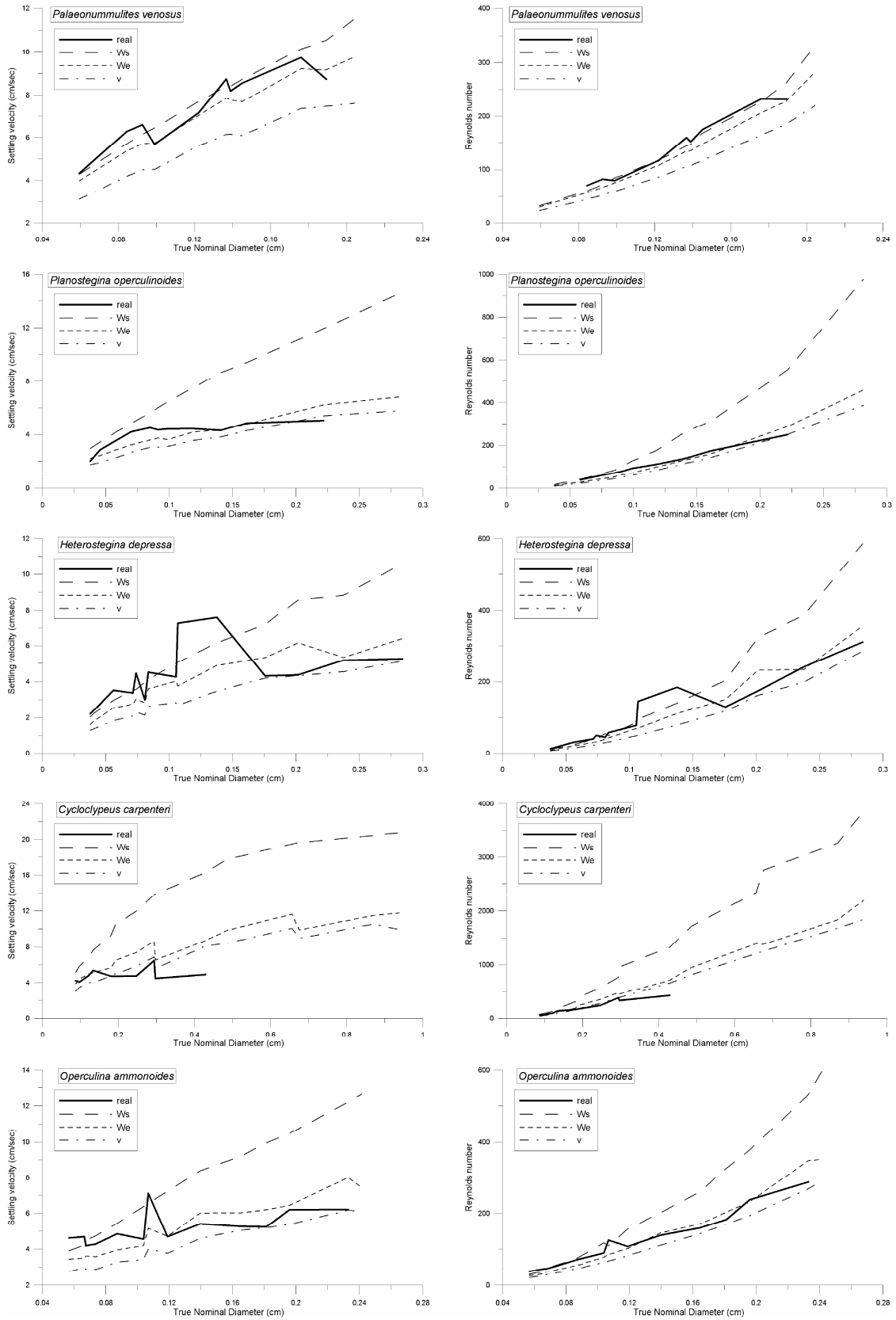


FIGURE 5 – Comparison between real (measured) and calculated settling velocities on the left and between real (measured) and calculated Reynolds numbers on the right. The True Nominal Diameter, proposed by Waddel (1939), on the x-axis calculated with the formula $TND = 2(3V/4\pi)^{1/3}$ where V represents the volume of the test. It allows linear comparisons of different tests sizes without taking into account shapes differences.

The shape entropy equation is based on the geometry of an ellipsoid and can be calculated with

$$H_r = [(p_l \ln p_l) + (p_i \ln p_i) + (p_s \ln p_s)] / 1.0986 \quad (12)$$

where p_l , p_i and p_s , are the proportions of the major (L), intermediate (I) and minor axes (S) of the ellipsoid

$$p_i = I / (L + I + S)$$

$$p_l = L / (L + I + S)$$

$$p_s = S / (L + I + S)$$

The third formula used was proposed by Allen (1984) for bivalve shells:

$$v^2 = 2gV(p_s - p_f) / C_d p_f A \quad (13)$$

where V is the volume, C_d is the drag coefficient and A is the area of the shell/test facing the water during sinking, which was calculated as reported in Briguglio and Hohenegger (2009).

The following formula was used to calculate the Reynolds number to quantify the particle's buoyancy

$$Re = p_f D_n v / \mu_f \quad (14)$$

where D_n is the True Nominal Diameter proposed by Le Roux (1997a) and v is the particle's settling velocity. The Reynolds number provides information on test buoyancy. It considers test settling velocity, drag coefficient and density, making it important to examine its correctness and to correlate it with the experimental values obtained in the laboratory.

For comparison with the daily and constant energy input at the sea bottom, the best-fitted settling velocity for every species was used. This comparison reveals how and how much the water motion (under normal fair weather conditions) may or may not influence test distribution. According to Hohenegger (personal observation, 1999), to get a good representation of the environment under fair weather conditions, the wave parameters in equation (4) could be: $T = 9$ s and $H = 1$ m.

The obtained function may be represented as an exponential function $y = a \exp^{bx}$ where x is depth, a is the velocity at the depth 0 m and b is very close to 0.

On settling velocity, the statistical limits $\bar{x} \pm 1.96s$ including 95% of all cases were calculated and were used to estimate the transport/deposition boundary as well as accumulation. These results are shown in figures 6 and 7.

The calculated BOV function was used as reference and, on this function, the distribution of living and optimally preserved specimen was reported (specimens number per 500g of sediment). The settling velocity range of every species is represented on the top of every graph with a double arrows line.

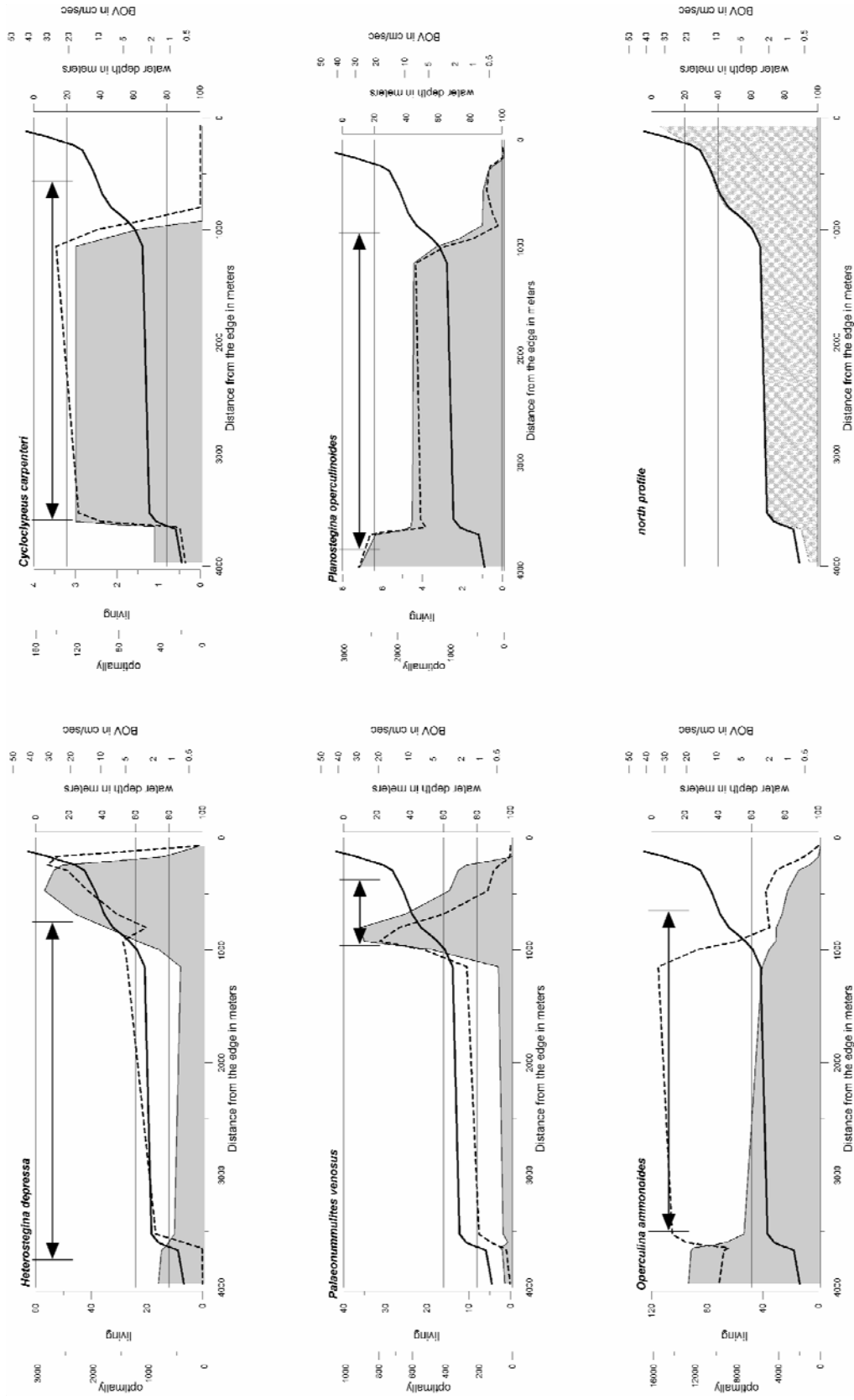


FIGURE 6 – Depth distribution of living foraminifera (dotted line) and optimally preserved tests (grey area) along the northern transect. The thick black line indicates the BOV profile varying accordingly to water depth. The depth range of the settling velocities is represented by the two arrows line at the top of every graph. The bottom right image shows the transect morphology (grey area) together with the BOV profile calculated at the given conditions.

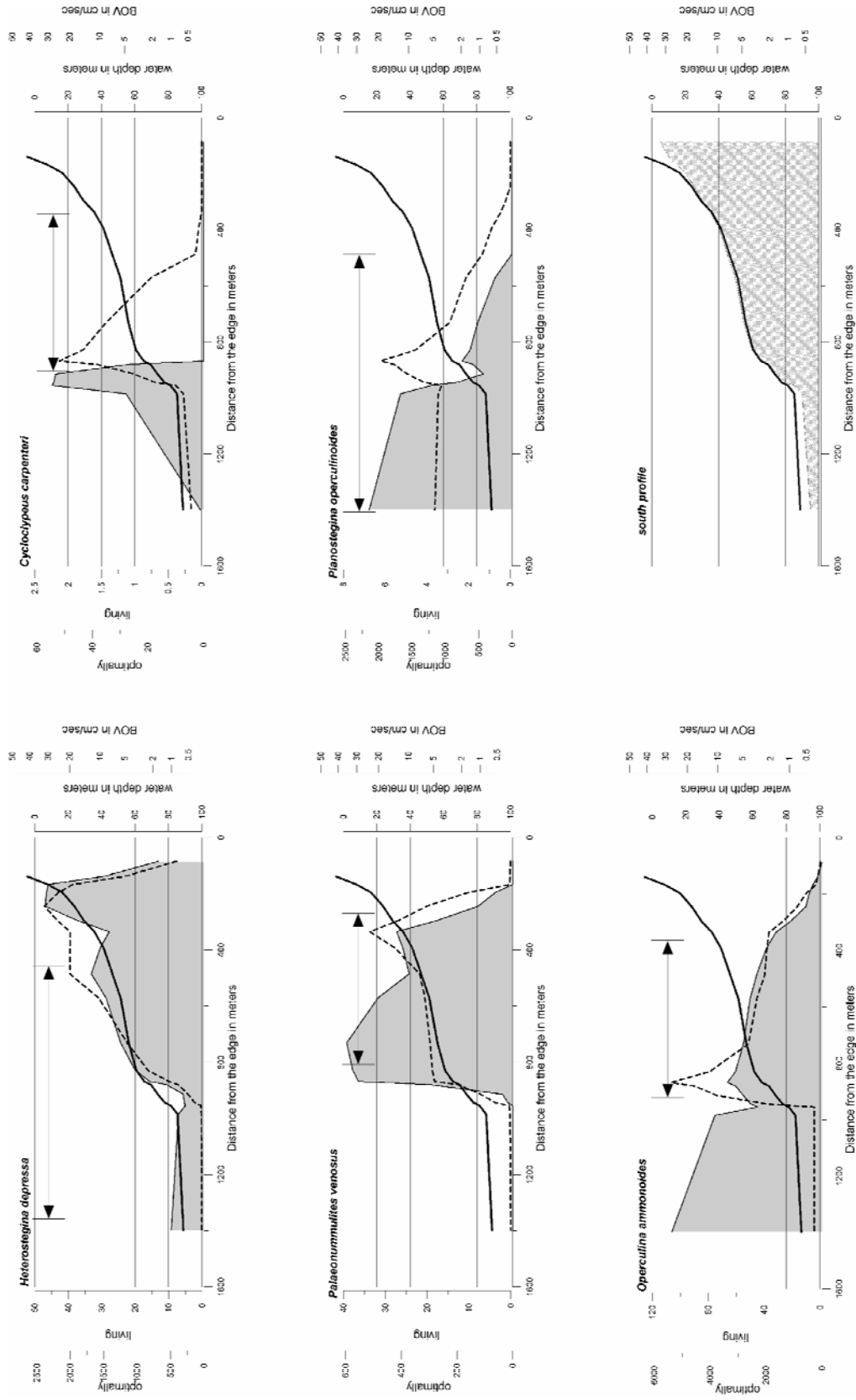


FIGURE 7 – Depth distribution of living foraminifera (dotted line) and optimally preserved tests (grey area) along the southern transect. The thick black line indicates the BOV profile varying accordingly to water depth. The depth range of the settling velocities is represented by the two arrows line at the top of every graph. The bottom right image shows the transect morphology (grey area) together with the BOV profile calculated at the given conditions.

3. Results

The hydrodynamic behaviour of nummulitids obtained by mathematical approach fits very well with the results obtained by experiments using a settling tube (Yordanova and Hohenegger, 2007). Up to the settling velocity and to the Reynolds numbers (Fig. 5), calculations are consistent with experimental results, both in smaller and in larger specimens. In figure 2, comparisons between the two methods are displaced. For every taxon, the three settling velocity equations 10, 11 and 13 were used to check which one fits the experimental data best.

In fact, depending on the specimen's shape entropy (equation 12), one of the three calculated settling velocities fits best. Considering the shape entropy parameter, the most accurate equation for calculating the settling velocity of specimens with $H_r > 0.95$ (i.e., well-rounded tests like *P. venosus*) is equation (10), which assumes the falling object is spherical. The most accurate settling velocity equation for specimens with $H_r < 0.85$ (i.e., disk-like test such as *C. carpenteri*) is equation (13), where the volume/half-surface ratio significantly reduces the sinking effect. For specimens with $0.85 < H_r < 0.95$ (i.e., plate-like tests or not rounded tests) the best mathematical calculation, which correlates well with the experimental data, is equation (11). Here, shape entropy becomes important strongly reducing the settling velocity of a sphere.

The combination of the energy scenario (i.e., the orbital velocity calculated with equation (4) with the hydrodynamic behaviour of every single test (i.e., the settling velocity as results of calculated size shape and density) provides the key to evaluate the depth transport distribution along the transect. As already stated, to permit transport, together with the necessary orbital velocity, a secondary force must be available: it is here the case due to the influence of tidal currents and downwelling by the Kuroshiy Current, which passes the location from the south (Hohenegger et al., 1999). It means that the sampling area can be considered as an indicative location to investigate and quantify hydrodynamics. The two transects, with different morphologies but with almost the same diversity in foraminifera may allow quantification on the influence of slope morphology on living foraminifera distribution and transport, deposition and accumulation of empty shells due to water dynamics.

The hydrodynamic equilibrium conditions allow estimating the water depth where a shell, with its hydrodynamic parameters, may be transported or deposited, i.e., the transport - deposition boundary. In figures 6 and 7 the representation of the transect morphology and the relative BOV are reported for the northern and the southern transects at the bottom right of every figure. Obviously, the BOV follows the profile morphology in both transects. In figures 6 and 7 the distribution of living and optimally preserved foraminiferal tests are displaced as dotted line and as grey area, respectively. The referring specimen numbers are reported on the y-axes on the left side of every graph. On the right side the y-axis for the BOV, which is distinguishable by a thick black line, is reported as well as the scale for water depth calculation; the transect profile is not reported because of its similarity with the BOV line. On the top of every schema, a double arrow is illustrated: it represents the distribution of settling velocities. Its depth boundaries embrace 95% of all individuals within a species according to normal distributions.

Concerning test morphologies, the distribution of living individuals matches the settling velocity vs. BOV equilibrium, i.e., the ecological optimum for every species is identified by the hydrodynamic behaviour of the tests. Concerning transportability of tests, living and optimally preserved tests distributions do not show significant transport evidences. Only in a few cases, settling velocity is lower than BOV: in such condition, tests are transported downslope until those depths, where water energy does not play any role for this specific test form.

In the following chapters the living and empty test distributions on the transects accordingly to its hydrodynamic behaviour are discussed for the investigated nummulitid species.

3.1 Hydrodynamic behaviour of the investigated taxa.

3.1.1 Palaeonummulites venosus (Fichtel and Moll)

It is restricted to sandy bottom in both transects and lives in the uppermost sand layer. Within the nummulitidae, *P. venosus* is the species with highest settling velocities. It allows individuals living in shallower water without being transported by water motion. The tests can easily being entrained together with the surrounding sand grains and put in

suspension; the rounded test, characterized by a high settling velocity, make the foraminifer sink faster than the smaller carbonate grains and in case of burial, its peculiar lenticular shape is favourable for relatively quickly climbing up through the sediment again (Hohenegger et al., 1999).

The hydrodynamic equilibrium between settling velocity and BOV is located at water depths between 40 and 50 meters and the 95 % distribution's tails are located at 33 and 59 meters water depth. The same value of BOV for such water depth is revealed by the settling velocity of the measured tests. It means that the tests built by *P. venosus* at the water depth where they live may contrast water motion without being transported out of their habitat; in fact, the optimally preserved tests curve follows consistently the living specimens one. Because of the steeper morphology in the shallower part of the northern transect respect to the southern one, the depth distribution of the settling velocities (calculated for the tests belonging to this species between 35 and 60 meters water depth) covers only 100 meters in length; on the southern transect the same depths range is more than 400 meters length. It results that, on the southern transect, the distribution of the tests (both living and optimally preserved) covers a broader surface accordingly to the calculated depth.

A mere morphological analysis of the transect would expect deposition and accumulation in the deepest part of the profile just below the distribution of living organisms. It is not the case: even with a very steep slope, water energy is not able to keep the tests in suspension and move them downslope. In the fossil record, the estimation of paleodepth by settling velocity calculation of such high entropy shells would have been correct.

3.1.2 *Cycloclypeus carpenteri* Brady

It lives on sandy substrates in the medium euphotic zone. In both transects, *C. carpenteri* lives on the flat part of the slope and close to its steeper part. There, the ecological optimum, visible by the highest specimens number area, is displaced at the water depth between 45 and 68 meters. This depth range is defined also by the range of the settling velocity.

In the northern transect such water depth is characterized by a vary flat profile, on which *C. carpenteri* is well distributed and represented and, because at that water depth the equilibrium between settling velocity and BOV is reached, shells are not

transported. On the southern transect, the water depths at which *C. carpenteri* is abundant are perfectly comparable to the northern transect but the topography becomes important. At this water depth, the profile is steeper and the optimum for *C. carpenteri* is reached in a very restricted area. The settling velocity BOV comparison also considers this depth as the equilibrium depth. However, a very steep slope starts exactly at this water depth; all specimens are transported and accumulated downslope. This is possible by any small variation of the energy input; a higher wave period or a longer wavelength would be able to keep tests in suspension and move them downslope easily due to gravity.

3.1.3 *Operculina ammonoides* (Gronovius) including *O. complanata* (Defrance)

They frequently inhabits fine-grained bottoms of lagoons behind patch reefs; it is abundant on sand, and has similar frequencies on soft bottoms and firm substrates along the slope of the northern transect (Hohenegger et al., 1999). This species avoids the reef edge and is rare in the uppermost 10 m of the slope. It prefers lower-energy environments with medium light intensities. Settlement in shallower waters is restricted to firm substrates with well-structured surfaces, where the individuals resist hydrodynamic forces by hiding within small grooves and holes (Hohenegger et al., 1999). Abundance is higher on sandy versus hard substrates in both transects.

In both transects, hydrodynamic is important. In fact, the distribution of living tests reflects the depth calculated by settling velocity analysis. Not only the 95% limits of settling velocities coincide with the test distributions, but also accumulation is visible after the deeper limit, where any test at the given environmental conditions is further transportable.

3.1.4 *Planostegina operculinoides* Hofker

It lives on sandy bottoms in the deepest parts of the euphotic zone (Hohenegger and Yordanova, 2001) but it is present on the transects from 20 meters down to more than 100 m. The distributions of living individuals and optimally preserved tests in both transects reflects non-transport. Transportability is strongly reduced because *P. operculinoides* has a very broad spectrum of settling velocities in case of very different shape entropies. Such characteristic is advantage permitting the taxon living at different environment with different energetic conditions. The ecological optimum seems to be

located for *P. operculinoides* in much deeper condition, below 70 meters water depth along the northern profile and at about 65 meter for the southern profile. The steeper morphology of the southern transect shows the distribution of *P. operculinoides* with much more details. Even if the species can live in deeper environments, it seems that its maximum is located around 65 meter water depth. After that depth, tests are accumulated without any transport evidence.

3.1.5 *Heterostegina depressa* d'Orbigny

It hides itself in small holes within carbonate rocks or between thalli of macroalgae. According to Yamano et al. (2002), *H. depressa* prefers firm substrates. The size, form and completely smooth surface in shallow-living individuals are very similar to *P. venosus* (Hohenegger and Yordanova, 2001). This species is rare near the reef edge, but its abundance suddenly increases at 10 m. Because of its hiding peculiarity, *H. depressa* may live in very shallow environment without being affected by water motion, which reduces drastically in holes of rocks and in vegetated sea bottom. That is why high abundance of individuals of both living individuals and optimally preserved tests occur. If hidden in holes or between algae, water motion can transport neither living nor death individuals. The settling velocity analysis would still give quite good results in the fossil record concerning depth distribution of optimally preserved tests.

4 Discussion

The comparison between wave orbital velocity and settling velocity for a particle is not new in coastal engineering and marine geology, but it is for palaeontologists. The hydrodynamic equilibrium concept and the study of the transportability to approach the shell's functional morphology are also new in palaeontology. Such approach is proposed here within a very few species of LBF, but it can be expanded to the different families in both recent and fossil record as the physic laws acting on the hydrodynamic distributions can be considered the same as now as in the past.

The measurements of density, shape and size and the succeeding calculations give consistent results on all the analyzed specimens and help to interpret accurately the hydrodynamically induced depth distribution of tests. Even if shape, size and density

can be considered as the main parameters to approach hydrodynamics, they still need some attention by scientists.

Concerning LBF, the density issue remains open. It can be measured in recent specimens, but no fixed values are known for fossil forms. In recent nummulitids, the density ranges between 1.1 and 1.9 g/cm³ (Yordanova and Hohenegger, 2007) but values are most concentrated, for adult specimens, at 1.4 g/cm³. Other approximations for density in fossil specimens yield slightly higher values. According to Jorry et al. (2006), the apparent density value of fossil *Nummulites* ranges from 1.4 to 2.61 g/cm³, but for water-filled specimens the range drops down to 1.7 and 1.9 g/cm³; an average value of 1.8 g/cm³ was used for predicting hydrodynamics of the fossil *N. globulus* (Briguglio and Hohenegger, 2009). Using X-ray computed tomography, a value of 1.75 g/cm³ was calculated for *P. venosus* and of 1.46 g/cm³ for *O. ammonoides*. This does not consider surface microporosity, which decreases values by 10 - 20 % to 1.2 - 1.4 g/cm³ (Briguglio et al., in press). However, although a fixed value (or a species-specific range including growth stages) is not yet available for fossil species, the used data are consistent with the calculated hydrodynamic scenario.

Size and shape, beside density, play a fundamental role in the overall calculation and drive the sequence of equations. For LBF transportability, the main deviation from classical particle sorting involves shape. Particle shape is an even more complex subject than density or size; during the last decades different shapes indices have been proposed. Flatness index (Wentworth, 1922), oblate–prolate index (Dobkins and Folk, 1970), disk-rod index and rod index (Illenberger, 1991), several measures of sphericity (Wadell, 1932; Rubey, 1933; Krumbein, 1941; McNown and Malaika, 1950; Aschenbrenner, 1956; Janke, 1966; Hofmann, 1994) are only the most cited and used indices within a much longer list (Le Roux, 2005). Some of these shape indices help to determine the settling velocity of non-spherical particles (Komar and Reimers, 1978; Baba and Komar, 1981a,b), which are very useful for nummulitids tests. Le Roux (1996, 1997b) demonstrated that the Hofmann (1994) shape entropy H_r gives the best results for ellipsoidal grains, and thus can be considered as well suited for nummulitids (Briguglio & Hohenegger, 2009).

The importance of modelling shape to contrast water motion has often been taken into account in the story of nummulitids hydrodynamics and of functional test morphology; but a quantification of how the shape must vary or how intense water input must be to

transport a test to a certain water depth, is so far unknown. Some methods to evaluate distribution of tests along a transect or a geologic profile consider the calculation of the diameter/thickness ratio as the main parameter for test shape hydrodynamics. But the calculation of nummulitid's hydrodynamics is much more complicated and can give much more insights within a single species. The calculation of the diameter/thickness ratio is only an approximation and does not take into account density (which may significantly vary between species and changes during growth) and size. The mathematical procedure here used (extensively published in Briguglio & Hohenegger, 2009) is very simple and can be reproduced without using advanced mathematics programs.

The shape effects determined here finally solve the problems inherent in the subjective and not useful morphological definitions such as "disk-like", "plate-like", "lens-shaped", "egg-shaped", "globular" and "elongate" test form. Shape entropy and its calculation is a powerful parameter to differentiate test forms and to compare forms that are apparently different, but which may have similar hydrodynamic behaviour. In fact, it is very common in both recent and fossil environments to find, within the same assemblage, very different test shapes possessing similar shape entropy. The shape entropy ranges outlined here lead to different settling velocity calculations and thus to different depth ranges where the test is not transportable any more. This methodology leads to more detailed and exact interpretations of depositional environments even in the case of monospecific associations, especially the nummulite bank concept: such banks are mainly composed of almost monospecific assemblages with a relative high abundance of B-forms (Papazzoni, 2008). It remains unclear whether such facies represent biological accumulation and thus show nummulitids in living positions, or whether they represent the result of sorting and displacement due to turbulence (Reynolds number) and comparable settling velocities.

The hydrodynamic analysis demonstrates how to approach such problems by an energetic point of view without considering side effects of functional reaction, which must be taken into account to avoid misinterpretations. The habitat of high shape entropy tests (e.g., *P. venosus*) is characteristic for a high-energy scenario, but, as in the study area presented here, such environment also contains tests with low shape entropy. Such tests have a very low settling velocity and can be transported very easily by water motion, thus should not belong to such high energy scenario; in fact, such species, have

developed transport resistance methods as hiding (*P. operculinoides* or *H. depressa*) or anchoring (*Amphistegina bicirculata* Larsen). For palaeoenvironmental reconstructions, high shape entropy tests will remain as potential fossils in the same habitat because of their settling velocity, thus useful for paleodepth calculations. Use of settling velocity for low shape entropy tests in high energy scenario can lead to misinterpretations but are most important to support ecological adaptations (e.g., anchoring or hiding strategies, or infaunal lifestyle). Such differences in shape may help to differentiate autochthonous from allochthonous sediments solely by analysing the shape entropy of tests. The importance of shape and its correlation with water depth may be explained by considering shell functionality in hydrodynamic environments. On the one hand, larger foraminifera, because of their symbiont-bearing character, have to build tests with a high surface/volume ratio to get enough light to obtain positive net rate in photosynthesis; on the other hand, the resulting shell must somehow have a hydrodynamically convenient shape or assuming strategies avoiding transport (i.e., anchoring, hiding, density increase). Such coexistence of strong light dependence and bauplan intelligence causes foraminifera to live within a strictly delimited water depth range characterized by BOV always lower than the tests settling velocity. The investigated taxa fit to this rule. Additionally, LBF ecological optimum depth, defined by the largest number of individuals and always located within the settling velocities range, occupies for every species the shallowest depth just below the boundary with the transport area. It is convenient for a cell to live where not only transport is avoided but also where the maximum light penetration is available, i.e., at the shallowest depth just below the transport deposition boundary. If the species is not hiding or has not developed any anchoring system, the evaluation of water depth by comparison between settling velocity and BOV is precise even if the equations proposed do not consider transect morphology. Only the widths of settling velocity range depend on morphology, the calculated water depth where the transport/deposition boundary occurs does not vary.

The deeper boundary, obtained by the lowest settling velocity of all the tests belonging to the same species, explains the water depth where the wave-induced BOV does not play any role in suspending tests anymore. Suspension, at the given energy condition, is unreliable but the lower light penetration does not allow some species to live at such

water depths. The deep tail of the species-specific distribution curve must depend on the endosymbiont's need for light and not on the hydrodynamic behaviour of the tests.

Consequently, the lower boundary should be recognized by the lower limit of a positive net rate in photosynthesis for the symbionts (Lee et al. 1980, Hohenegger 2004) and by elevated test structures concentrating light (Hottinger, 2006) thus having few relation with hydrodynamics. Therefore, the lower hydrodynamic boundary should be considered as the specific water depth where transport becomes unimportant, but also can be considered as the water depth, where accumulation of all tests starts expecting a high number of individuals without any evidence of transport. Considering the studied taxa, transport below the deep hydrodynamic boundary occurs in restricted cases depending on very steep morphologies.

All species studied here are adapted to species-specific water depths where test geometries are able to resist water motion; the cells can live and reach reproduction without being transported out of their habitat if the energetic conditions are typical for fair weather as we have supposed and calculated. By varying the weather conditions and increasing the time span of exposition of test to water movement, the distributions of empty test of not optimal preservation are, for every species, moved significantly downslope (Yordanova & Hohenegger, 2002).

5. Conclusion

The hydrodynamic approach we used to estimate the transport deposition boundary and to evaluate shell functionality gave important results and is worthy for palaeoenvironmental and palaeohydrodynamic reconstructions. The requested measurements are easy to obtain and already known in the literature, the proposed calculation can be carried out by any calculator and even if equations must be considered only as a mere approximation of the real hydrodynamic behaviour of the shells, it is evident how much consistent they are with the values obtained experimentally.

Up to the Reynolds number, the equation sequence is rigorous and mirrors the experimental results and its diversity of parameters, given by the study of shape, density and size, allowing the use in a very broad spectrum of applied tasks. Even if such calculation requires more data than the mere diameter/thickness ratio, it allows much

more detailed palaeoenvironmental reconstructions and hypotheses on the energetic scenario in fossil shallow water environments.

Comparing the depth distributions of living individuals and empty tests helps to interpret the transport, deposition, and reworking of sediments. Different transport intensities between species along the same transect reflect varied test buoyancies caused by differences in shape and settling velocity. In the presented study, shell functionality is valued by its resistance to water motion and thus by its capability not to be transported out of its habitat, at least during life time. Once the energetic input by water motion at the seafloor has been defined and the settling velocity has been calculated for every test, the result we obtained is that tests are characterized by settling velocities comparable to the orbital velocity at the water depth where the ecological optimum occurs. The settling velocity of a foraminiferal shell can, consequently, be considered as the main hydrodynamic parameters, because it depends on shape, size and density. It may also be considered as the key parameter to predict water depth where the same shell can live resisting water input and this is very usable in the fossil record. For the studied taxa, it seems that the test geometry and the relative entropy are functionally perfect and let the foraminifer survive within its ecological optimum without being transported away at least during fair weather condition as supported by the depth distribution of optimally preserved tests. Such evidence underlines the potentiality of the use of bottom orbital velocity for paleontological analyses to the much broader spectrum of the fossil nummulitids which have been subdivided in many hundreds of species and all of them possess a specific geometry which could have provided different entropy and then settling velocity and thus different water depths.

However, this study clearly shows a quantitative correlation between shell morphology, ecological optimum, water depth and wave induced bottom orbital velocity. Such correlations may be most useful to characterize monospecific assemblages or highly diverse associations, broadly deposited during Palaeocene and Eocene periods.

In addition with sedimentological observations, the hydrodynamic approach we used can be applied to reconstruct the paleoenvironment of LBF and to define their shallow-water energetic scenario. This makes transport calculation mandatory both in paleoenvironmental reconstructions and in energetic scenario characterisations.

6. Acknowledgement

7. References

- Adabi, M.H., Zohdi, A., Ghabeishavi, A., and Amiri-Bakhtiyar, H., 2008. Applications of nummulitids and other larger benthic foraminifera in depositional environment and sequence stratigraphy: an example from the Eocene deposits in Zagros Basin, SW Iran. *Facies*. 54, 499–512.
- Allen, J.R.L., 1984. Experiments on the settling, overturning and entrainment of bivalve shells and related models. *Sedimentol.* 31, 227–250.
- Aschenbrenner, B.C., 1956. A new method of expressing particle sphericity. *J. Sediment. Petr.* 26, 15–31.
- Baba, J., and Komar, P.D., 1981a. Settling velocities of irregular grains at low Reynolds numbers. *J. Sediment. Petr.* 51, 121–128.
- Baba, J., and Komar, P.D., 1981b. Measurements and analysis of settling velocities of natural sand grains. *J. Sediment. Petr.* 51, 631–640.
- Beavington-Penney, S.J., 2004. Analysis of the effects of abrasion on the test of *Palaeonummulites venosus*: implications for the origin of Nummulithoclastic sediments. *Palaios*. 19, 143–155.
- Beavington-Penney, S.J., Wright, V. P. and Racey, A., 2005. Sediment production and dispersal on foraminifera-dominated early Tertiary ramps: the Eocene El Garia Formation, Tunisia. *Sedimentol.* 52, 537–569.
- Briguglio, A., and Hohenegger, J., 2009. Nummulitids hydrodynamics: an example using *Nummulites globulus* Leymerie, 1846. *Boll. Soc. Paleont. It.* 48, 105–111.
- Briguglio, A., Metscher, B., Hohenegger, J., (in press). Growth rate biometric quantification by x-ray microtomography on larger benthic foraminifera: three-dimensional measurements push nummulitids into the fourth dimension. *Turk. J. Earth Science*.
- Cookman, J.L., and Flemings, P.B., 2001. STORMSED1.0: hydrodynamics and sediment transport in a 2-D, steady-state, wind- and wave-driven coastal circulation model. *Computers & Geosciences*. 27, 647–674.
- Dobkins, J.E., and Folk, R.L., 1970, Shape development on Taiti-Nui. *J. Sediment. Petr.* 40, 1167–1203.

- Hallock, P., 1979. Trends in test shape in large, symbiont-bearing foraminifera: J. Foraminiferal Res. 9, 61-69.
- Hallock, P., Röttger, R., and Wetmore, K., 1991. Hypotheses on form and function in foraminifera, *in*: Lee, J.J. and Anderson, O.,R., eds., Biology of Foraminifera, Academic Press, 41-72.
- Haynes, J., 1965. Symbiosis, wall structure and habitat in Foraminifera. Contr. Cushman Found. Foraminiferal Res. 16, 40-43.
- Hofmann, H.J., 1994. Grain-shape indices and isometric graphs. J. Sediment. Res. 64, 916- 920.
- Hohenegger, J., 1996. Remarks on the distribution of larger Foraminifera (Protozoa) from Belau (Western Carolines). Reprinted From Occasional Pap. Kagoshima Univ. Res. Cent. S. Pac.30, 85- 90.
- Hohenegger, J., 2000. Coenoclines of larger foraminifera. Micropaleontol. 46, 127-151.
- Hohenegger, J., 2004. Depth coenoclines and environmental considerations of western pacific larger foraminifera. J. Foraminiferal Res. 34, 9–33.
- Hohenegger, J., 2005. Estimation of environmental paleogradient values based on presence/absence data: a case study using benthic Foraminifera for paleodepth estimation. Palaeo3. 217, 115– 130.
- Hohenegger, J., 2006. The importance of symbiont-bearing benthic foraminifera for West Pacific carbonate beach environments. Mar. Micropaleontol. 61, 4–39.
- Hohenegger, J., 2009. Functional shell geometry of symbiont-bearing benthic Foraminifera. Galaxea, J. Coral Reef Stud. 11, 1-9.
- Hohenegger, J., Yordanova, E.K., Nakano, Y., and Tatzreiter, F., 1999. Habitats of larger foraminifera on the upper reef slope of Sesoko Island, Okinawa, Japan: Mar. Micropaleont. 36, 109–168.
- Hohenegger, J., and Yordanova, E.K., 2001. Displacement of Larger Foraminifera at the Western Slope of Motobu Peninsula (Okinawa, Japan). Palaios. 16, 53–72.
- Hottinger, L., 2006. The depth-depending ornamentation of some lamellar-perforate foraminifera. Symbiosis. 42, 141-151.
- Hunt, J. N., 1979, Direct solution of wave dispersion equation. J. Waterways, Ports, Coast. Ocean Division, ASCE. 105, 457-459.
- Illenberger, W.K., 1991. Pebble shape (and size!). J. Sediment. Petr. 61, 756– 767.

- Janke, N.C., 1966. Effect of shape upon settling velocity of regular convex geometric particles. *J. Sediment. Petr.* 36, 370–376.
- Jorry, S.J., Hasler, C.A., and Davaud, E., 2006. Hydrodynamic behaviour of *Nummulites*: implication for depositional models. *Facies*. 52, 221-235.
- Komar, P.D., 1998. Wave erosion of a massive artificial coastal landslide: *Earth Surf. Processes and Landforms*. 23, 415-428.
- Komar, P.D., and Reimers, C.E., 1978, Grain shape effects on settling rates. *J. Geology*. 86, 193–209.
- Krumbein, W.C., 1941. Measurement and geological significance of shape and roundness of sedimentary particles. *J. Sediment. Petr.* 11, 64– 72.
- Le Roux, J.P., 1996. Settling velocity of ellipsoidal grains as related to shape entropy. *Sediment. Geology*. 101, 15– 20.
- Le Roux, J.P., 1997a. An Excel program for computing the dynamic properties of particles in newtonian fluids. *Computers & Geosciences*. 23, 671-675.
- Le Roux, J.P., 1997b. Comparison of sphericity indices as related to the hydraulic equivalence of settling grains. *J. Sediment. Res.* 67, 527– 530.
- Le Roux, J.P., 2005. Grains in motion: A review. *Sediment. Geology*. 178, 285–313.
- Lee, J.J., McEnery, M.E., Garrison, J.R., 1980. Experimental studies of larger foraminifera and their symbionts from the Gulf of Elat on the Red Sea. *J. Foraminiferal Res.* 10, 31-47.
- Li, M.Z, and Amos, C.L., 2001. SEDTRANS96, the upgraded and better calibrated sediment-transport model for continental shelves: *Computers & Geosciences*. 27, 619-645.
- McNown, J.S., and Malaika, J., 1950. Effect of particle shape on settling velocity at low Reynolds numbers. *American Geophys. Union Trans.* 31, 74– 82.
- Papazzoni, C.A., 2008. Preliminary palaeontological observations on some examples of “nummulite banks”: sedimentary or biological origin?. *Rend. online Soc. Geol. It.*, 2, note brevi, 135-138.
- Pecheux, M.J.F., 1995. Ecomorphology of a recent large foraminifer, *Operculina ammonoides*. *Geobios*. 28, 529-566.
- Rasser, M.W., Scheibner, C., and Mutti, M., 2005. A paleoenvironmental standard section for Early Ilerdian tropical carbonate factories (Corbieres, France; Pyrenees, Spain): *Facies*. 51, 217–232.

- Renema, W., 2002. Larger foraminifera as marine environmental indicators. *Scr. Geologica*, 124, 1-260.
- Resig, J.M., 2004. Age and preservation of *Amphistegina* (foraminifera) in Hawaiian beach sand: implications for sand turnover rate and resource renewal. *Mar. Micropaleont.* 50, 225-236.
- Röttger, R., and Hallock, P., 1982. Shape trends in *Heterostegina depressa* (Protozoa, Foraminiferida). *J. Foraminiferal Res.* 12, 197-204.
- Rubey, W., 1933. Settling velocities of gravel, sand and silt particles. *American J. Science.* 25, 325– 338.
- Schutten, J., Dainty, J., Davy, A.J., 2004. Wave-induced Hydraulic Forces on Submerged Aquatic Plants in Shallow Lakes, *Annals of Botany.* 93, 333-341.
- Serra-Kiel, J., and Reguant, S., 1984. Paleoecological conditions and morphological variation in monospecific banks of *Nummulites*: an example, *in* Oertli, H.J., ed., *Benthos '83, 2nd Internat. Symp. Benthic Foraminifera*, Pau 1983, 557-563.
- Soulsby, R.L., 1987. Calculating bottom orbital velocity beneath waves: *Coast. Eng.* 11, 371-80.
- Soulsby, R., 1997. *Dynamic of marine sands.* Thomas Telford, London.
- Wadell, H., 1932. Volume, shape, and roundness of rock particles. *J. Geology.* 40, 443–451.
- Wentworth, C.K., 1922. The shapes of beach pebbles: U.S. Geological Survey, Professional Paper.131-C, 75- 83.
- Wiberg, P.L., and Sherwood, C.R., 2008. Calculating wave-generated bottom orbital velocities from surface-wave parameters. *Computers & Geosciences.* 34, 1243–1262.
- Yamano, H., Kayanne, H., Matsuda, F., and Tsuji, Y., 2002. Lagoonal facies, ages, and sedimentation in three atolls in the Pacific. *Mar. Geology.* 185, 233-247.
- Yordanova, E.K., and Hohenegger, J., 2002. Taphonomy of larger foraminifera: relationships between living individuals and empty tests on flat reef slopes (Sesoko Island, Japan). *Facies.* 46, 169–204.

Yordanova, E.K., and Hohenegger, J., 2007. Studies on settling, traction and entrainment of larger benthic foraminiferal tests: implication for accumulation in shallow marine sediments. *Sedimentology*. 54, 1273-1306.

Chapter 4

To be submitted.

*Si tibi forte anumum tali ratione tenere
versibus in nostris possem, dum perspicis omnem
naturam rerum, qua constet compta figura.*

Titus Lucretius Carus: *De rerum natura*, I, 948-950.

NUMMULITIDS HYDRODYNAMICS:
BRIEF REVIEW AND APPLICATIONS

ABSTRACT

The main physical variables influencing the hydrodynamic behavior of nummulitid tests are size, density and shape. Transport and sorting thus vary among nummulitid species and life stages because of different test buoyancies. A mathematical calculation to get the settling velocity of every test was used on well-preserved specimens collected on a profile in the Early Eocene sediments of the Tremp basin in Spain. On consolidated material, several thin sections were studied and the obtained results coming from the microfacies analysis were used to crosscheck information gotten from the settling velocity dataset. This work demonstrates the potential and the importance of the settling velocity to describe the hydrodynamic behavior of a particle in aquatic realms. Its study may explain transport, deposition and accumulation processes based on the comparison among different genera normally of common occurrence within the same sample as the case of nummulitids.

The calculations we ran, gave information on the palaeobiology of foraminifera, on the habitat they might have lived, and on adaptive shell morphology strategies, according to species-specific and assemblage-specific hydrodynamic parameters they possessed.

The good quality of results, based on the mathematic calculation of hydrodynamic parameters compared with experimental analyses, allows shallow-water zonation reconstruction based on transportability boundaries and functional shell morphologies coenoclines based on species-specific hydrodynamic behavior.

INTRODUCTION

Larger benthic foraminifera (LBF) living in shallow water environments formed sedimentary beds of considerable thickness and lateral extent at different geological time, especially in the late Palaeozoic (Fusulinids) and Palaeogene (Nummulitids) (Wilson, 1975; Aigner, 1985). Sequences of layers, banks or build-ups consisting of almost monospecific accumulation but counting a large number of specimens can be found in many localities around the world (Buxton & Pedley, 1989; Beavington-Penney et al., 2005)

Palaeogene nummulitid limestones, as important hydrocarbon reservoirs (Decrouez & Lanterno, 1979; Racey, 2001), are exploration targets in the Middle East (Beavington-Penney et al., 2005). Therefore, the palaeoenvironment of *Nummulites* has been debated over the last 50 years because modern analogues of such enormous fossil accumulations do not exist.

Because of these difficulties, very few information are available to palaeontologist to provide palaeoenvironmental reconstructions and to provide insights on the palaeobiology of such organisms. The reaction of larger benthic foraminifera to water depth is considered as the major variable that influences the distribution of tests (Hohenegger, 2000) on a slope. Temperature, light, hydrodynamics, substrate and trophic resources are water depth dependent factors and therefore they must be taken into account to approach LBF distribution (Hohenegger 2004). Furthermore, all these primary factors depend on the geographic latitude and on the topography of shore (including the hinterland) and of the sea floor.

Additionally to such physical laws affecting marine environments, chemistry also plays an important rule; in fact, due to the various taphonomic processes acting extremely in shallow water environments (Martin and Liddell, 1991), the preservation of LBF tests within their habitat is not common. While transport, sorting, fragmentation and abrasion demonstrate the influence of hydrodynamics, the effects of corrosion, dissolution, cementation, neomorphism and recrystallization reflect the influence of pore water chemistry and porosity of the sediments, where the tests are embedded (Fluegel, 2004). Beside these problems, primary environmental factors can be estimated by actualistic approaches. First, modern LBF are restricted to warm water, where they cannot fall for longer time (e.g., a few weeks) below a threshold value of 14°C. Therefore, they are

restricted to the tropic and warm temperate ocean, where the base of the thermocline determines their depth limit (Hollaus & Hottinger, 1997; Langer & Hottinger, 2000; Hohenegger, 2004).

It is well known and demonstrated that modern LBF's react to decreasing light intensity by test flattening optimizing the surface/volume ratio (Larsen & Drooger, 1977; Hallock, 1979; Renema, 2005) or by thinning of the walls (Hallock and Hansen, 1979). This strong dependence on light intensity has been recently challenged (Nobes et al., 2008), explaining the presence of large and flat LBF with a high surface/volume ratio in very shallow, quiet water environments (e.g. *Planostegina giganteiformis* in Middle Miocene shallow water limestones between coral patch reefs; Gross et al., 2008).

Substrate is important to resist hydrodynamics (Hohenegger, 2004): many LBF living in shallowest regions anchor themselves to hard substrates like rocks thanks to their structured surfaces or spines or they hide themselves below the sediment particles. Nevertheless, high-energy events as tropical cyclones can remove living LBF transporting them into inconvenient regions, where they can survive for a few days but not reproduce (Hohenegger et al., 1999). However, because of the low density of foraminifera shells and depending of their external morphology, smooth currents or wave induced bottom orbital velocity may keep such tests in suspension and transport them in quieter region (Hallock, 1979; Jorry et al., 2006; Yordanova & Hohenegger, 2007; Briguglio and Hohenegger, 2009; Briguglio & Hohenegger, 2010).

Therefore, the main task for a foraminifer cell, building its test within such energetic scenario, seems to meet two requirements: optimize light receipt and resistance to hydrodynamics at least until reproduction. Adapted strategies for optimizing light receipt are visible as variations of the wall composition (e.g., glassy versus non-transparent walls) and as differences of test geometry (e.g., wall thickness and surface/volume ratio through test flattening). Resistance against hydrodynamics can be optimized by the development of spines for anchoring in sandy or rocky substrates or by special fixing mechanisms of flat tests on smooth surfaces (e.g., soritids) or by building hydrodynamic convenient test shapes able to contrast, with their size, form and density, marine energetic inputs.

As LBF are restricted within the euphotic zone, tests are always exposed to hydrodynamics, which can be stronger or weaker depending on the source of the energy input and on the water depth. After death or reproduction, anchoring systems decay

and tests are at the mercy of water motion; on the contrary, hydrodynamics convenient shapes will continue contrasting water motion within certain energetic limits. In the fossil record, potentially, every test might have been transported out of its habitat. Because of water motion, always inferring depth distribution of LBF tests both during their life time (*in vita*) and after their death (*post mortem*), many hypotheses have been proposed over the past decade to interpret the biostratinomy of LBF accumulation. Several depositional models have been developed for understanding palaeoecology, palaeoenvironments and hydrodynamic behavior of nummulitids to explain their depth distribution (Davies, 1970; Hohenegger and Yordanova, 2001a,b; Yordanova and Hohenegger, 2007). Several authors point out that the hydrodynamic behavior of *Nummulites* is a key-factor controlling such distribution (e.g., Jorry et al., 2006; Yordanova & Hohenegger, 2007; Briguglio & Hohenegger, 2009). Consequently, transport varies among species and among generations because of different test size, shape and densities. Physical processes, which are modeled by mathematical equations, could be helpful to explain disturbances and modifications of communities leading to fossil associations: i.e., the biostratinomy of the tests.

During the last two years, the mathematic process characterizing LBF shells hydrodynamics has been explained (Briguglio & Hohenegger, 2009) and its importance to get information on shell morphology and functional test construction has been also exposed (Briguglio et al., in press; Briguglio & Forchielli, 2010; Briguglio & Hohenegger, 2010). A further step in nummulitids hydrodynamic, i.e. the explanation how such mathematic calculation can be a useful tool to give some advantages in palaeoenvironmental reconstruction on a field geologic profile, is a further goal of this work.

MATERIALS AND METHODS

The study area is situated in the westernmost part of the province of Lerida (Catalunya, Spain), in the region of Tremp. The samples studied were collected from an outcrop located on the road connecting Guardia de Tremp to Santa Lucia close to the fork junction to Estorm (Figure 1). The location area was chosen because of the optimal preservation of foraminiferal tests. In addition, the outcropping nodular limestone lithology of sediments allows both the study on thin sections and the measurements on

isolating specimens. On the outcrop, 14 layers were sampled; thin sections were obtained from lithified material, while unconsolidated samples were treated with 10% hydrogen peroxide then sieved (0.125 mm). On the sieved material, all optimally preserved specimens were collected, photographed, measured and used in this work. The mathematical results have been crosschecked with data from microfacies analysis (made on thin sections). 97 thin sections have been obtained from the lithified material and 645 specimens of nummulitids were used for the mathematical calculation. Additionally, several specimens were split on the equatorial section for classification and stratigraphic purposes.

The sampled profile corresponds to the "*Nummulites globulus* shales" of Luterbacher (1970, 1973) and can be stratigraphically assessed to the upper part of the middle Ilerdian *sensu* Tosquella & Serra-Kiel (1996), *Assilina corbarica* zone *sensu* Hottinger (1960) and SBZ 8 *sensu* Serra-Kiel et al. (1994) (Figure 2).

The composition of the samples is mainly made by hyaline LBF belonging to the genera *Nummulites* and *Assilina*, while *Discocyclina* is rare. Some species belonging to the genus *Assilina* have been assessed to the subgenus *Operculina* (*Operculina*) for long time because of their "operculinids" growth geometry (*sensu* Hottinger, 1960). As this characteristic leads to a very different hydrodynamic behavior of such forms, the operculinids have been always considered independently in this work. Among the taxa presented, the following species belong to operculinids: *Assilina ammonica ammonica*, *Assilina subgranulosa* and *Assilina douvillei*; not included into the operculinids is the taxon *Assilina leymeriei*. Porcelaneous foraminifera are abundant in the lower part of the profile and represented by the genera *Alveolina*, *Orbitolites* and *Opertorbitolites*. From the washed samples, well-preserved tests were selected to carry on this work as they can be regarded as members of the same time-averaged biocoenosis and thus relieve an interpretation of the fossil environment (Yordanova and Hohenegger, 2002, 2007). After washing the sediment, specimens were measured using the vector image analysis program CanvasX. Basic calculations and statistics were performed in Microsoft EXCEL, while SPSS for Windows, Release 16.0.1, was used for complex statistical analyses. On every specimen the calculations proposed by Briguglio & Hohenegger (2009) were performed. On some specimens, classified at species level, a species-specific study to validate the taxonomic accuracy of the mathematical approach was carried on. At the sample scale (comprehending the genera *Nummulites*, *Assilina*

and operculinids), the results of the calculation applied were used to define transportability of LBF and water depth estimation based on the transport - deposition boundary study (Briguglio & Hohenegger, 2010).

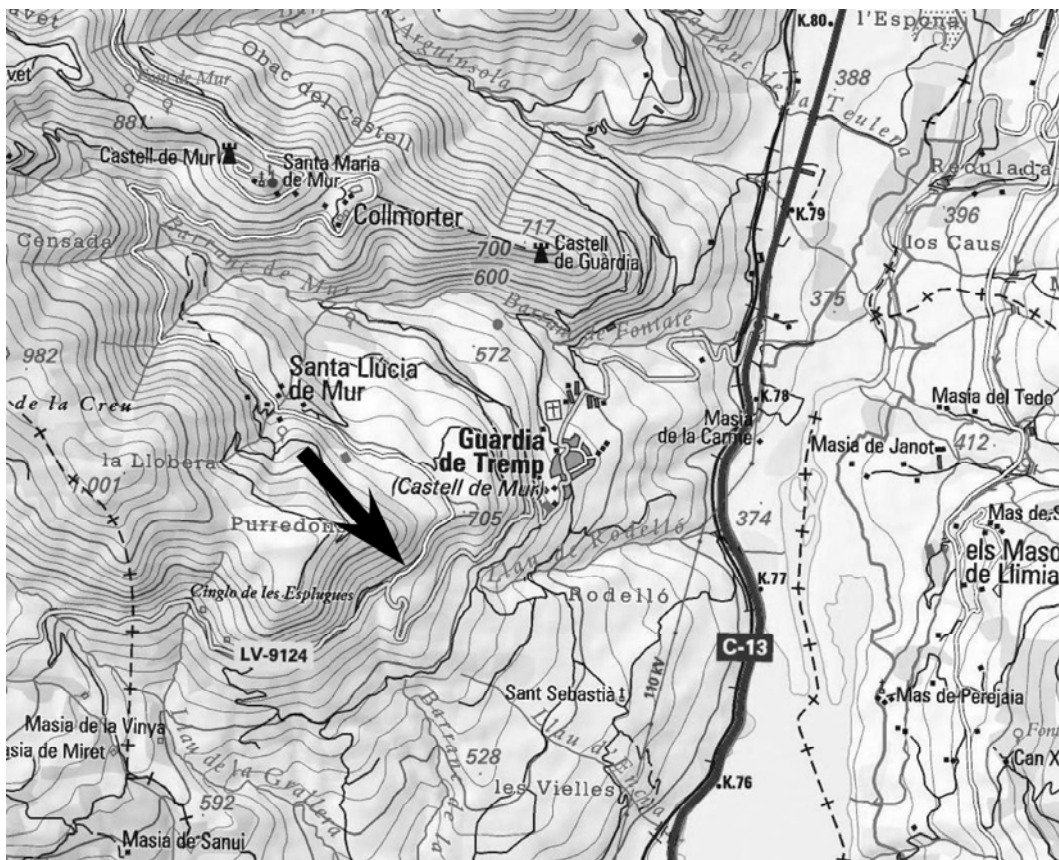
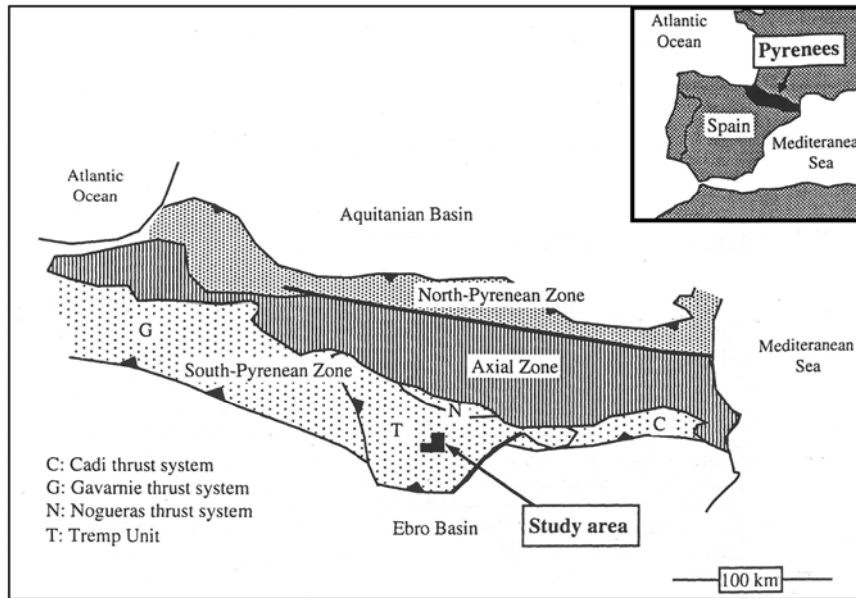


Figure 1: location of the study area (modified after Waehry, 1999) and of the presented outcrop (arrow)

Chronostratigraphy		Allostratigraphy		Biostratigraphy			
Haq et al. (1987)		Schaub (1981)	Modified after Mutti & Sgavetti (1994)		Hottinger, 1960	Tosquella & Serra-Kiel, 1996	Serra-Kiel et alii, 1994
Eocene	Ypresian	Cuisian	Castigaleu Group				
		Ilerdian	Figols Group		<i>Alveolina trempina</i>	<i>Nummulites involutus</i>	SBZ 9
			Upper Tremp-Ager Group	Alveolina Limestone	<i>Alveolina corbarica</i>	<i>Assilina leymeriei</i> <i>Nummulites exilis</i>	SBZ 8
					<i>Alveolina moussoulensis</i>	<i>Assilina aranensis</i>	SBZ 7
					<i>Alveolina ellipsoidalis</i>	<i>Nummulites bigurdensis</i>	SBZ 6
Upper Tremp-Ager Group	Alveolina Limestone	<i>Alveolina vredenburgi</i>	<i>Assilina dandotica</i>	SBZ 5			
Paleocene	Thanetian	Thanetian	Continental Red Beds				

Figure 2: Stratigraphic interval modified after (Waehry, 1999)

ACCURACY OF THE MATHEMATICAL APPROACH

Tests of foraminifera, acted on by fluids, behave mathematically as sedimentary grains (Pye, 1994).

The three main parameters, density, size and shape are responsible for differences in the behavior of sediments grains in fluids (Yordanova and Hohenegger, 2007) and the definition of these parameters, representing LBF shell morphology, is a pivotal factor to get information on their hydrodynamic behavior.

The calculation proposed by Briguglio & Hohenegger (2009), which provides a complete set of data on the hydrodynamics of ellipsoidal tests, needs some auxiliary explanations and a short review to allow its use in the fossil record.

DENSITY

Density data from recent foraminifera and their usage to extinct species could be wrong. Although the canal system and microstructures are similar, fossil nummulitids often show internal structural complexity higher than recent forms. Jorry et al. (2006) deduced the density of fossil nummulitids from weight and volume measurements, the latter obtained by immersion in mercury (Hg). They made these calculations on several nummulitids characterized by a minimum of diagenetic modifications and well-preserved intraskeletal porosity. Considering porosity is important to get insight on the hydrodynamics of LBF. Beside the macroscopic porosity, represented by the many chambers contained in the cell's test, a dense network of micropores in the chamber walls may let vary density in every test. Modern foraminifera develop also perforations for gas exchange through the wall (Leutenegger and Hansen, 1979). Gas exchange is of particular significance when foraminifera are associated with endosymbiotic algae, which develop light-regulation devices to avoid photo-inhibition (Hottinger, 2000). However, micropores with 1 – 2 μm diameter, representing tubular holes perpendicular to the wall surface, range from 25 to 36% of the wall volume, while the chamber volume (macroscopic porosity) ranges from 30 to 42% (Jorry et al., 2006). Therefore, the total porosity of *Nummulites* varies from 47.5 to 62.9%. A pore space of 30% for *Nummulites* reduces test wall density in empty tests from 2.72 g/cm^3 in walls consisting of solid low-magnesium calcite to 2.21 g/cm^3 in porous walls (Briguglio et al., in press). The density of a foraminiferal test changes with growth due to the variable proportion between test wall and chamber volume and cannot be used as a fixed value (Yordanova and Hohenegger, 2007).

Living foraminifera show densities similar to empty tests filled with seawater because the protoplasm possesses densities similar to seawater. According to Jorry et al. (2006), the apparent density of *Nummulites* thus ranges from 1.7 to 1.9 g/cm^3 , when macro- and micropores are filled with seawater.

In the calculations proposed by Briguglio & Hohenegger (2009), the average value of 1.8 g/cm^3 was used to represent density of *Nummulites globulus* (Leymerie, 1846) tests. The same value is here proposed to simulate the hydrodynamic behavior of fossil *Nummulites*. Concerning the genera *Assilina* and the operculinids, both abundant along the measured profile, slightly lower values are used: 1.6 for *Assilina* and 1.4 for operculinids because of their internal structure (Briguglio et al., in press). Such density

differences are consistent also for recent LBF (Yordanova & Hohenegger, 2007). Unfortunately, no realistic data are available in the literature concerning density of LBF, some three dimensional reconstructions of nummulitids (Briguglio et al., in press) gave some advices but more precise studies on density reconstruction are due to get more precise information on nummulitids hydrodynamic behavior at the species level and between generations. However, the differentiation here proposed seems to fit very well with the calculation.

SIZE

The parameters length (L), width (I), height (S), equatorial area and axial area were measured on all the selected specimens. Length (L) could be directly obtained on oriented thin sections or by image analysis; I was measured perpendicular to L crossing in the middle of the protoconch; and S was measured in axial section (see Figure 1 in Briguglio & Hohenegger, 2009). Equatorial and axial area was measured by image analysis.

Some parameters, used for the last 15 years to express mathematically shapes and forms of test and shells, have been used here on the 645 measured specimens and some considerations are mandatory.

Beside the calculation of the volume, which can be performed in many ways depending on the geometry of the test (see Yordanova & Hohenegger, 2007; Briguglio, 2008), a linear variable representing the diameter of the sphere possessing a given volume is the most important size parameter. The possibility to deal with linear parameters allows easier calculations and practical comparisons between different forms and sizes. This advantage is most useful in palaeontology where comparisons among assemblages, samples or association, even if composed by different taxa, are very common. Such tool can be useful also in further analyses of functional dependencies (Yordanova and Hohenegger, 2007).

The most famous linear parameter representing the diameter of a sphere possessing a certain volume (V), is

$$TND = 2 \left(\frac{3V}{4\pi} \right)^{1/3} \quad (1)$$

where *TND* is the true nominal diameter proposed by Wadell (1932).

A similar value to equation (1) could be obtained using another formula proposed by Le Roux (1997):

$$D_n = \sqrt[3]{D_l D_i D_s} \quad (2)$$

It requires only calculating the three diameters of the shell. In figures 3 and 4, the correlations between equations (1) and (2) are shown. The value of the slope is close to 1. According to this congruence, equation (2) is preferable to equation (1) for nummulitids, because measuring the three axes is much easier than calculating the volume and transferring it to the TND, especially for poorly preserved tests.

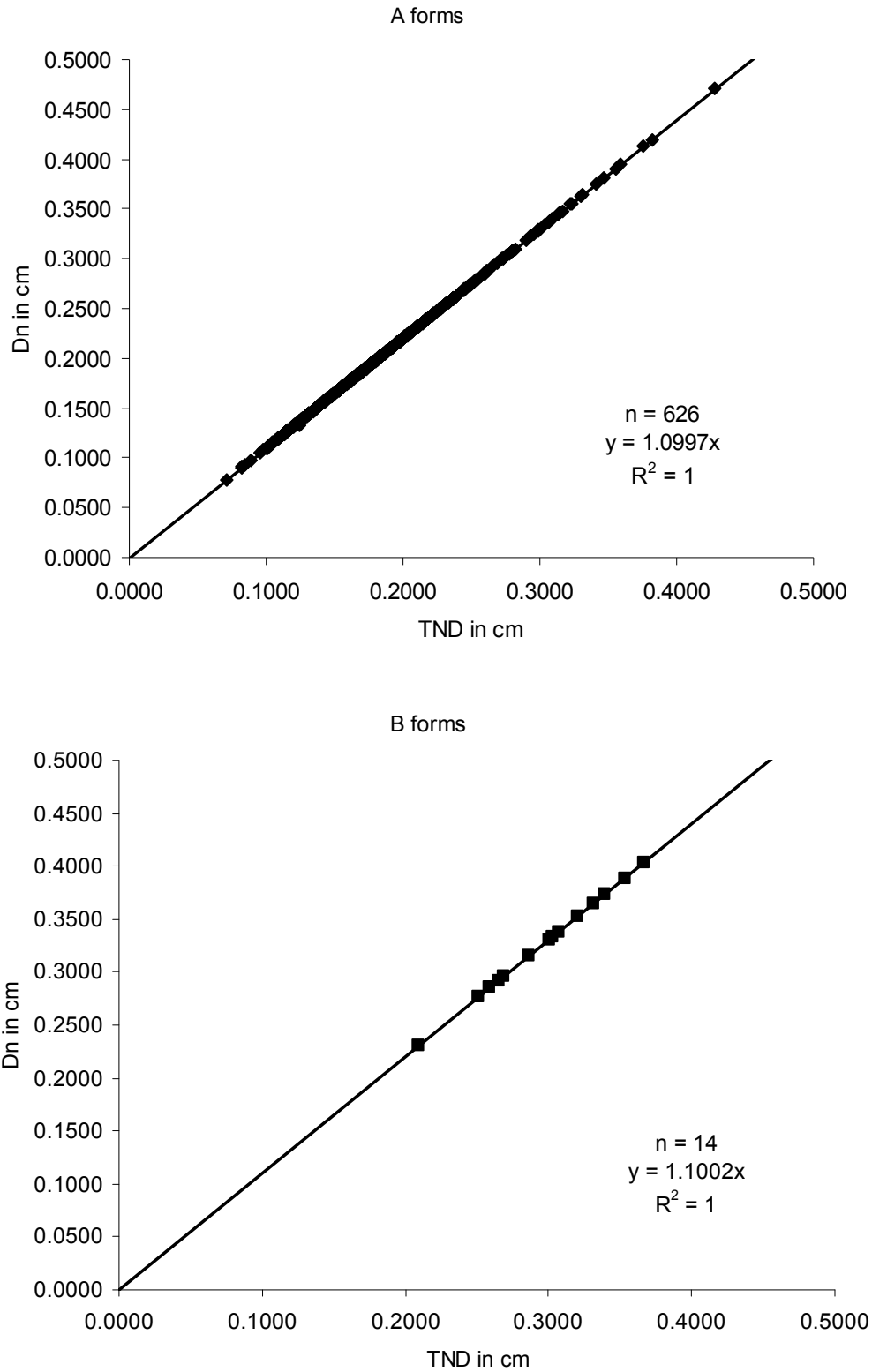


Figure 3: Correlation between the true nominal diameter TND (equation 1) and D_n (equation 2) in both A-forms (above) and B-forms (below) of all investigated specimens comprehending the genera *Nummulites*, *Assilina* and operculinids.

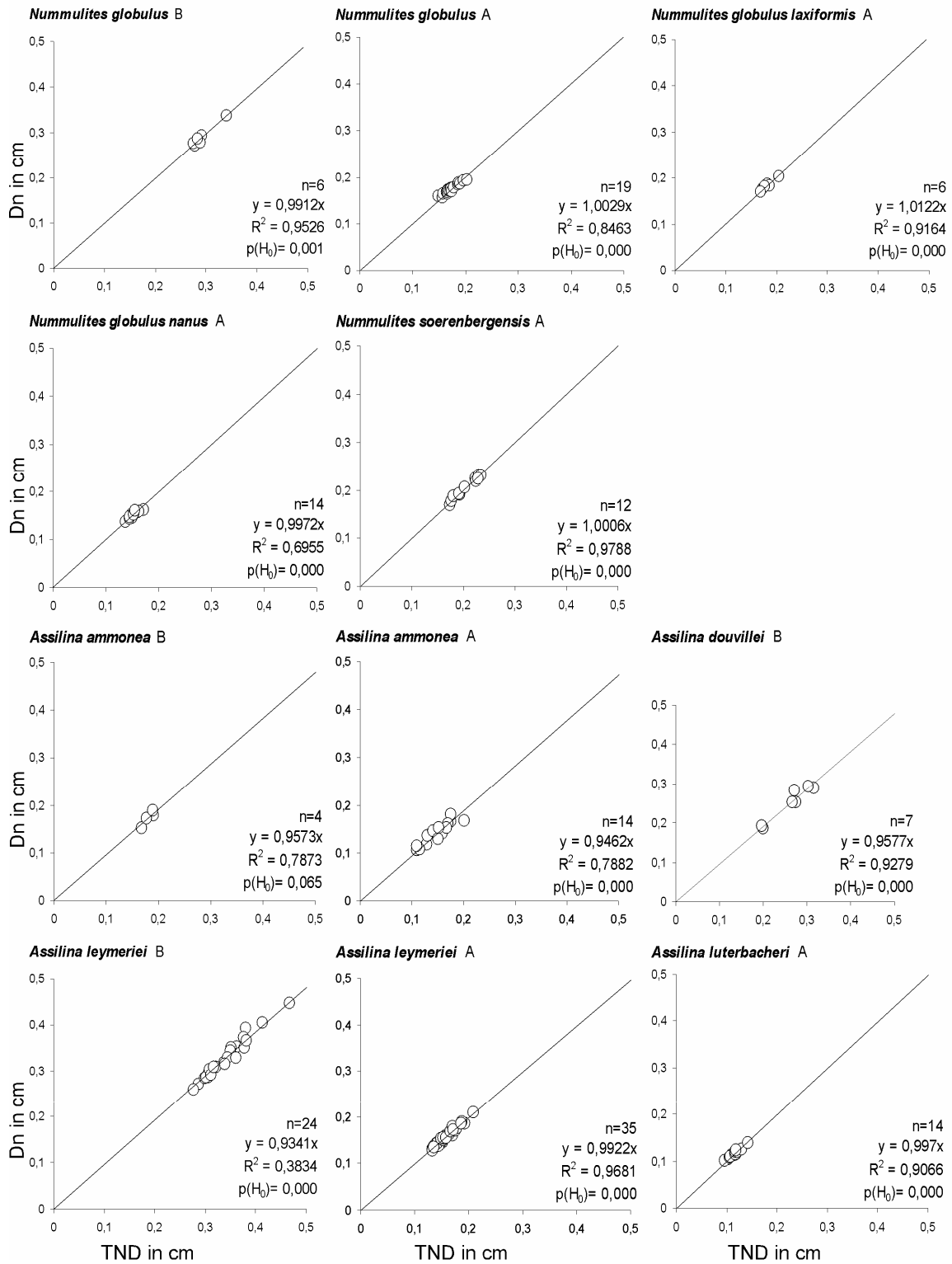


Figure 4: Species-specific correlation between the true nominal diameter TND (equation 1) and D_n (equation 2) on some selected specimens.

SHAPE

Shape is often considered as the key parameter driving the equations sequence to calculate the hydrodynamics of a particle (Briguglio & Hohenegger, 2009; Briguglio & Hohenegger, 2010). Very flat shapes versus rounded shapes behave very differently under the same energy input. Le Roux (1996, 1997, 2005) compared different sphericity indices in use and concluded that the shape entropy proposed by Hofmann (1994) is the best suited for predicting the settling velocity of an ellipsoidal grain. Jorry et al. (2006) and Briguglio & Hohenegger (2009) tested such parameter on nummulitids with good results. The Hofmann's shape entropy parameter is also quite convenient to calculate because the requested parameters to be measured are the three diameters of the ellipsoid L , I and S .

Settling velocity is directly related to particle shape. The difference between settling velocity of a sphere and a non-spherical particle possessing the same volume can be very large. Among the many formulas known in the literature, giving realistic values on settling velocity (i.e. dimensional velocity, there are other formulas giving dimensionless velocity, see. Briguglio & Hohenegger, 2009), three are considered the most important for modeling nummulitids hydrodynamic behavior.

The settling velocity of a non-spherical grain (W_e) and the settling velocity of the equivalent sphere (i.e. possessing the given volume) (W_s) were proposed by Le Roux (1996). Allen (1984), studying the sinking behavior of bivalve shells proposed a third formula where the projected area of the shell facing the flow during sinking plays a pivotal role. As reported in figures 5, 6, and 7, 8 these three different formulas give three different results. In fact, depending on the "roundness grade" of the test one settling velocity equation can be more realistic than another one. More specifically, according to some comparisons between measured settling velocities and calculated one on recent tests (Briguglio & Hohenegger, 2010), the equation best representing the sinking speed of very flat test (i.e. plate-like or disk-like) is represented by the value proposed by Allen (1984). For lense shaped shells the best solution is given by the value W_e , and for rounded test or egg-shaped the most realistic solution is given by the equation of W_s . The differentiation among different shapes is defined by the Hofmann's shape parameter. The use of selected formulas depending on the shape entropy parameter is followed in the present work.

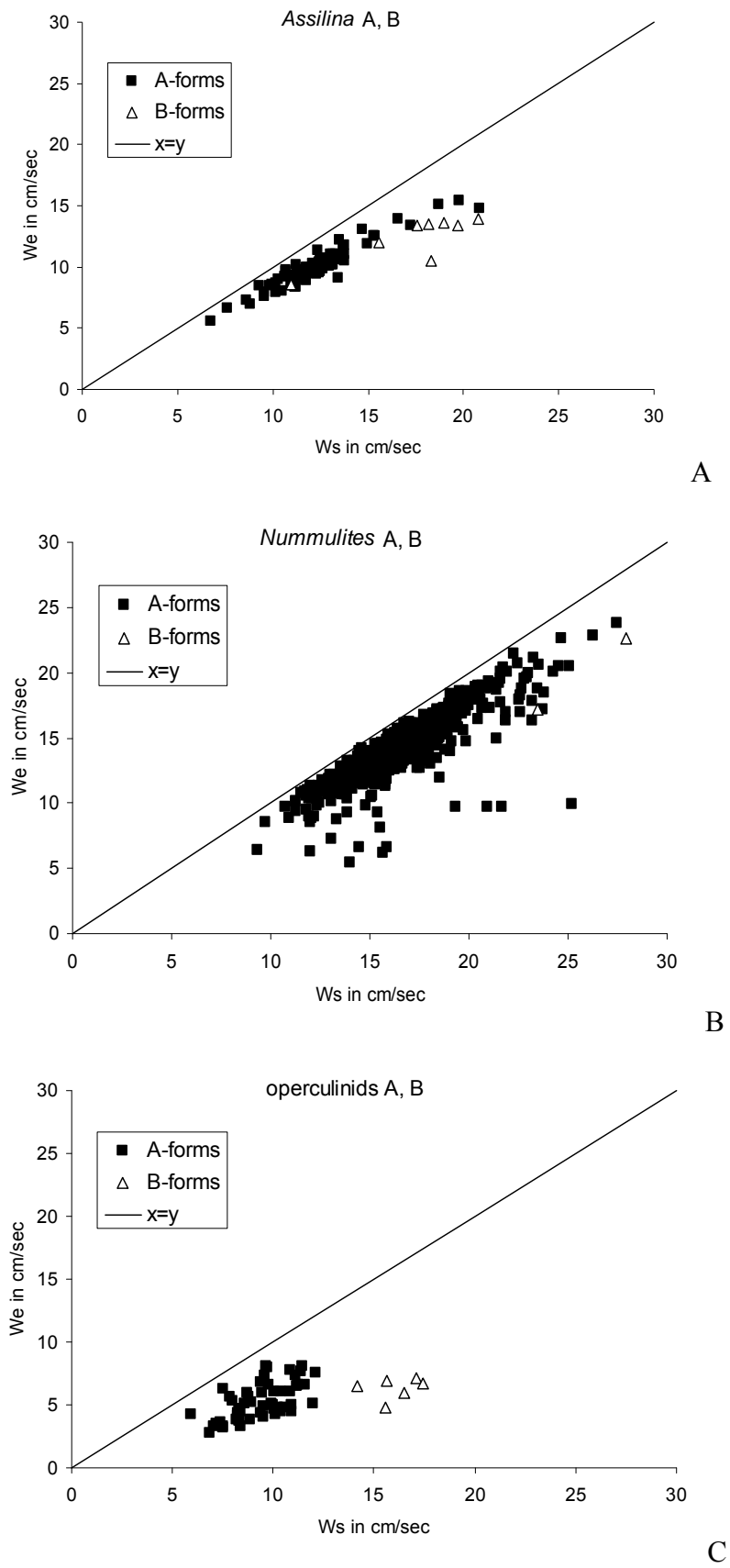


Figure 5: Correlation between settling velocities W_s and W_e on all the specimens' dataset.

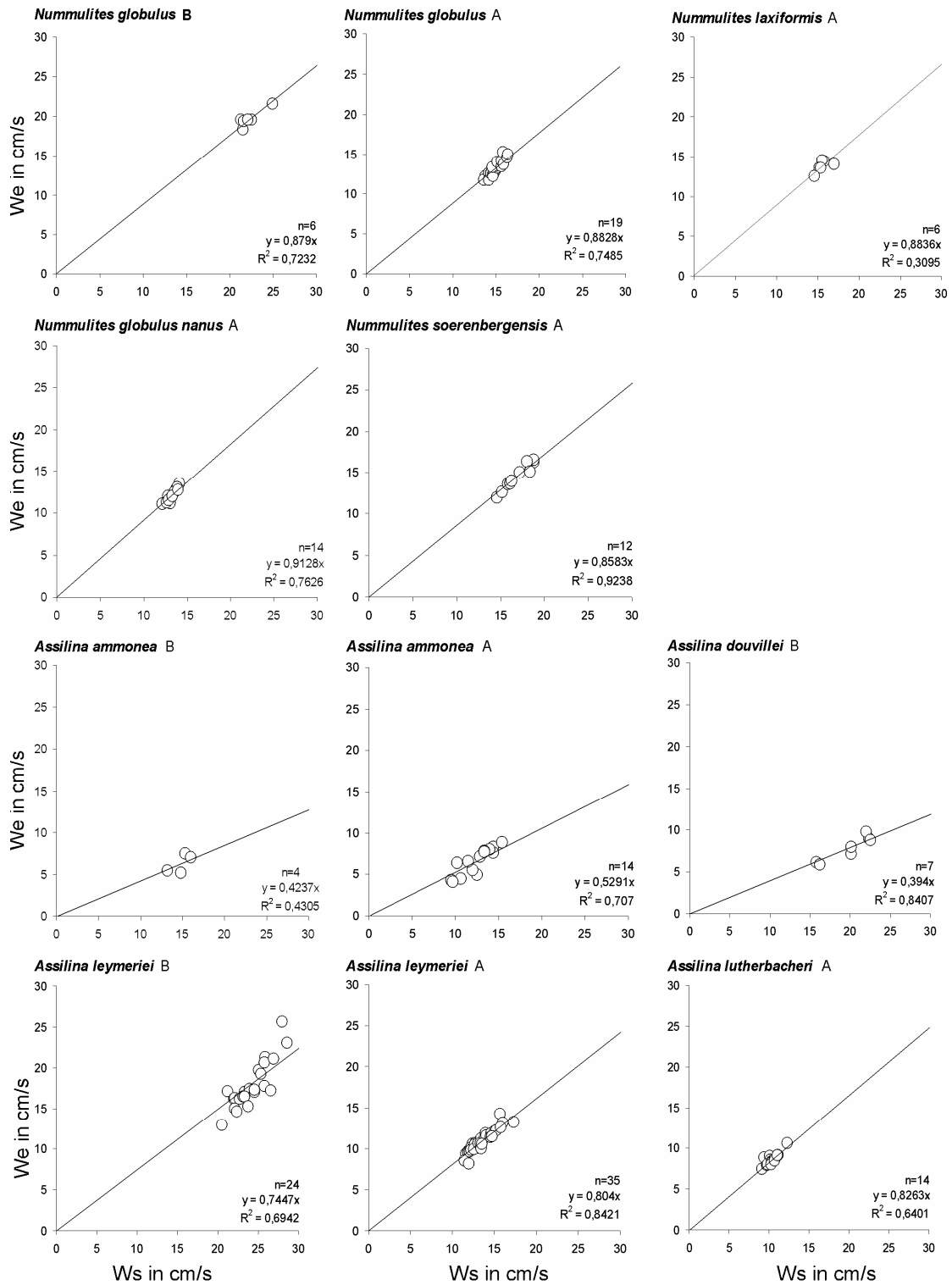


Figure 6: Species-specific correlation between settling velocities W_s and W_e on some selected specimens.

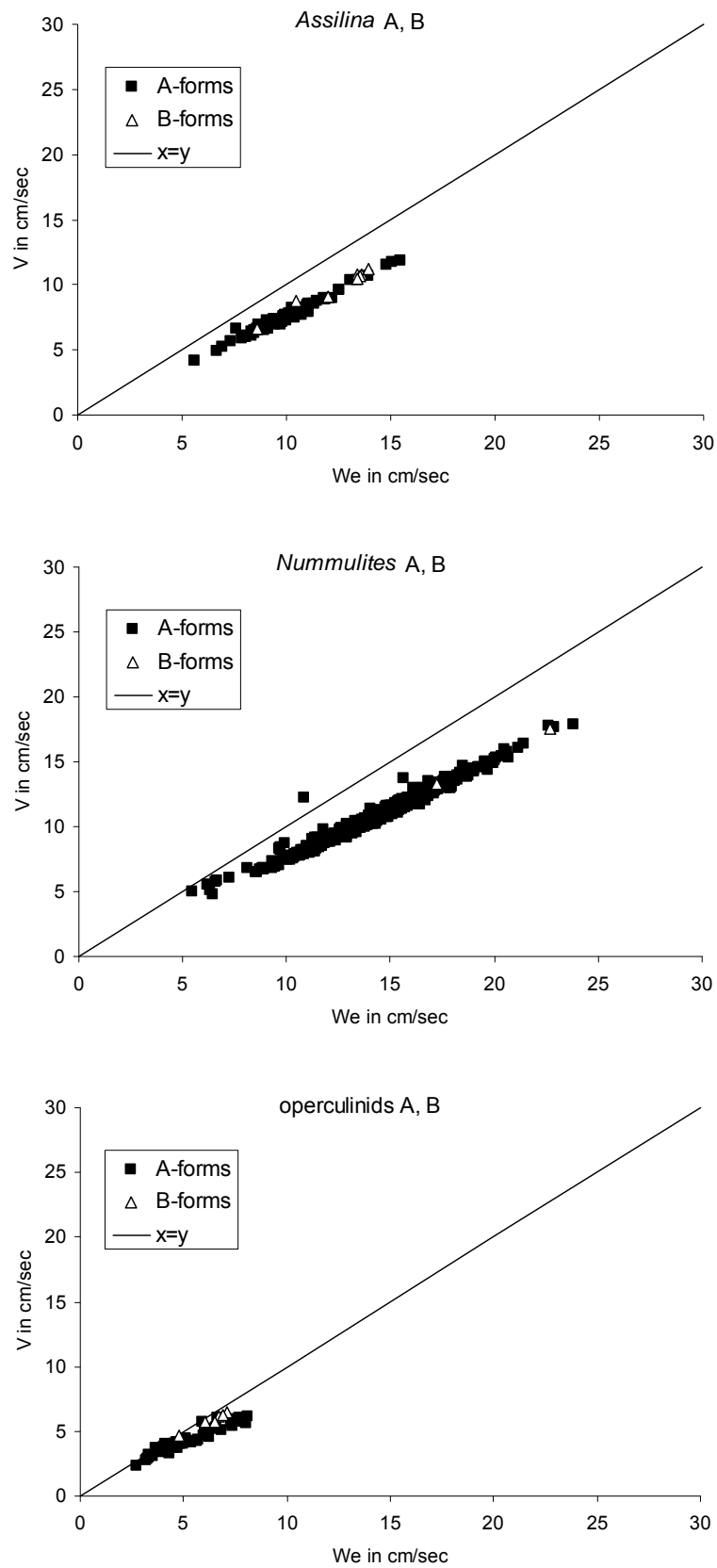


Figure 5: Correlation between settling velocities W_e and V on all the specimens' dataset.

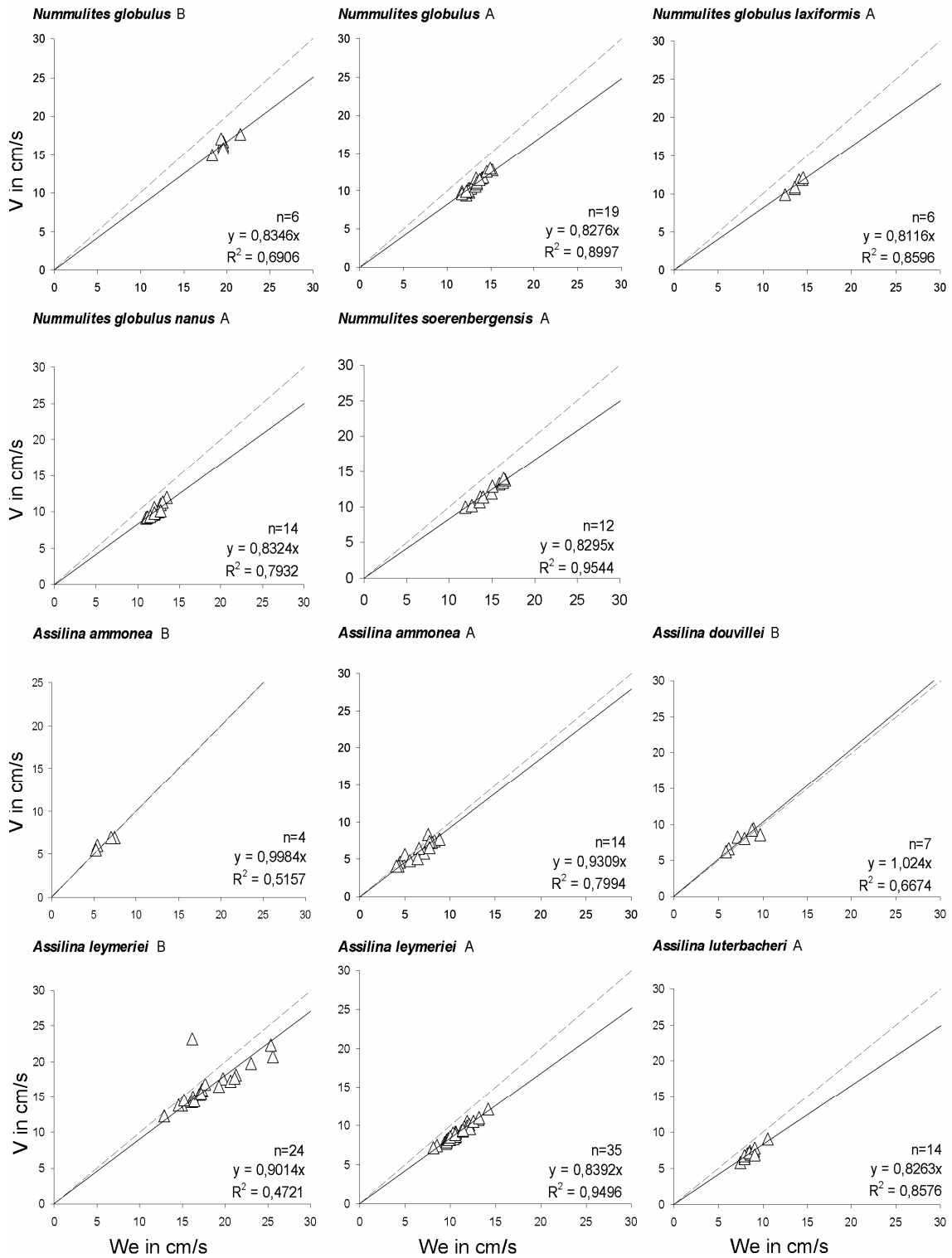


Figure 8: Species-specific correlation between settling velocities W_e and V on some selected specimens.

FIELD APPLICATIONS OF NUMMULITIDS HYDRODYNAMICS

The use of the settling velocity to characterize the hydrodynamic behavior of particles has a long history; the application of data as such is very broad and often a complete dataset on the hydrodynamic of sand particles helps sedimentologist in understanding currents direction, intensities and providing energetic quantifications of fossil environments. Concerning nummulitids, this history has not yet begun. The work of Jorry et al. (2006), which deals with settling velocity and its possible applications, concludes that the peculiar hydrodynamic behaviour of *Nummulites* tests can explain the diversity of the depositional models and that bottom streams and wave currents may induce the formation of in situ winnowed bioaccumulations. So far, no relationship is given between settling velocity and environment. A more comprehensive approach is provided by the work of Yordanova & Hohenegger (2007) in which the settling velocity is inverse related to transport distance: the higher is the settling velocity the shorter is the transport; e.g. *Palaeonummulites venosus* (Fichtel & Moll, 1798) living on coarse sand, is entrained with neighbouring grains but may be transported along shorter distances than other grains because of its high settling velocities. A much more complex approach, proposed by Briguglio & Hohenegger (2010), tries to compare the velocity pushing the particle on the ground due to gravity (i.e. settling velocity) with the requested energy to keep the given particle in suspension. Such energy can be expressed in terms of velocity pulling the particle vertically detaching it from the sea-floor. Wind-generated waves induce – in sufficiently shallow water (*sensu* Soulsby, 1997) – orbital motion within the water column to a depth roughly equal to half the wavelength of the source waves. When water depth is less than half the wavelength, this wave-induced orbital motion affects particles lying on the seabed. Such orbital motion can be decomposed as vertical horizontal vectors. The magnitude of the vector vertically directed can be expressed as the bottom orbital velocity, which is able to keep particles in suspension if they possess a lower settling velocity value. Consequently, given a wind-induced sea surface wave by the definition of its period and amplitude, a quantification of the bottom orbital velocity is calculable along water depth. Particles lying at water depths where orbital velocity is higher than their settling velocity can be kept in suspension; consequently particles lying at water depths where the orbital velocity is lower than their settling velocity will not be kept in suspension. This

statement does not include transport occurrence, neither its direction nor its intensity; it deals only with the capability for wave motion to keep or not particles in suspension, depending on water depth and on particles hydrodynamic characteristics (i.e. size, shape and density). LBF, under the effect of water motion, react, basically, similar to particles. The only difference from sand grains is that in some species, cells anchor themselves on rocks with their pseudopodia. After death, this only difference, instantaneously, disappears. Because LBF tend to live at water depth where they are not transported at least until reproduction, the comparison between bottom orbital velocity and settling velocity gives a quantification of the water depth where every test is not kept constantly in suspension by water motion and thus, not at the mercy of directional currents. Such depth can be considered as the best location to get the maximum light for symbiosis avoiding transport. That is the reason why the calculation of the settling velocity can provide much information about the quality of the sample, insights on its transportability and on its depositional environment also in terms of water depth.

On all the optimally preserved specimens found in the samples collected from the profile, the settling velocity (according to the Hofmann's shape entropy parameter) was calculated and the data obtained are reported schematically in figure 9 at the side to the geological profile and in detail in figure 10. The comparison to bottom orbital velocity is not given because no data are available in the literature to model surfaces sea wave in the lower Eocene Tresp basin, but some assumptions can be done for fair weather and storm weather conditions.

GEOLOGICAL SETTING OF THE STUDY AREA: PREVIOUS WORKS.

Early attempts to subdivide stratigraphically the Eocene deposits in the south-central Pyrenees date back to the late sixties. The proposed methods evolved progressively from a lithostratigraphic to an allostratigraphic approach. According to the allostratigraphic framework (Mutti & Sgavetti 1994; Mutti et al. 1988), the uppermost Cretaceous to Eocene strata can be subdivided into five allogroups, including the Tresp-Ager Group, Figols Group, Castigaleu Group, Castisent Group and Santa Liestra Group. The studied stratigraphic interval includes the upper part of the Tresp-Ager Group and the Figols Group (Figure 2). The profile here presented (Figure 9) starts from

the uppermost part of the so called Upper Tremp-Ager Group (UTAG). The whole group includes: the uppermost part of the Continental Red Beds, corresponding to the upper part of the Tremp Formation or to the lower part of the Serraduy Sequence (Luterbacher et al. 1991, Eichenseer & Luterbacher 1992) and the *Alveolina* Limestones.

Stratigraphically, the profile represents the last sequences of the *Alveolina* limestone passing to the Figols group (Figure 2). The *Alveolina* limestone formation is equivalent to the Cadi Alveoline Limestone formation (Mey et al, 1968), the lower part of the Ager Formation (Luterbacher, 1969, 1970; Mutti et al., 1972; Nijman & Nio, 1975), the lower part of the Figols sequence (Mutti et al., 1985; Fonnesu, 1984), the *Alveolina* Limestone and the lower part of the Figols Group (Mutti et al., 1988) or the Ager sequence (Luterbacher et al., 1991; Eichenseer & Luterbacher, 1992). The Figols Group, investigated here only at its stratigraphic base, includes the Roda Formation (Mey et al. 1968), the upper part of the Ager

Formation and the lower part of the Montanyana Formation (Luterbacher 1969, 1970), the upper part of the Ager Formation and the Castigaleu Formation (Nijman & Nio 1975), the upper part of the Figols Sequence (Mutti et al. 1984, Fonnesu 1984), and the Llimiana, Alinya and Oden sequences and the lower part of the Castigaleu Group (Luterbacher et al. 1991, Eichenseer & Luterbacher 1992).

DESCRIPTION OF THE PROFILE:

MICROFACIES ANALYSIS AND NUMMULITIDS HYDRODYNAMICS

On the profile three different facies have been recognized based on microfacies analyses on thin sections.

F1: *Alveolina* limestone facies. The rocks of this facies type are grey or beige limestones. It contains bryozoans, echinoderms fragments, alveolines, miliolids, *Orbitolites*, *Opertorbitolites*; rotalids and textularids abundant at various proportions, some gastropods and pelecypods, including oysters, and locally abundant *Lucina*. Some layers also contain red algae. Geopetal fabrics are common in more micritic layers. The beds are nodular at various degrees. In very nodular layers the bedding planes are difficult to identify, thus giving these rocks a poorly stratified and massive aspect.

Within the study area, nodular milioline packstones to grainstones form decimetric to metric units. According to the literature, *Alveolina* limestone of the Tresp area, are believed to represent the principal source area of the miliolids dominated sediments. In fact, the fine-grained carbonate lithology and the absence of any physical structures point to a low-energy setting where the carbonate sediments could be produced (Wearhy, 1999 and reference therein). However, the diversified faunal assemblage points to a shallow water, normal marine to slightly restricted setting (Heckel 1972, Plaziat 1984), characterising muddy lagoons, bays or shallow shelves.

F2: Nodular micritic wackestone with small *Nummulites* with large operculinids.

This facies consists essentially of shaly, locally slightly sandy, grey-brown to yellowish wackestones to packstones composed by hybrid arenites with abundant calcareous siltstones. The most characteristic macrofossil in these beds is the pelecypod *Spondylus*. Among the nummulitid foraminifera, large operculinids are particularly abundant. Alveolinids and *Orbitolites* are absent, if present, they are very poorly preserved. Echinoderms furnish abundant fragments, and small to medium sized spatangoids occur locally still in life-position. The beds are very nodular and characterised by an important lateral extension (sampled by the Author from Moror to Sant'Adrià for more than 10 km). On thin section analysis the medium size for well preserved nummulitids is very small in respect to the well preserved operculinids which may reach up to 3 mm. Large sized nummulitids, when present, are always poorly preserved. The abundance of micrite and the absence of porcelanaceous foraminifera assess this facies as deeper as F1. Hydrodynamically, small rounded nummulitids and large flat operculinids behave similarly.

F3: Larger nummulitids and transported porcelanaceous foraminifera.

Sediments are here classified as low-angle and hummocky cross-stratified nummulitic hybrid arenites. Besides nummulitids, the faunal assemblage includes echinoderm fragments, oyster shells, and locally bryozoans, *Orbitolites*, alveolines and miliolids. Many porcelanaceous foraminifera are very poorly preserved. Bioturbations occur abundantly. Discocyclinids are common in some layers, in subordinate proportions.

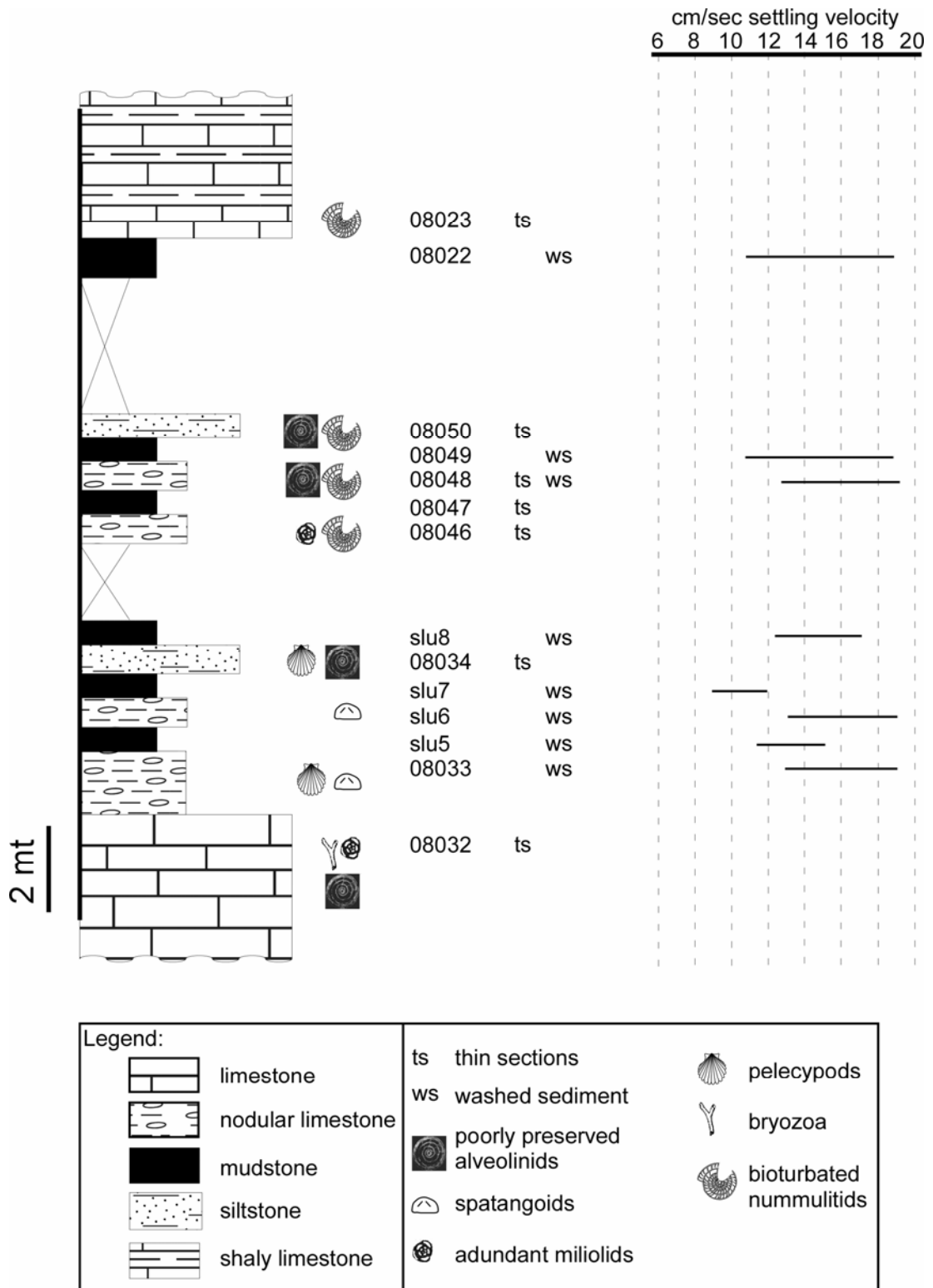


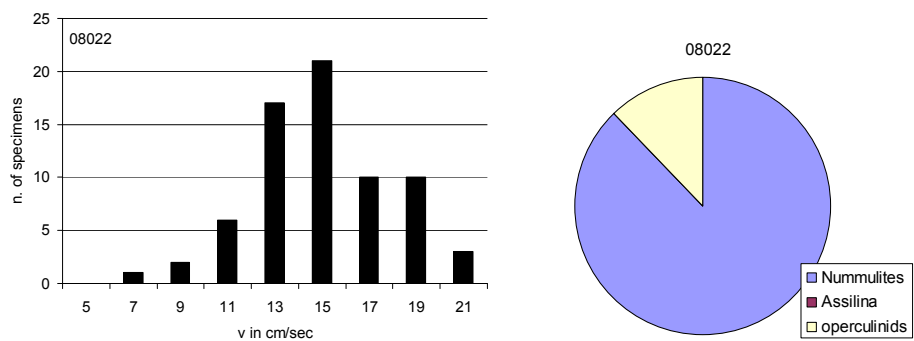
Figure 9: studied profile.

STRATIGRAPHIC INTEGRATED STUDY OF MICROFACIES ANALYSIS
AND HYDRODYNAMICS OF NUMMULITIDS

A description of all investigated layers is reported. In the cases of samples with isolated specimens, a cake diagram is reported with the taxa differentiations together with a settling velocity distribution diagram. In cases of lithified material, a description of the microfacies is reported. Raw data on settling velocity of nummulitids for each layer are reported in figure 10.

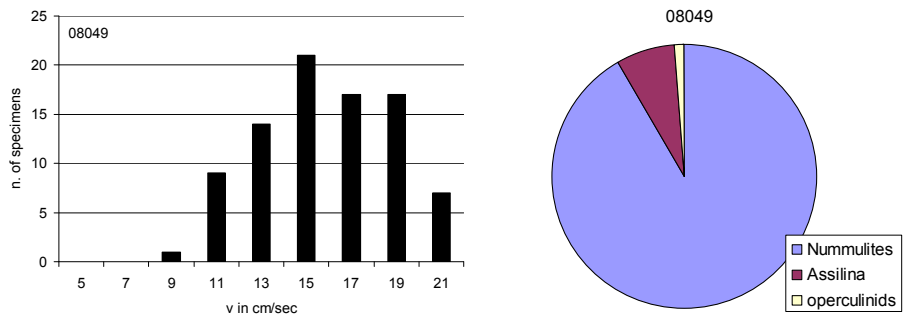
Layer	Facies	Description
08023	F3	Bioclastic packstone with abundant discocyclusinids and well preserved operculinids. Abundant well preserved small nummulitids; larger test are often bioturbated or destroyed (Plate 8).

08022

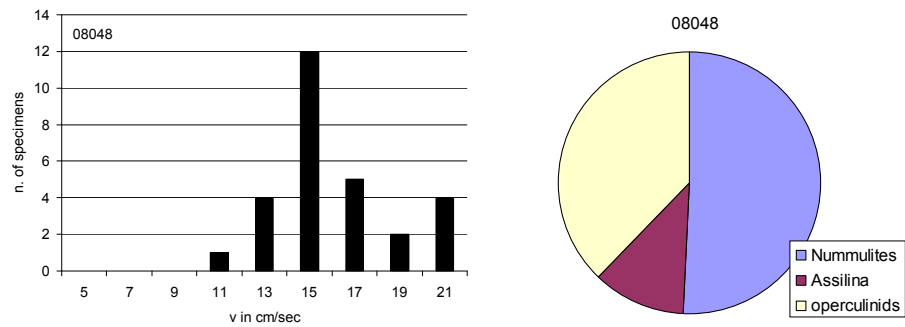


08050	F3	Micritic wackestone with medium size nummulitids and operculinids optimally preserved. Rare orbitolids and alveolinids. Some thin sections show transported material and on larger tests bioturbation occur. Rare poorly preserved alveolinids indicate long distance transport (Plate 7).
-------	----	--

08049



08048 F3



Abundant bioclastic debris testifies transport processes and deposition of tests belonging to shallower environments. Bioturbation occurs often on larger tests. Well-preserved discocyclinids are common. The presence of rare and poorly preserved alveolinids testify long distance transport. (Plate 6).

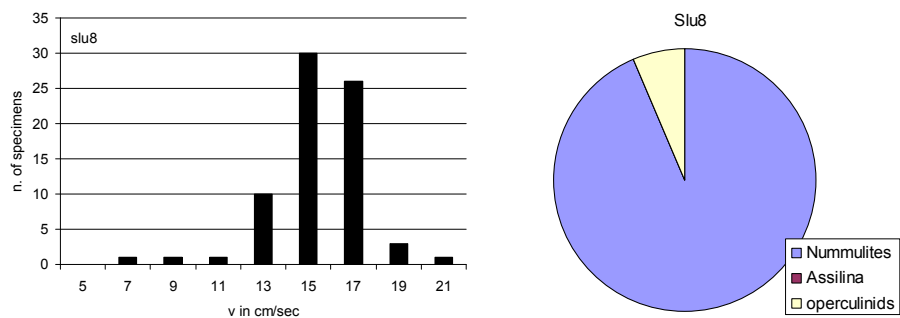
08047 F2

Wackestone with well-preserved small nummulitids and middle sized to large operculinids. Very rare large nummulitids always broken or destroyed. Calm environment with micritic matrix (Plate 5).

08046 F2

Well preserved *Assilina* and operculinids within a micritic wackestone is the most common situation among the studied thin sections. Quite calmer environment respect to the formers, few bioclastic debris and rare broken or abraded nummulitids are not evidence for intensive transport. The abundance of foraminifera is strongly reduced in respect to the layers below. The absence of discocyclinids infers a shallower environment (Plate 4).

Slu8

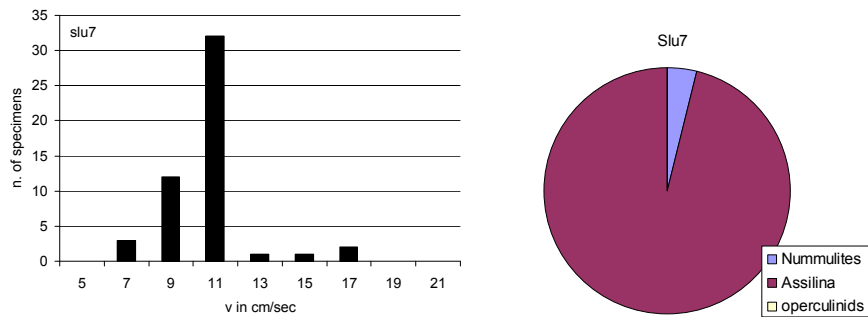


08034 F3

Packstone with transported nummulitids, operculinids and echinoids. Transport flows from shallower regions deposited bioclastic detritus made by broken nummulitids. Abundant terrigenous input and very rare and badly preserved *Alveolina* testify shallow water sediment input

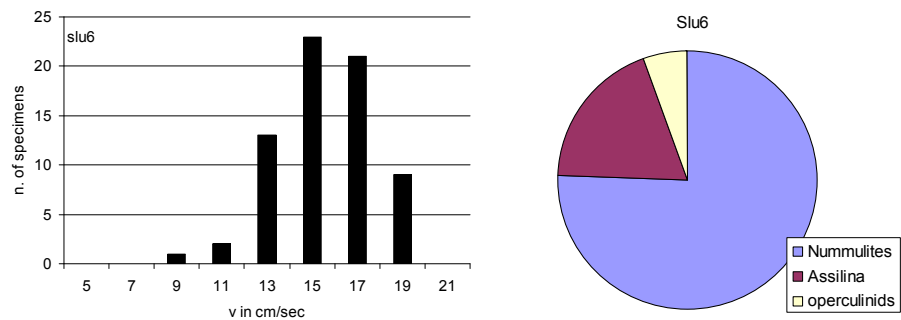
within sustained energetic inputs. The only forms, which present a moderate, but not optimal, preservation grade are large discocyclinids and few *Assilina*. According to this evidences, the "heavier" nummulitids test must be considered transported from long distant shallower depths. Rewashing may be the case for abrasion also in small nummulitids heavily subjected to suspension and re-deposition due to weak water inputs. Rewashing may have affected operculinids also, but their strongly reduced settling velocity allows them a longer time in suspension reducing collisions with other faster settling grains. Abundance of discocyclinids suggests deeper water environments (Plate 3).

Slu7



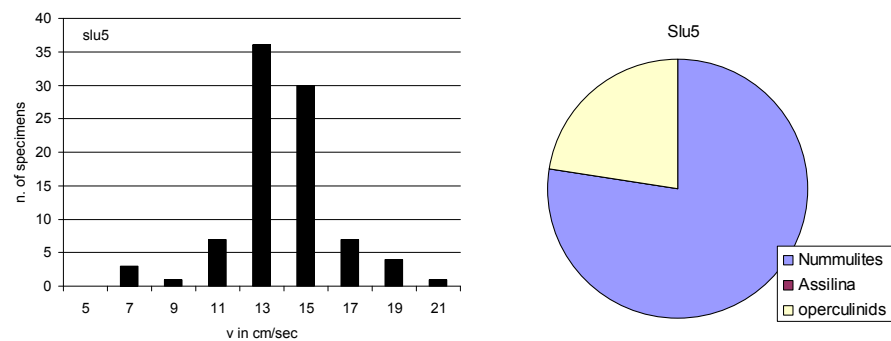
Sample's photos are shown in plate 2.

Slu6



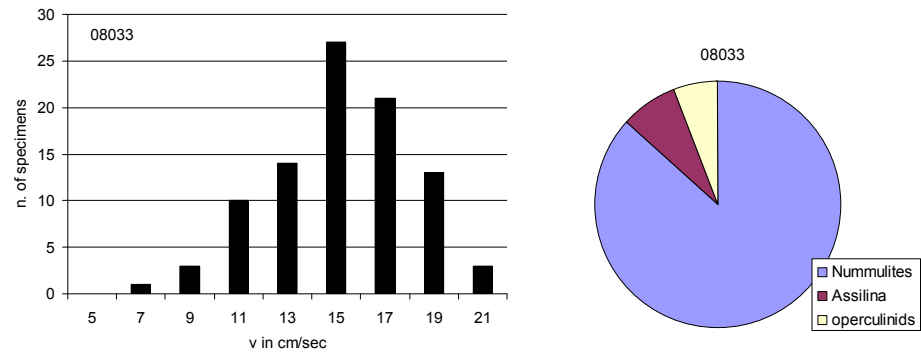
Sample's photos are shown in plate 2.

Slu5



Sample's photos are shown in plate 2.

08033



08032 F1 *Alveolina* limestone: grey or beige limestone. It contains bryozoans, echinoderms fragments, alveolines, miliolids, *Orbitolites*, *Opertorbitolites*, *rotalids* and textularids.

Beside the good preservation of most of the tests, some *Alveolina* specimens are very poorly preserved: some broken shells and abraded surfaces are, in some layers, common. The elevated porosity of the sediment is replaced by sparitic calcite. This wackestone can be associated with a quite protected scenario as a lagoon or backreef zone. *Orbitolites*, when not broken, are compacted one above the other with few micrite in between (Plate1).

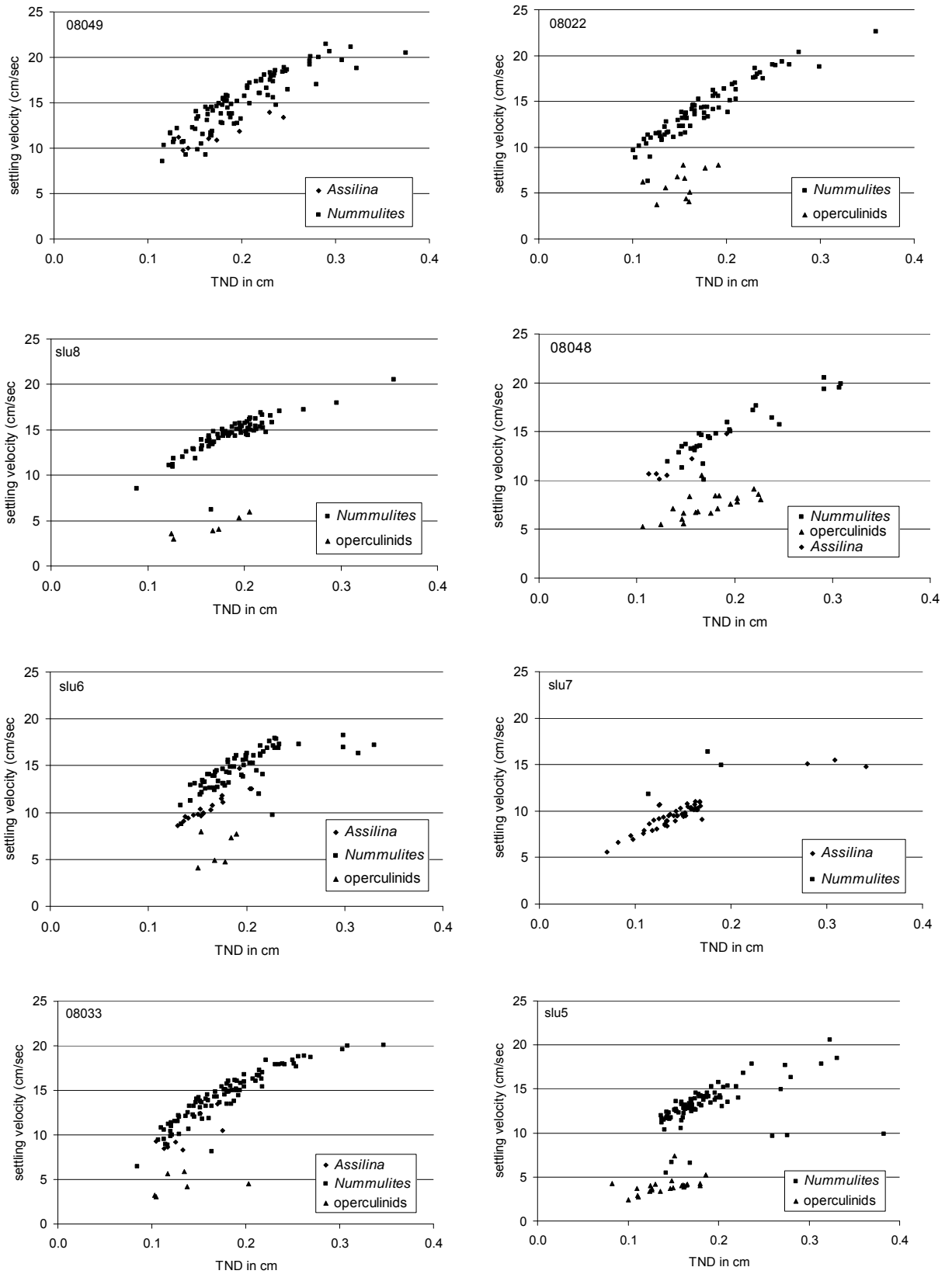


Figure 10: Raw data on settling velocities of all measured specimens of all sampled layers where isolated specimens were available.

INTERPRETATION OF THE PROFILE:
DEPOSITIONAL PROCESSES, ENVIRONMENTS AND HYDRODYNAMICS

The mixture of terrigenous sand and silt with nummulitids foraminifera points to an open marine, shallow to moderately deep and delta-influenced setting (mixed sedimentation). According to the literature, abundant within the area, nummulitic delta front and shelf sandstones hybrid arenites and siltstones are deposited in open marine setting with a high influx of terrigenous sand and silt. Such terrigenous-dominated areas may develop near deltas (Waerhy, 1999). With increasing distance from the delta, the nummulitic delta front to shelf deposits pass into nummulitic carbonate sediments (at the end of the profile, beginning of the Figols group) (Mutti et al., 1994). Milioline nearshore sediments are deposited, with respect to the associated hybrid arenites, in areas of influx of terrigenous sand. The locally observed contact of nummulitic shelf wackestones and packstones over milioline nearshore grainstones and packstones (at the beginning of the profile) points to rapid transgression.

Sharp and locally erosive basal bedding planes, abundance of clasts within the thin sections indicate that beds, mainly the ones belonging to facies F3, have been deposited by gravity-flows. The *Alveolina* limestone (which may be considered as part of a ramp system) consists of nearshore and shallow shelf limestones rich in alveolinids, *Orbitolites*, *Opertorbitolites* and other small miliolids.

The nearshore facies may include tidal flat, lagoon, beach and tidal bar deposits. Such facies association are represented by bioturbated platforms and bioclastic to calcilutitic gravity-flows (Facies F3).

The platform is considered as the "sediment factory" of the system (Waehry, 1999). Sea grass bottoms may have played an important role in sedimentary production and in differentiating the hydrodynamics, reducing the energy produced by waves at the seafloor. The nummulitic carbonate ramp system is dominated by nummulitid grainstones and wackestones. Bioclastic beaches, bars, and coral-, coralgal- and sponge-dominated carbonate buildups are common structures often only partially preserved. The shelf includes platform and gravity-flow dominated deposits.

Concerning hydrodynamics, lower or higher settling velocities ranges differentiate the sampled layers. Higher settling velocity tests layers are comparable with high energy

environments; consequently, low settling velocity tests assemblages indicate quieter or calmer sedimentary conditions. A correlation of the settling velocity with the bottom orbital velocity can provide a quantitative estimation of the water depth where the foraminifera have lived or have been transported in. After the first layers in the lower part of the profile, where high energetic environments are represented by the *Alveolina* limestone and grains supported matrix, variable deeper and shallower conditions are displaced within the sedimentary record. The first layers, where isolated specimens were measured (i.e. 08033, Slu5, Slu6 and Slu7), indicate an interesting trend in settling velocities: first reducing from 13-17 cm/sec to 13-15 cm/sec, after increasing in Slu6 falling drastically down with the almost monogeneric association of the deeper assilinitids in Slu7. According to the lithologic variations, samples Slu5 and Slu7 are coming from unconsolidated sediments with abundant muddy fraction respect to the samples 08033 and Slu6 which are characterized by more sandy or silty cemented lithologies. Consequently, Slu5 and Slu7 contain tests belonging to less energetic environments with lower settling velocities. Above the relatively deep water association of Slu7, characterized by a low settling velocity monogeneric association in a mud supported lithology, a sharp base layer crops out containing bioclastic debris made by broken nummulitids. The deepening trend is confirmed by the abundant and well preserved discocyclinids. From the muddy sediment above it seems that the water depth is slightly changing and tends to a new sea level fall. Measured tests in Slu8, mainly nummulitids and no *Assilina*, possess a "well sorted" settling velocity between 15 and 17 cm/sec. The regression sequence, hydrodynamically visible from with Slu8, continues with 08046 with absence of discocyclinids. Larger nummulitids also occur and are always poorly preserved as a consequence of the erosional surfaces due to the regressive system. The same facies remains constant until layers 08048 and 08049 occur, where the settling velocity increases covering a broad spectrum (i.e., much broader distribution) probably because specimens with optimal test preservation but transported from higher energetic environments (i.e. shallower regions) have been included in the calculation. The sedimentary environment in 08050 shows a typical deeper shallow water fauna within a protected area. Few transport events produced the evidence of rare and poorly preserved alveolinids; the regressive trend is continuing in 08022. Similarly to Slu5, abundant high settling velocity nummulitids testify an energetic environment in shallower areas. According to the lithology (micritic mudstone) we supposed that the

environment can be similar to the facies F2 with small nummulitids and large operculinids with the presence of some well preserved transported specimens, which shift the diagram to higher settling velocities. Such hypothesis is confirmed by the following layer possessing characteristics of deeper water sediments with abundant discocyclinids and well preserved operculinids.

RESULTS

Concerning the accuracy of the mathematical approach we used to get palaeoenvironmental information from the presented profile, many important results can be observed for further analyses. The correlation coefficients between the methods proposed by Yordanova and Hohenegger (2007) and Le Roux (1997) to represent test size independently from shape and density show a significant linear relationship (Fig. 1). Additionally, there is no difference between genera; *Nummulites*, *Assilina* and other operculinids possess the same slope. Even at the species level, no significant differentiation is present within genera and between generations; additionally no deviation from the linear function $x=y$ is noted. Even for the very different geometries of *A. ammonica* generations, the correlation is always consistent. According to Hottinger (1977), this species belongs to the subgenus *Operculina* (*Operculina*): the main characteristic of this species is its growth rate, which is fast and strongly evolute. In A-forms, a third whorl chamber could be more than three times higher than the corresponding chamber of the second whorl. Unfortunately, the abundance of B-forms in the samples was quite poor for manifesting these differences. Thus, the use of TND or D_n is a powerful tool to express test size in nummulitids; both generations of the three genera here presented can be investigated with the same parameter. This result allows size comparison among samples and within genera; it allows the use of the nominal diameter as a linear variable for multivariate representations.

As the nominal diameter represent the "size" of a shell possessing a certain volume, the shape factor is playing a major role within the grain size description. That is the reason why, to have a better quantification of settling velocity, the shape factor was taken into account. As the shape entropy parameter was calculated on every test, the use of the best-suited settling velocity equation give a consistent result for every single test. The nummulitids always posses the highest settling velocity respect to species belonging to

the genus *Assilina* and to operculinids, which are always characterized by lowest settling velocity values.

The operculinid's shape generates strong resistance against water during sinking, thus causing the deviation from a sinking sphere. Rather globular forms such as *N. globulus*, *N. globulus nanus* (Schaub, 1981) or even *A. luterbacheri* (which does not belong to the operculinids) show a slope of the regression line slightly below 1 (figs: 6 and 8); this documents the inefficiency of shape entropy in globular forms, thus justify the use of a different formula. The use of the settling velocity in further works is highly solicited as such parameter defines the grain in all its aspects. Settling velocity in its calculation includes density shape and size and therefore is the most suitable parameter to define the behavior of a particle (or a shell) within the water column or lying on the seafloor. Therefore, such parameter can be used also for planktonic foraminifera even if the settling velocity calculation should take into account several more parameters reducing sinking speed almost to zero such as spines (e.g., in globigerinids) or highly perforated surfaces (e.g., orbulinids). Diameter/thickness ratio calculation is important as well but too superficial to get into the hydrodynamic behavior of such a divers group as the nummulitids is. Such ratio can be very useful in the field to have a fast quantification of differences among layers and outcrop (as this ratio is dimensionless it is usable as linear parameter); however it is not suitable for detailed study or for publications.

The application of all the mathematic calculation to the collected samples along the profile gave extraordinary results both crosschecking the microfacies analyses obtained by thin sections and producing quantitative data to assess palaeodepths. Sea level fluctuations are visible and can be visible in longer profiles both in small- or large-scale events just by reproducing the calculation proposed. The settling velocity range obtained characterized depths between 20 to 50 meters water depth with a normal fair-weather condition swell (Briguglio & Hohenegger, 2010).

DISCUSSION

The use of hydrodynamics and settling velocity to investigate samples or geological profile may lead to some misinterpretations. A particle possessing a certain settling velocity is able to resist water motion if the energy input acting on the particle is vectorially reverse to gravity and shorter in magnitude. It does not mean that the particle

can resist all kinds of transport. In fact, critical shear velocities, which quantify the minimum velocity required for an energy input to entrain a particle without keeping it in suspension, for investigated tests are much lower than their settling velocity. Thus, transport may always occur as entrainment or traction on the seafloor and can move heavier tests. Test damages are considered the evidence of these events but some studies do not agree (Beavington-Penney, 2004). Additionally, the used calculation of the settling velocity is a mere theoretical approach. It does not consider bed friction and roughness of sea floor given by sedimentary grains, it does not consider turbulence, which may vary the real velocity felt at seafloor. The value of the settling velocity is a good representation of the environment but with the many limits belonging to a model. The general decrease of the settling velocity correlated with increased test flatness explains the capability for flat forms to be kept in suspension easier, while rounded forms are less easily transportable because of their higher settling velocity. Because of these transportability differences, fragile forms as the here studied operculinids must testify very quiet environments. However, the constant presence of operculinids within the samples we have presented must be discussed.

Operculinids do not possess a settling velocity similar to nummulitids; they are hydrodynamically incompatible. Possessing such higher settling velocity, nummulitids can live in shallower environment respect to the flat operculinids, which, because of their broader surfaces, may host a major number of endosymbionts and thus may inhabit much deeper and less illuminated environments. The most convenient solution for LBF is to live at the shallowest depth possible below that boundary given by higher bottom orbital velocity. Such depth may provide the highest illumination possible for symbionts. Only in very few cases, symbionts do not require such abundant light intensity (Holzmann et al., 2001). Consequently, if both large nummulitids test and large operculinids test are present within an assemblage, without considering upslope transport events, nummulitids must be considered as transported. The poor preservation of the majority of the larger tests within the samples of facies F2, is a logical consequence of such process. The higher settling velocity of such large tests may justify also their poor preservation due to re-suspension and rewashing effects. In recent environments, operculinids do not live abundantly together with nummulitids, and if they do, than the hydrodynamics of their test has comparable settling velocities to the

water depth of nummulitids, i.e. they have not a flat shape (Yordanova & Hohenegger, 2007; Briguglio & Hohenegger, 2010).

Beside these considerations, many others can be the analyses the settling velocity study can give.

Because the main parameters to be calculated are the three diameters and the main test geometry can be represented only by the major and the minor axes, the calculation proposed can be used also on axial oriented sections, normally most available on thin sections. A further step in the study of the hydrodynamics of nummulitids accumulations will be the study of the correlation between sediments and faunal association, where orbital velocity and gravity should have been acted the same. However, the calculation of the settling velocity, with its accuracy and speediness permits a broad use of such parameter in many environmental science branches.

CONCLUSIONS

This study provides a contribution to the interpretation of fossil accumulations, on reworking phenomena and on transportation and re-distribution of living/dead nummulitids.

More than 600 well-preserved nummulitids from the lower Eocene of the Pyrenean area were measured and investigated to understand how and how much their hydrodynamic behavior influenced their distribution in a shallow water environment. Thin sections were made on the same sediments to crosscheck hydrodynamics with microfacies analysis.

The calculation used provides some parameters for a better definition of hydrodynamics of tests and of entire samples. Shape-independent parameters, which describe size of grains, are most suitable for correlation among different tests. A precise calculation of the shape factors for ellipsoidal tests helps in observing different hydrodynamic behaviors among tests belonging to the same taxon.

The settling velocity, here broadly used and discussed, is the only parameter really representing the particle in all its characteristics within an aquatic realm. As the equation to get the settling velocity considers density of the particle and its shape and volume (i.e., its size), the value obtained can be considered as the most important one to

understand many physical processes as transport, deposition and to have insight on the energy of the environment where the particle lies or has been transported in.

Together with the calculation of the Reynolds number and the drag coefficient, the settling velocity is a pivotal parameter to analyze and interpret particles accumulation and distribution with a correlation to the energetic input they have been deposited. Such analysis fits very well studies on nummulitid accumulations. On a geological profile, characterized by particularly abundance of nummulitids tests, the range of settling velocities of all the tests has been calculated for each layer. Such settling velocity range was used to evaluate the energy of the depositional environment, which was characterized by water depth variations and by transport mechanisms often altering the quality of the samples. Autochthonous from allochthonous material was differentiated thanks to the hydrodynamic compatibility of the taxa for each layer. The comparison with the bottom orbital velocity gives impressive results such as a quantitative definition of the water depth and of the energy of the environments in term of sea waves and currents occurrences producing depth transport.

ACKNOWLEDGEMENTS

REFERENCES

- Aigner, T., 1985, Biofabrics as dynamic indicators in nummulite accumulations: *Journal of Sedimentary Petrology*, v. 55(1), p. 131-134.
- Allen, J.R.L., 1984, Experiments on the settling, overturning and entrainment of bivalve shells and related models: *Sedimentology*, v. 31, p. 227–250.
- d'Archiac, A., and Haime, J., 1853, Description des animaux fossiles du groupe nummulitique de l'Inde, précédée d'un résumé géologique et d'une monographie des Nummulites, Gide et J. Baudry (eds.), Paris, 373 p.
- Beavington-Penney, S.J., 2004, Analysis of the effects of abrasion on the test of *Palaeonummulites venosus*: implications for the origin of Nummulithoclastic sediments: *Palaaios*, v. 19, p. 143–155.
- Beavington-Penney, S.J., Right, P.V., and Racey, A., 2005, Sediment production and dispersal on foraminifera-dominated early tertiary ramps: the Eocene el Garia Formation, Tunisia: *Sedimentology*, v, 52, p. 537-569.

- Briguglio, A., 2008, *Nummulites*: ein einfaches geometrisches Verfahren zur Bestimmung hydrodynamischer Parameter: *Berichte der Geologischen Bundesanstalt*, v. 75, p. 8. 14. Jahrestagung Österreichische Paläontologische Gesellschaft. Dornbirn.
- Briguglio, A., and Hohenegger J., 2009, Nummulitids hydrodynamics: an example using *Nummulites globulus* Leymerie, 1846: *Bollettino della Società Paleontologica Italiana*, v. 48(2), p. 105-111.
- Briguglio, A., Metscher, B., and Hohenegger, J., (in press) - Growth Rate Biometric Quantification by X-ray Microtomography on Larger Benthic Foraminifera: Three-dimensional Measurements push Nummulitids into the Fourth Dimension. *Turkish Journal of Earth Science*.
- Briguglio, A., and Hohenegger, J., 2010, Biostratinomy in shallow water environments: how to tackle the larger benthic foraminifera depth distribution. Third International Palaeontological Congress IPC3, London.
- Briguglio, A., and Forchielli, A., 2010, Transportability of Larger Benthic Foraminifera. Third International Palaeontological Congress IPC3, London.
- Buxton, M.W.N., and Pedley, H.M., 1989, Short paper: a standardised model for Tethyan Tertiary carbonate ramps: *Journal of the Geological Society of London*, v. 146, p. 746–748.
- Davies, G.R., 1970, Carbonate bank sedimentation, eastern Shark bay, Western Australia: *Memoir - American Association of Petroleum Geologists*, v.13, p.85-168.
- Decrouez, D., and Lanterno, E., 1979, Les "bancs a *Nummulites*" de l'Eocene mesogéen et leurs implications. The Nummulites banks of the Mesogaeic Eocene and their implications: *Archives des Sciences*, v. 32(1), p. 67-94.
- Eichenseer, H., and Luterbacher, H.P., 1992, The marine Palaeogene of the Tremp region (NE Spain) - depositional sequences, facies history biostratigraphy and controlling factors: *Facies*, v. 27, p. 119-152.
- Fichtel, L., and Moll, J.P.C., 1798, Testacea microscopica aliaque minuta ex generibus Argonauta et Nautilus ad naturam picta et descripta, in Rögl, F., and Hansen, H.J., 1984, Foraminifera described by Fichtel & Moll in 1798, A revision of Testacea Microscopica: *Neue Denkschriften des Naturhistorischen Museums in Wien*, v.3, p.1-143.

- Fluegel, E., 2004, Microfacies of carbonate rocks; analysis, interpretation and application: Springer, Berlin, 976 pp.
- Fonnesu, F. 1984: Estratigrafía física y análisis de facies de la secuencia de Figols entre el Rio Noguera Pallaresa e Iscles (provs. de Lerida y Huesca). Ph.D. Univ. Autònoma de Barcelona.
- Gross, M., Fritz, I., Piller, W.E., Soliman, A., Harzhauser, M., Hubmann, B., Moser, B., Scholger, R., Suttner, T.J., and Bojar, H., P., 2007, The Neogene of the Styrian Basin – *Guide to Excursions: Joannea –Geologie und Paläontologie*, v. 9, p. 117-193.
- Hallock, P., 1979, Trends in test shape with depth in large, symbiont bearing foraminifera: *Journal of Foraminiferal Research*, v. 9, p. 61–69.
- Hallock, P., and Hansen, H.J., 1979, Depth adaptation in *Amphistegina*: change in lamellar thickness: *Bulletin of the Geological Society of Denmark*, v. 27, p. 99–104.
- Heckel, P.H., 1972, Recognition of ancient shallow marine environments. In: Recognition of ancient sedimentary environments (Ed. by Stow, D.A.V. & Piper, D.J.W.). *Special Publications SEPM* v. 16, p. 226-286.
- Hofmann, H.J., 1994, Grain-shape indices and isometric graphs: *Journal of Sedimentary Research* v. 64(4), p. 916- 920.
- Hohenegger, J., 2000, Coenoclines of larger foraminifera: *Micropalaeontology*, v. 46 (1), p. 127-151.
- Hohenegger, J., 2004, Depth coenoclines and environmental consideration of Western Pacific larger foraminifera: *Journal of Foraminiferal Research*, v. 34, p. 9–33.
- Hohenegger, J., Yordanova, E., Nakano, Y., and Tatzreiter, F., 1999, Habitats of larger foraminifera on the upper reef slope of Sesoko Island, Okinawa, Japan: *Marine Micropalaeontology*, v. 36, p. 109–168.
- Hohenegger, J., and Yordanova, E., 2001a, Displacement of larger foraminifera at the western slope of Motobu Peninsula (Okinawa, Japan): *Palaios*, v. 16, p. 53–72.
- Hohenegger, J., and Yordanova, E., 2001b, Depth-transport functions and erosion-deposition diagrams as indicators of slope inclination and time – averaged traction forces: application in tropical reef environments: *Sedimentology*, v. 48, p. 1025–1046.

- Hollaus, S.S., and Hottinger, L., 1997, Temperature dependence of endosymbiotic relationships. Evidence from the depth range of Mediterranean *Amphistegina lessonii* (Foraminiferida) truncated by the thermocline: *Eclogae geologicae Helveticae*, v. 90, p. 591–597.
- Holzmann, M., Hohenegger, J., Hallock, P., Piller, W.E., and Pawlowski, J., 2001, Molecular phylogeny of large miliolid foraminifera (Soritacea Ehrenberg 1839). *Marine Micropaleontology*, v. 43, p. 57–74.
- Hottinger, L. 1960, Recherches sur les Alveolines paleocene et eocene. *Memoire suisse de Paleontologie*, v. 75-76.
- Hottinger, L., 2000, Functional morphology of benthic foraminiferal shells, envelopes of cells beyond measure: *Micropaleontology*, v. 46(1), p. 57-86.
- Hottinger, L., and Krusat, G., 1972, Un foraminifère nouveau intermédiaire entre *Opertorbitolites* et *Somalina* de l'Ilerdien pyrénéen: *Revista Española de Micropaleontologia*, Núm. Extraord. XXX Anivers. Empr. Nac. Adaro, Diciembre 1972, p. 249-271.
- Jorry, S.J., Hasler, C.A., and Davaud, E., 2006, Hydrodynamic behaviour of *Nummulites*: implication for depositional models: *Facies*, v. 52 p. 221-235.
- Langer M.R., and Hottinger, L., 2000, Biogeography of selected 'larger' foraminifera: *Micropaleontology*, v. 46, suppl. 1, p. 105–126.
- Larsen A.R., and Drooger, C.W., 1977, Relative thickness of the test in the *Amphistegina* species of the Gulf of Elat: *Utrecht Micropalaeontological Bulletin*, v. 15, p. 225–239.
- Le Roux, J.P., 1996, Settling velocity of ellipsoidal grains as related to shape entropy: *Sedimentary Geology*, v. 101(1), p. 15-20.
- Le Roux, J.P., 1997, An Excel program for computing the dynamic properties of particles in newtonian fluids: *Computers and Geosciences*, v. 23(6) p. 671-675.
- Le Roux, J.P., 2005, Grains in motion: A review: *Sedimentary Geology*, v. 178, p. 285–313.
- Leutenegger, S., and Hansen, H.J., 1979, Ultrastructure and radiotracer studies of pore function in Foraminifera: *Marine Biology*, v. 54, p. 11–16.
- Leymerie, A., 1846 Mémoire sur le terrain à Nummulites (épicrotacé) des Corbières et de la Montagne Noire: *Mémoires de la Société Géologique de France*, v. 1(2), p. 337-373.

- Luterbacher, H.P., 1969, Remarques sur la position stratigraphique de la Formation d'Ager (Pyrenees meridionales). *Mémoires. Bureau de Recherches Géologique et Minières*, v. 69/III, p. 225-231.
- Luterbacher, H.P., 1970, Environmental distribution of Early Tertiary microfossils, Tremp Basin, northeastern Spain: ESSO Production Research-European Laboratories. Houston, Texas.
- Luterbacher, H.P. 1973: La seccion tipo del Piso Ilerdiense: *Acta XIII Colloquio Europeo de Micropaleontologia*, Espana, e.N.G. ENADIMSA, Madrid, 113-140.
- Luterbacher, H.P., Eichenseer, H., Betzler, Ch. and Van den Hurk, A.M., 1991, Carbonate siliciclastic depositional systems in the Paleogene of the South Pyreneen foreland basin: a sequence-stratigraphic approach. In: Sedimentation, tectonics and eustasy (Ed. by Macdonald, D.I.M.). *Special Publication of the International Association of Sedimentology*, v. 12, p. 351-407.
- Martin, R.E., and Liddell, W.D., 1991, The taphonomy of Foraminifera in modern carbonate environments: implications for the formation of foraminiferal assemblages. In: The Processes of Fossilization (Ed. S.K. Donovan), Belhaven, London, p. 170–193.
- Massieux, M., 1973, Micropaléontologie stratigraphique de l'Eocène des Corbières septentrionales (Aude): *Cahiers Paléontologie*, CNRS, Paris, 146 pp.
- Mey, P.H.W., Nagtegaal, P.J.C., and Roberti, K.J., 1968, Lithostratigraphic subdivision of post-hercynian deposits in the south-central Pyrenees, Spain: *Leidse geol. Meded*, v. 41, p. 221-228.
- Mutti, E., Luterbacher, H.P., Ferrer, J. and Rosell, J., 1972, Schema stratigrafico e lineamenti di facies del Paleogene marino della Zona Centrale Sud-Pirenaica tra Tremp (Catalogna) e Pamplona (Navarra): *Memorie della Società Geologica Italiana*, v. 11, p. 391-416.
- Mutti, E., Rosell, J., Alien, G.P., Fomesu, F. and Sgavetti M., 1985, Stratigraphy and facies characteristics of the Eocene Hecho Group turbidite systems, south-central Pyrenees. In: Excursion guidebook: VI European Regional Meeting, Lerida Spain, Excursion 13 (Ed. by Mila, M.D. & Rosell, J.), p. 579-600.

- Mutti, E., Seguret, M., and Sgavetti, M., 1988, Sedimentation and deformation in the Tertiary sequences of the southern Pyrenees: AAPG Mediterranean Basin Conference, Special Publication, Università di Parma, Field trip 7.
- Mutti, E., and Sgavetti, M., 1994, Main stratigraphic units of the upper Cretaceous and Paleogene strata of the eastern sector of the south-central Pyrenees. In: The eastern sector of the southcentral folded pyrenean foreland: criteria for stratigraphic analysis and excursion notes (Ed. by Mutti, E., Davoli, G., Mora, S., and Sgavetti, M.): Second high-resolution Sequence Stratigraphy Congress, Tremp, Spain, p. 17-23.
- Mutti, E., Dattilo, P., Sgavetti, M., Tebaldi, E., Busatta, C., Mora, S., and Mutti, M., 1994: Sequence stratigraphic response to thrust propagation in the upper Cretaceous Aren Group, southcentral Pyrenees. In: The eastern sector of the southcentral folded pyrenean foreland: criteria for stratigraphic analysis and excursion notes (Ed. by Mutti, E., Davoli, G., Mora, S., and Sgavetti, M.): Second high-resolution Sequence Stratigraphy Congress, Tremp, Spain, p. 25-36.
- Nijman, W., and Nio, S.D., 1975, The Eocene Montaniana delta (Tremp-Graus basin, provinces of Lerida and Huesca, southern Pyrenees, N. Spain). In: The sedimentary evolution of the Paleogene South-Pyrenean basin. Part B (Ed. by Rosell, J., and Puigdefabregas, C.). XI International Congress IAS, Nice, France, p. 1-20.
- Nobes, K., Uthike, S., and Henderson, R., 2008, Is light the limiting factor for the distribution of benthic symbiont bearing foraminifera on the Great Barrier Reef?: *Journal of Experimental Marine Biology and Ecology*, v. 363, p. 48–57.
- d'Orbigny, A., 1850, Prodrôme de Paléontologie stratigraphique universelle des animaux mollusques et rayonnés. 1, i-lx + 1-392; 2, 1-427. V. Masson, Paris.
- Plaziat, J.C., 1984, Le Domaine Pyreneen de la fin du Cretace ala fin de l'Eocene - stratigraphie, paleoenvironnements et evolution paleogeographique. These Univ. Paris-Sud, France.
- Pye, K., 1994, Properties of sediment particles, in: *Sediment Transport and Depositional Processes*, K. Pye (ed.), Blackwell, Oxford, p. 1–24.
- Racey, 2001, A review of Eocene nummulite accumulations: structure, formation and reservoir potential: *Journal of Petroleum Geology*, v. 24(1), p. 79-100.

- Renema, W., 2005, Depth estimation using diameter-thickness ratios in larger benthic foraminifera: *Lethaia*, v. 38, p. 137–141.
- Schaub, H., 1951, Stratigraphie und Paläontologie des Schlierenflysches mit besonderer Berücksichtigung der palaeocaenen und untereocaenen Nummuliten und Assilinen. *Schweizerische Paläontologische Abhandlungen*, v. 68, 222 p.
- Schaub, H., 1981, Nummulites et Assilines de la Téthys paléogène. Taxinomie, phylogénese et biostratigraphie. *Schweizerische Paläontologische Abhandlungen*, v. 104, 236 p.
- Serra-Kiel, J., Hottinger, L., Caus, E., Drobne, K., Ferràndez, C., Jauhri, A. K., Less, G., Pavlovec, R., Pignatti, J.S., Samsó, J.M., Schaub, H., Sirel, E., Strougo, A., Tambareau, Y., Tosquella J. and Zakrevskaya E. (1998) – Larger foraminiferal biostratigraphy of the Thethyan Paleocene and Eocene: *Bulletin de la Societe Géologique de France*, v. 169(2), p. 281-299.
- Soulsby, R., 1997, Dynamic of marine sands: Thomas Telford (ed.), 249 p.
- Tosquella, J., and Serra-Kiel, J., 1996, Las biozonas de nummulitidos del Eoceno Pirenaico: *Principe de Viana - Suplemento de Ciencias*, v. 14/15, p. 155-193.
- Wadell, H., 1932, Volume, shape, and roundness of rock particles: *Journal of Geology*, v. 40, p. 443–451.
- Waehry, A.C, 1999, Facies analysis and physical stratigraphy of the Ilerdian in the eastern Tremp-Graus Basin (south central Pyrenees, Spain): *Terre & Environnement*, v. 15, XII + 191 p.
- Wilson, J.L., 1975 Carbonate facies in geologic history: Berlin- Heidelberg- New York, Springer, 471 p.
- Yordanova, E.K., and Hohenegger, J., 2002, Taphonomy of larger foraminifera: Relationships between living individuals and empty tests on flat reef slopes (Sesoko Island, Japan): *Facies*, v. 46, 169–204.
- Yordanova, E.K., and Hohenegger, J., 2007, Studies on settling, traction and entrainment of larger benthic foraminiferal tests: implication for accumulation in shallow marine sediments: *Sedimentology*, v. 54(6), p. 1273-1306.

TABLES

TABLE 1

Sample: 08032

1. *Alveolina aragonensis* (Hottinger, 1960);
2. *Alveolina sp.*;
3. *Orbitolites sp.* and *Opertorbitolites transitorius* (Hottinger & Krusat, 1972);
4. *Alveolina aragonensis* (Hottinger, 1960);
5. *Opertorbitolites sp.* and miliolids;
6. *Opertorbitolites latimarginalis* (Lehman);
7. facies characteristic wackestone;
8. facies characteristic wackestone;

Scale bar: 1 mm

Table 1

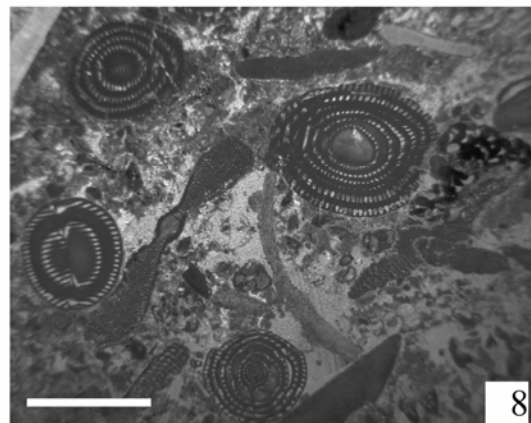
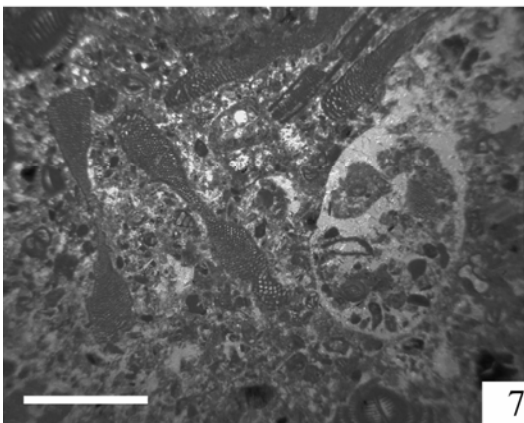
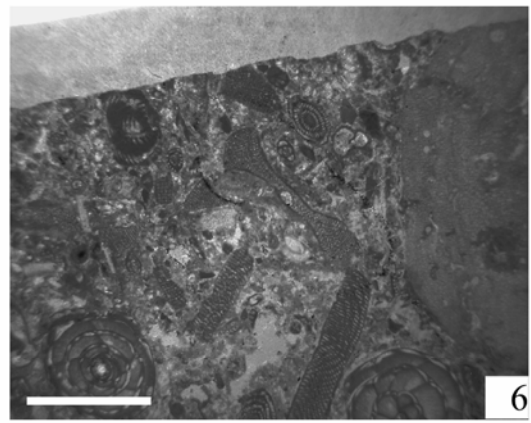
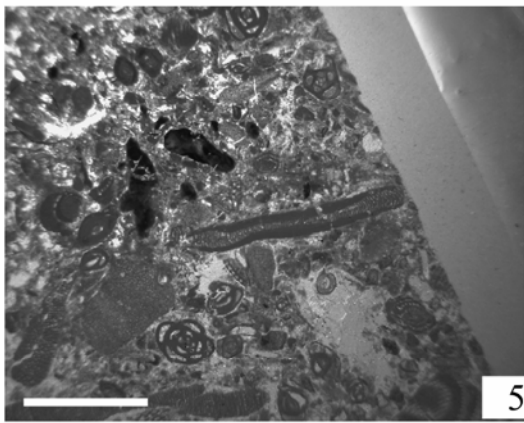
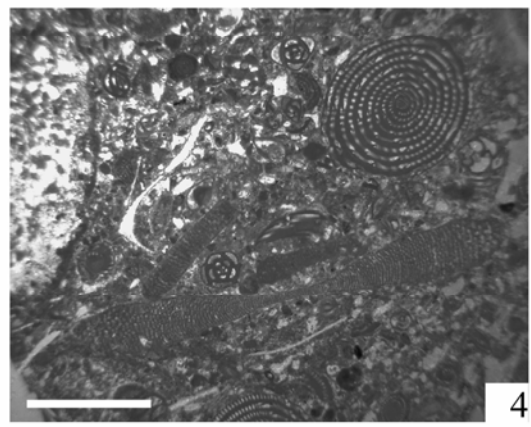
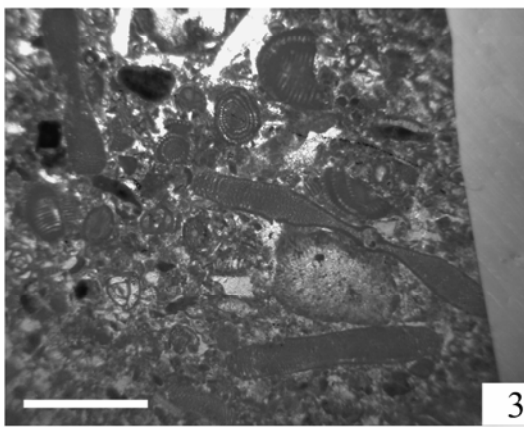
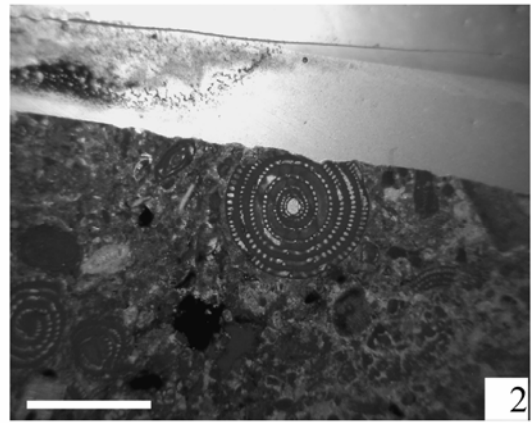
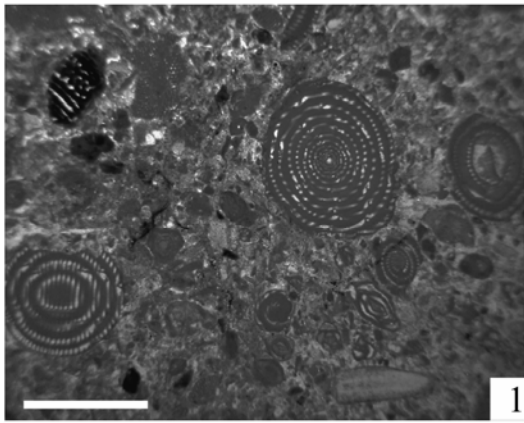


TABLE 2

Sample: Slu5 (1-5);

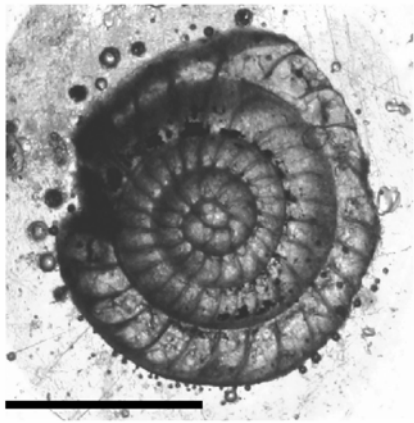
Sample: Slu6 (6);

Sample: Slu7 (7).

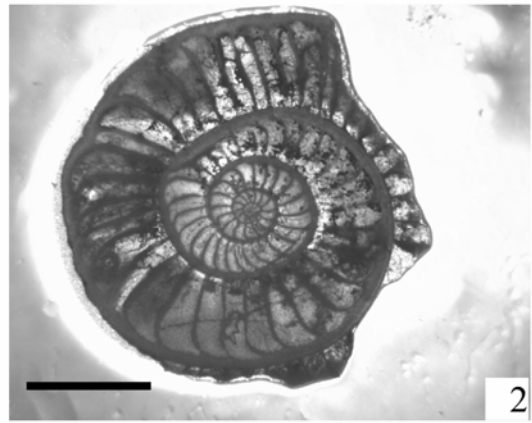
1. *Nummulites soerenbergensis* (Schaub, 1951);
2. *Assilina ammonia ammonia* (ex *Operculina*) (Leymerie, 1846);
3. *Assilina subgranulosa* (Ex *Operculina*) (d'Orbigny, 1850);
4. *Assilina subgranulosa* (Ex *Operculina*) (d'Orbigny, 1850);
5. *Assilina ammonia ammonia* (ex *Operculina*) (Leymerie, 1846);
6. *Operculina douvillei* (Doncieux, 1962);
7. *Assilina leymeriei* (d'Archiac & Haime, 1853).

Scale bar: 1 mm

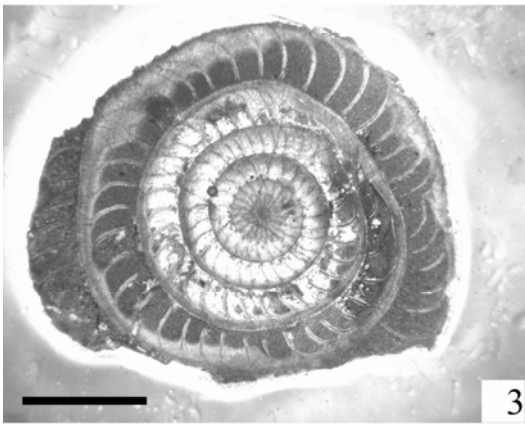
Table 2



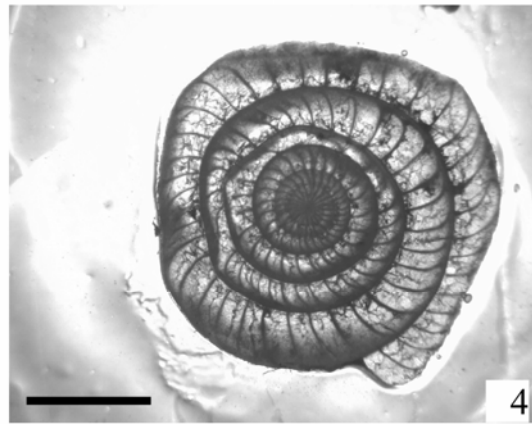
1



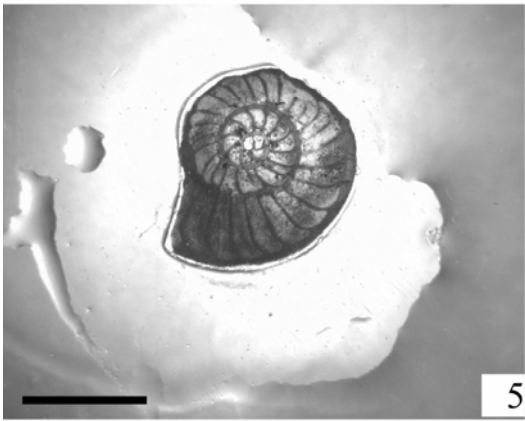
2



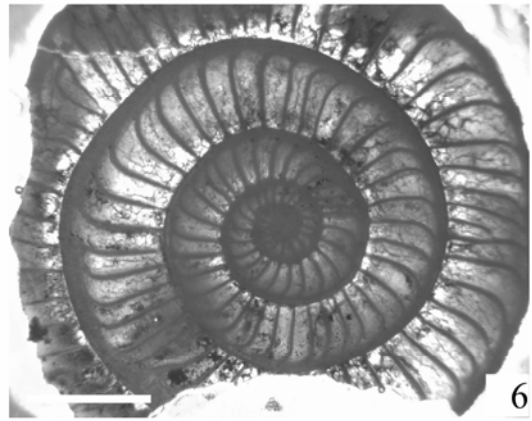
3



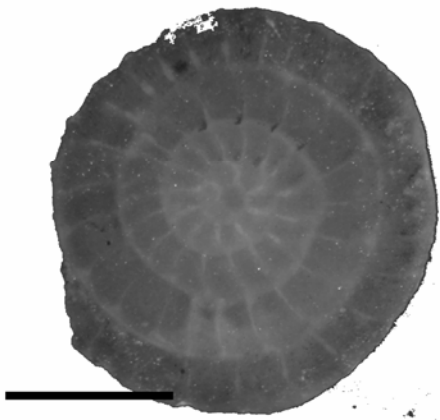
4



5



6



7

TABLE 3

Sample: 08034

1. Well-preserved discocyclinids and poorly preserved larger nummulitids;
2. rarely broken operculinids and common discocyclinids;
3. bioclastic debris with abundant broken and damaged nummulitids tests;
4. bioclastic wackestone;
5. well-preserved large operculinids;
6. well-preserved large operculinids and broken nummulitids tests;
7. wackestone with discocyclinids and larger bioturbated nummulitids;
8. nummulithoclast.

Scale bar: 1 mm

Table 3

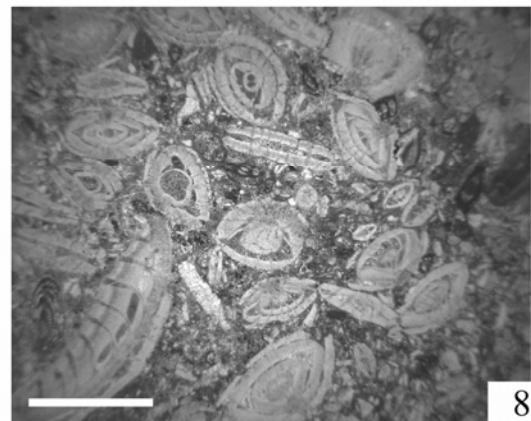
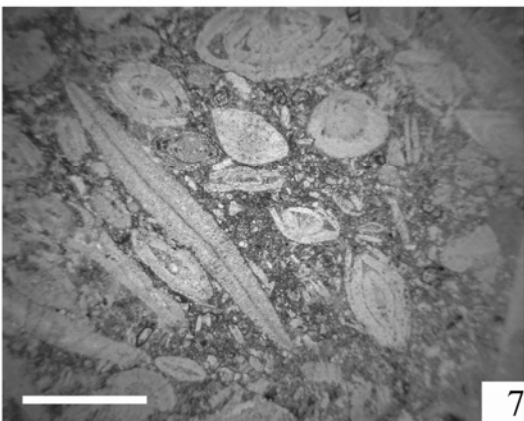
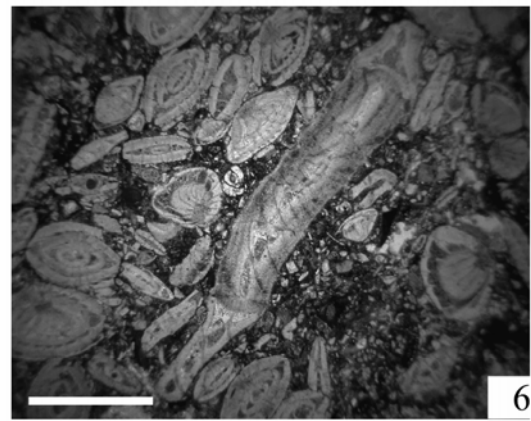
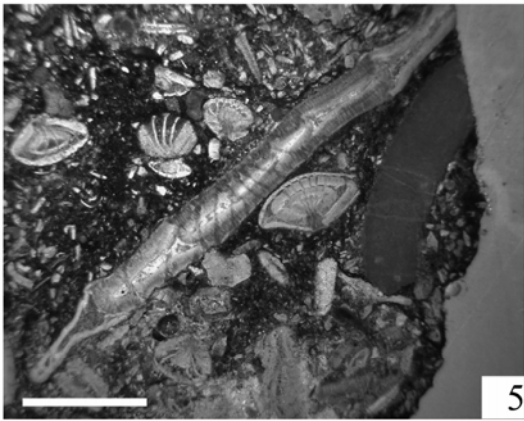
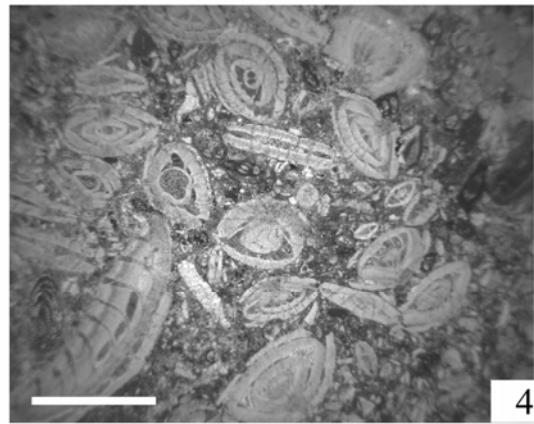
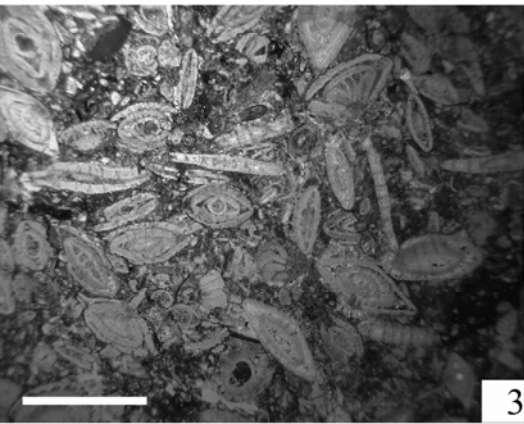
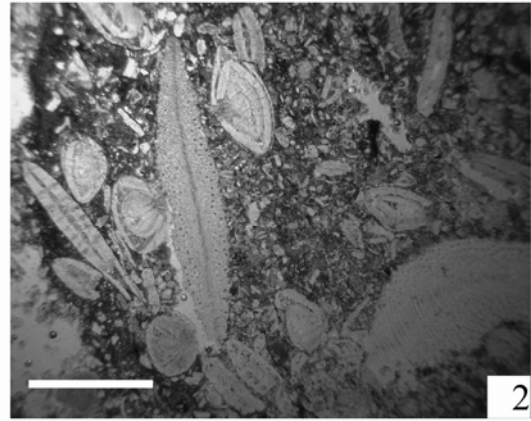
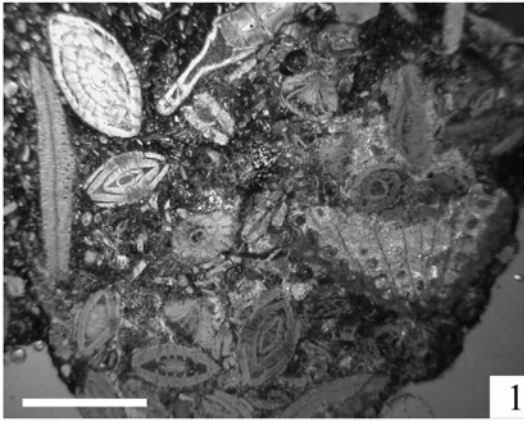


TABLE 4

Sample: 08046

1. *Assilina (leymeriei?)*;
2. bioturbation tracks on nummulitids B form;
3. bioclastic debris with rounded broken nummulitids;
4. wackestone with broken larger nummulitids tests;
5. *Nummulites globulus* (Leymerie, 1846);
6. well-preserved small nummulitids and poorly preserved larger tests;
7. wackestone with larger broken nummulitids tests, orbitolinids occur;
8. well-preserved operculinids and broken nummulitids tests.

Scale bar: 1 mm

Table 4

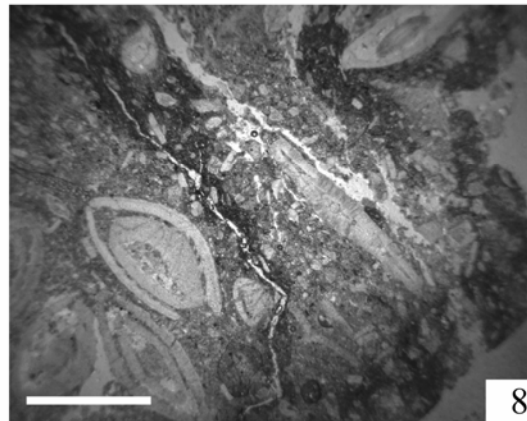
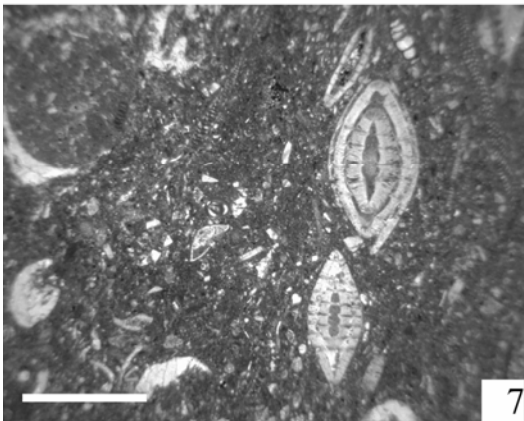
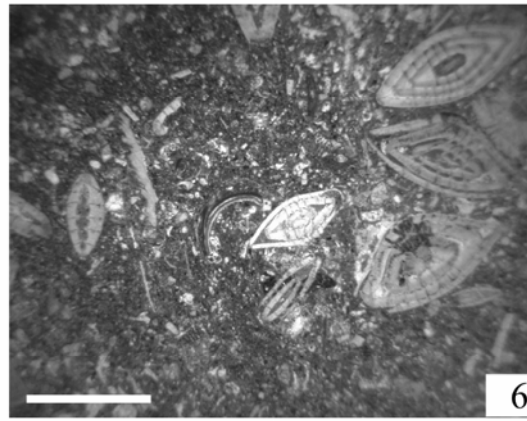
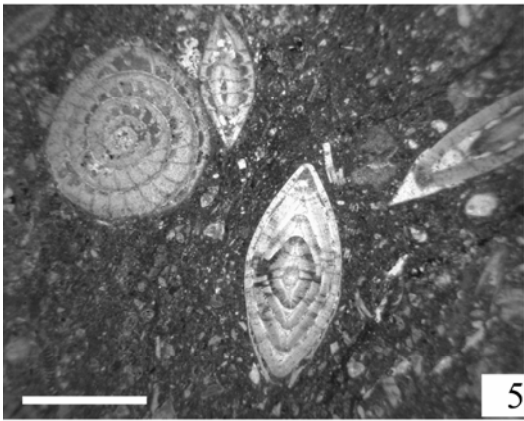
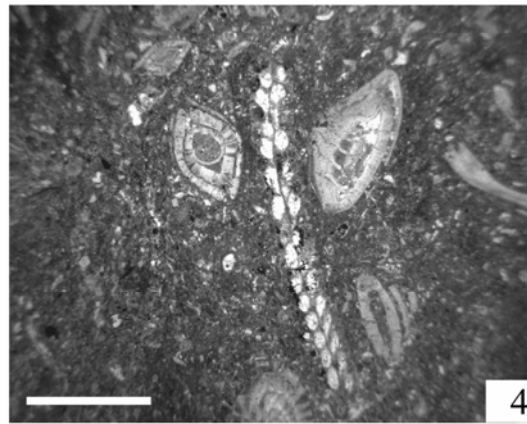
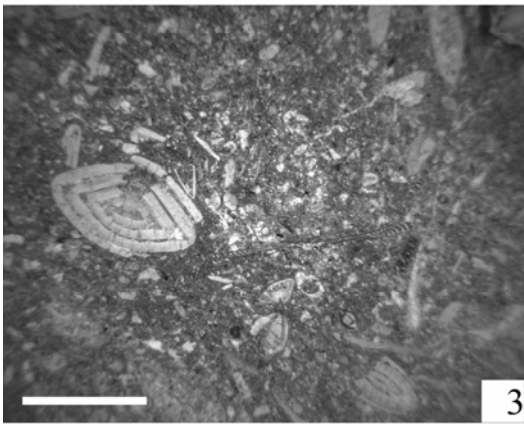
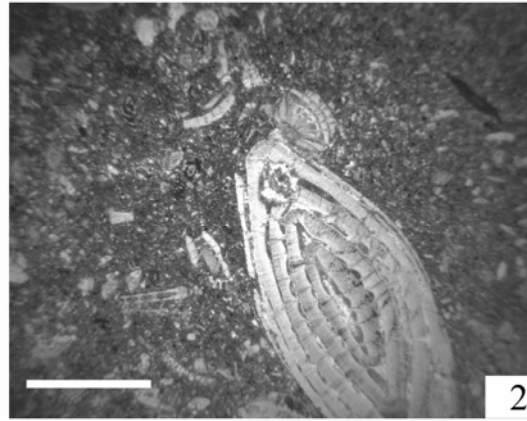
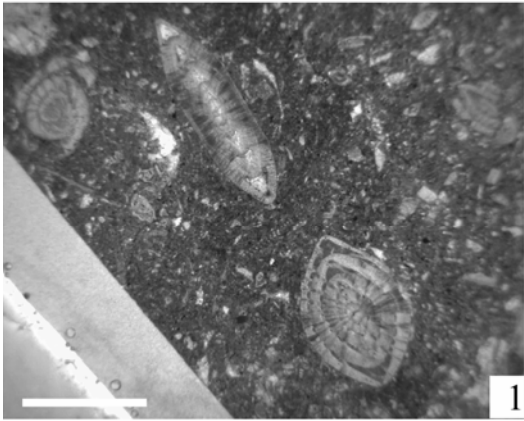


TABLE 5

Sample: 08047

1. Bioclastic debris with well-preserved small nummulitids;
2. wackestone with well-preserved small nummulitids and middle sized to large operculinids;
3. wackestone with *Nummulites soerenbergensis* (Schaub, 1951) and *N. globulus* (Leymerie, 1846);
4. operculinids with a much finer matrix testifying low energy environments;
5. bioclastic debris with *Assilina ammonica* (Leymerie, 1846);
6. example of facies;
7. broken nummulitids and well-preserved operculinids.

Scale bar: 1 mm

Table 5

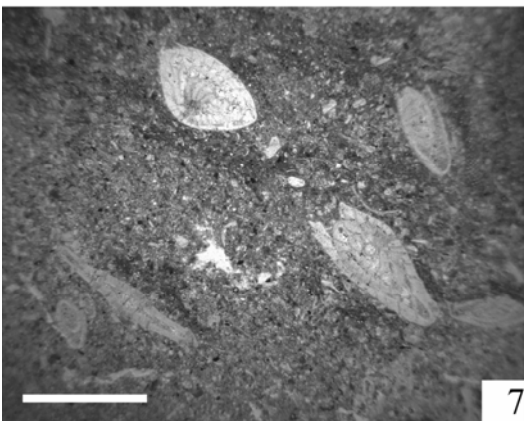
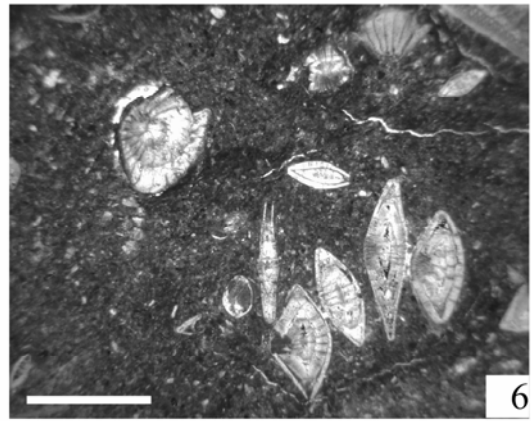
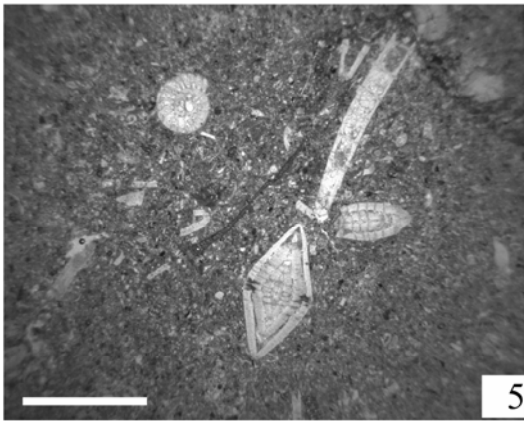
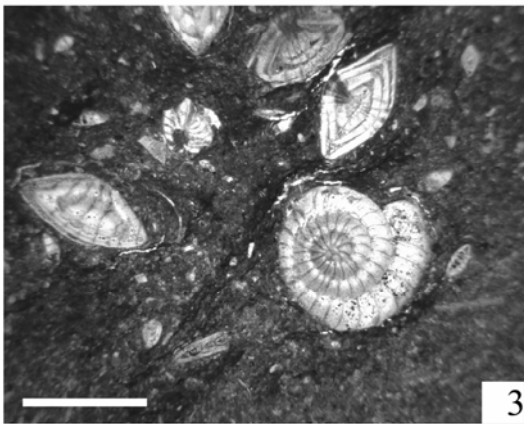
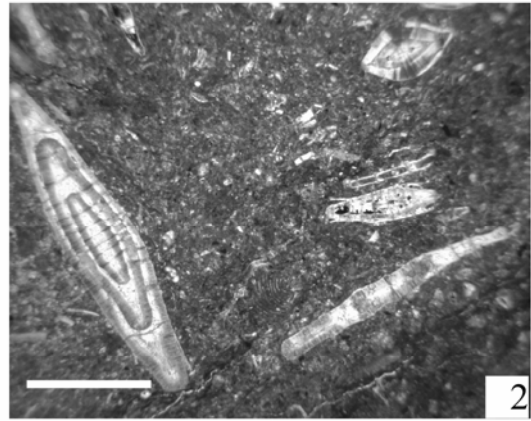
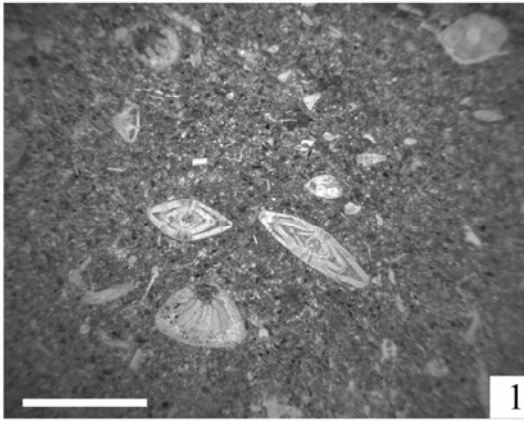


TABLE 6

Sample: 08048

1. Wackestone with poorly-preserved alveolinids and larger nummulitids;
2. broken nummulitids tests within a bioclastic debris;
3. poorly-preserved assilinids and nummulitids;
4. facies example;
5. well-preserved small nummulitids and small operculinids;
6. bioturbated larger nummulitid test;
7. nummulithoclast;
8. well-preserved discocyclinids within a bioclastic wackestone.

Scale bar: 1 mm

Table 6

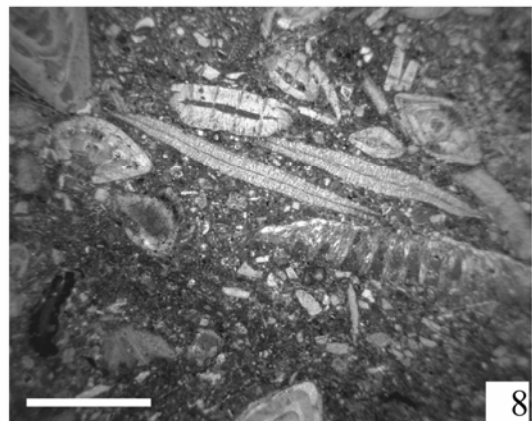
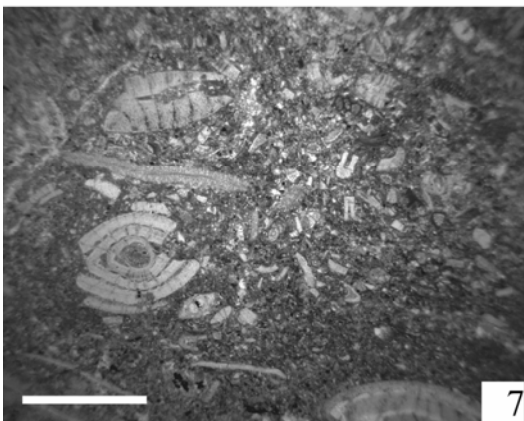
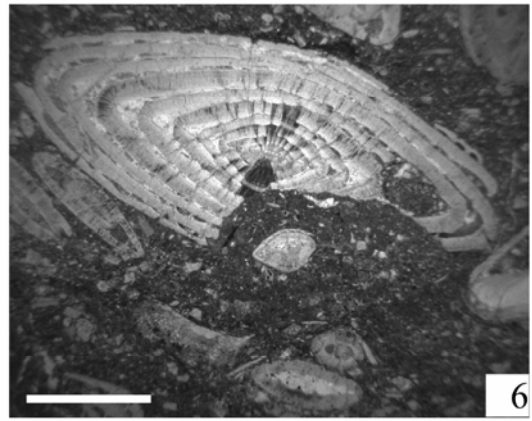
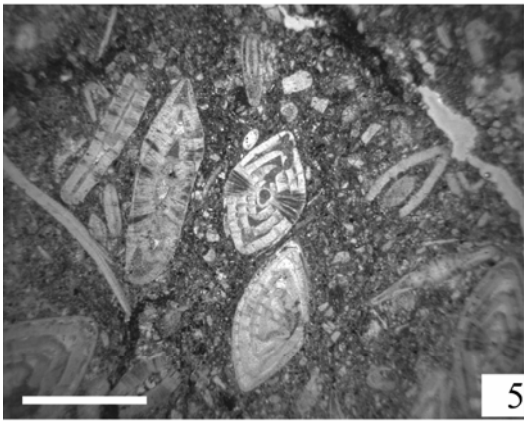
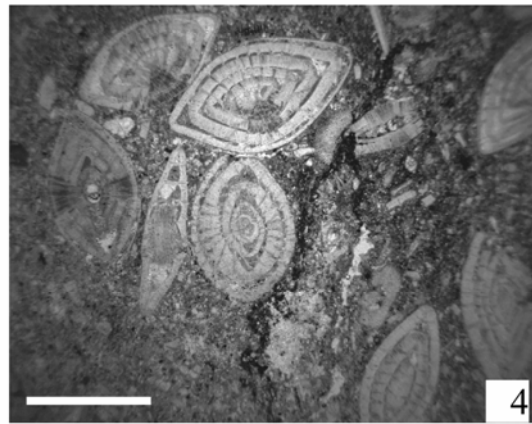
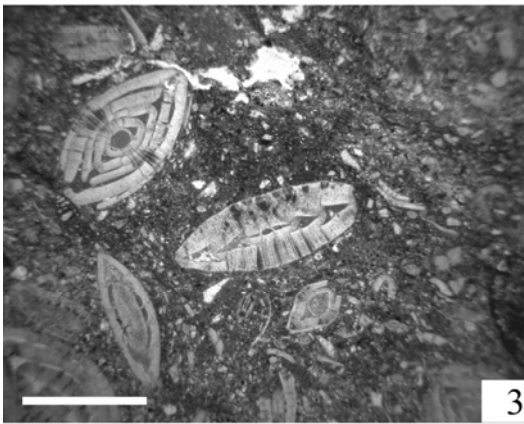
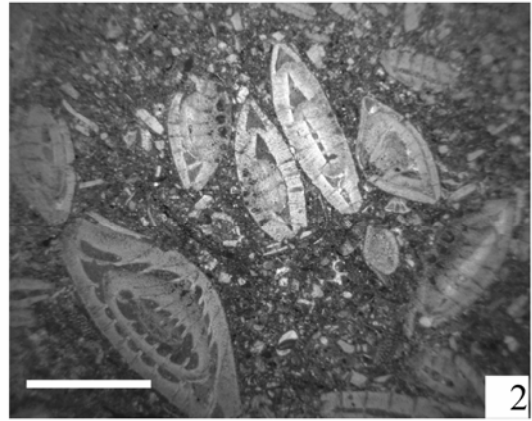
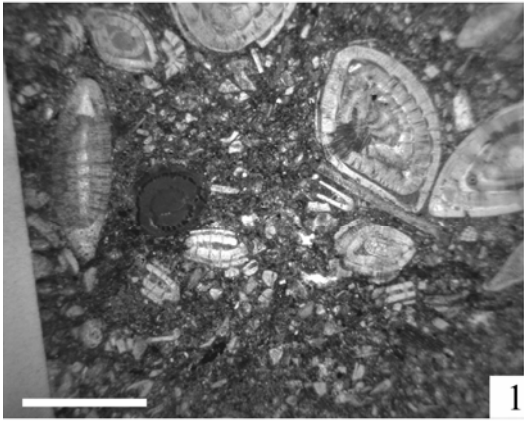


TABLE 7

1. Wackestone with nummulitids;
2. bioturbated large nummulitid test;
3. broken and bioturbated nummulitid test;
4. transported alveolinids with well-preserved nummulitids;
5. bioturbated larger nummulitid test;
6. broken and bioturbated nummulitid test;
7. *Nummulites globulus* (Leymerie, 1846) and *Assilina ammonica* (Leymerie, 1846);
8. facies example.

Scale bar: 1 mm

Table 7

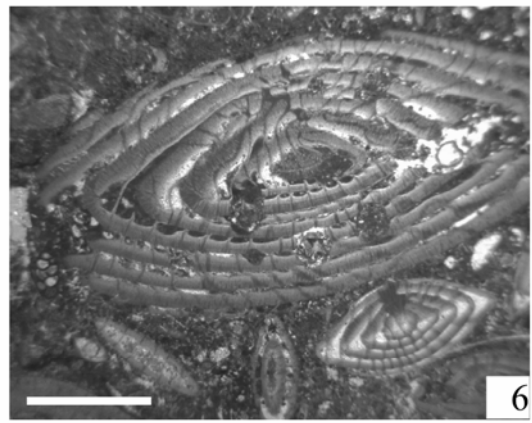
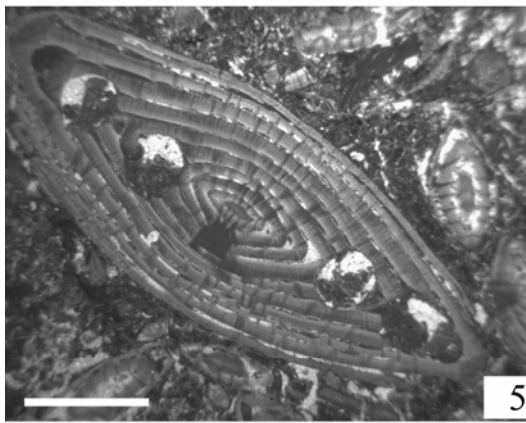
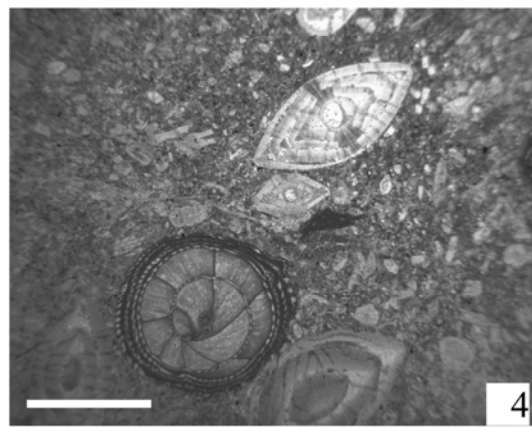
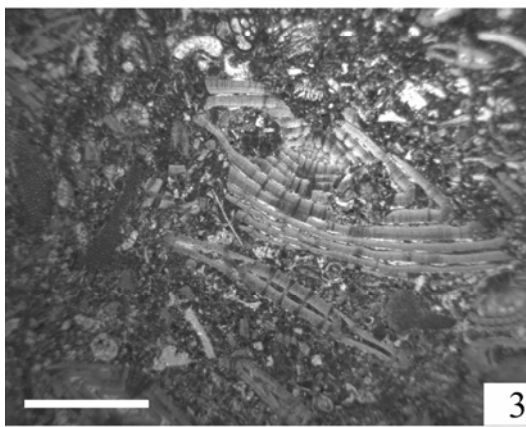
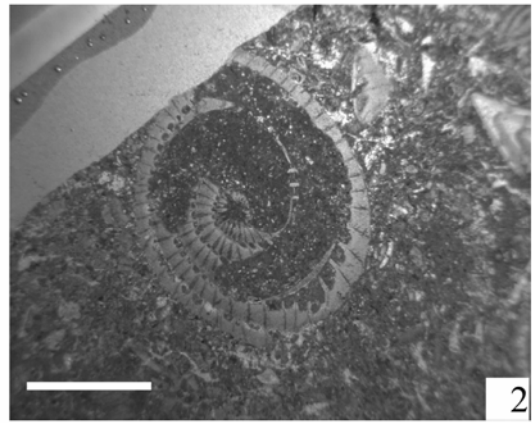
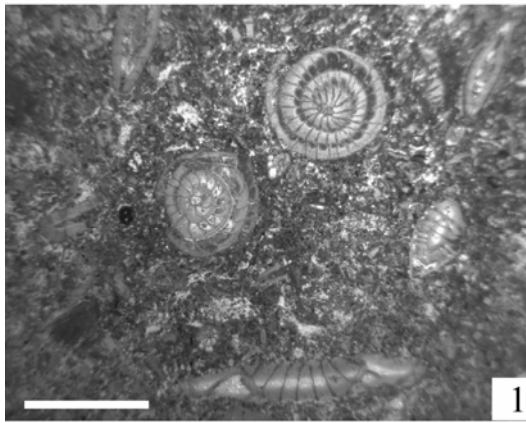
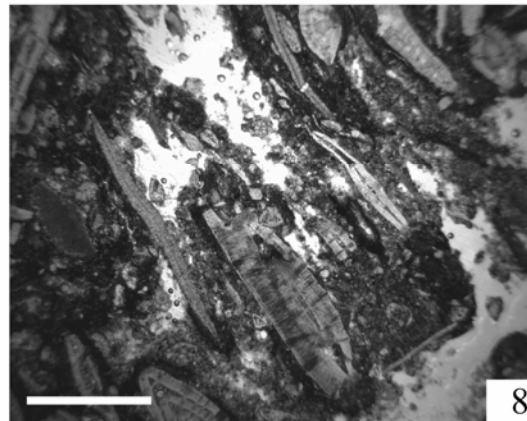
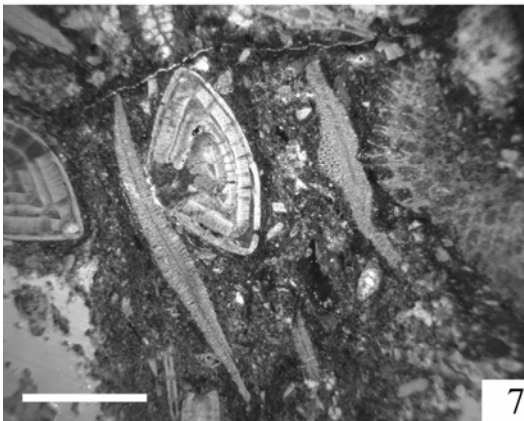
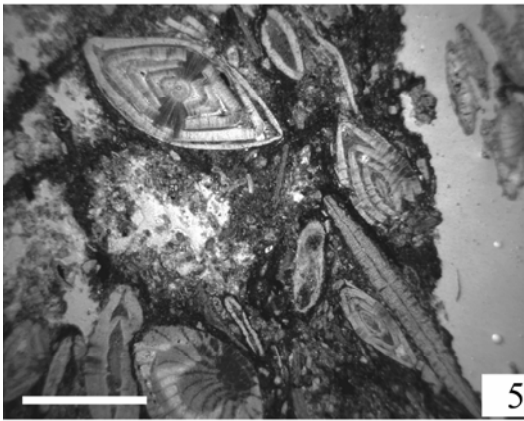
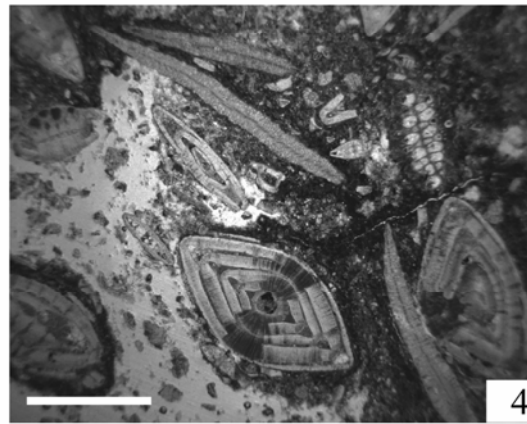
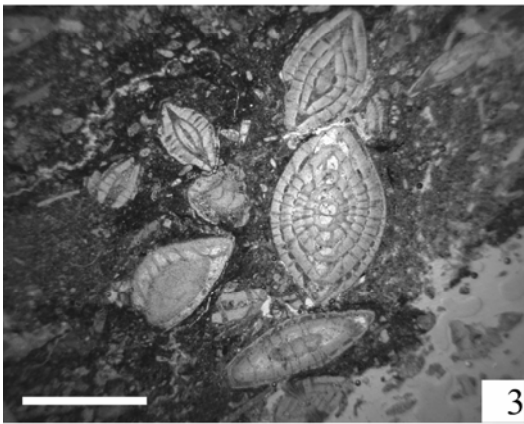
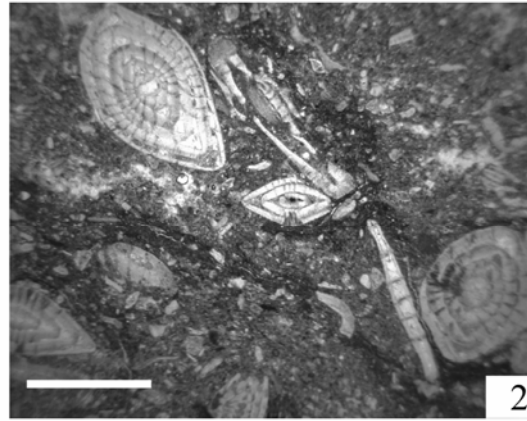
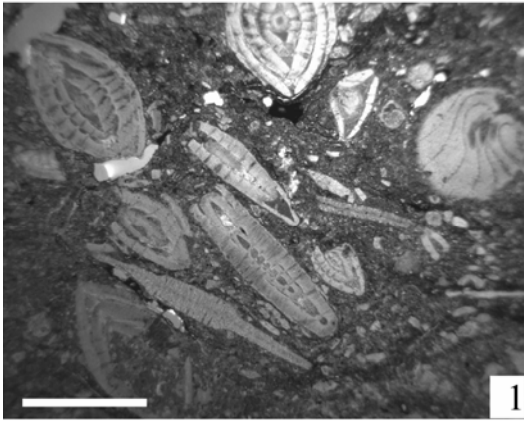


TABLE 8

1. Wackestone with broken nummulitids, and well-preserved discocyclinids;
2. well-preserved small operculinids and broken nummulitid tests;
3. facies example;
4. wackestone with well-preserved discocyclinids and abraded nummulitids;
5. wackestone with broken nummulitids, and well-preserved discocyclinids;
6. well-preserved operculinids (probably transported);
7. wackestone with well-preserved discocyclinids and abraded nummulitids;
8. well-preserved discocyclinids within a bioclastic debris.

Scale bar: 1 mm

Table 8



APPENDIX A

1	B	C	D	E
2	value	unit	definition	Excel formula
3				
4	g	cm/(sec ²)	gravity constant	981.0327
5	ρ_s	g/cm ³	density of the test	insert value
6	ρ_f	g/cm ³	density of the water	1.025
7	μ	Pa*s	dynamic viscosity	0.0108
8	μ^2	(Pa*s) ²		=E7^2
9	constant of Wd		to calculate Wd	=4.731*10^-6
10	constant of Ws		to calculate Ws	=((E6^2)/(E7*E4*(E5-E6))^(1/3))
11	constant of Dd		to calculate Dd	=(E6*E4*(E5-E6)/E8)^(1/3)
12	constant v		to calculate v	=(2*E4*(E5-E6))/E6
13	L	mm	major diameter	insert value
14	L	cm	major diameter	=E13/10
15	l	mm	intermediate diameter	insert value
16	l	cm	intermediate diameter	=E15/10
17	S	mm	minor diameter	insert value
18	S	cm	minor diameter	=E17/10
19	area eq	mm ²	area calculated on the equatorial section	=PI()*(((E13+E15)/2)^2)

Appendix A

20	area ax	mm ²	area calculated on the axial section	=E13*E17/2
21	V	mm ³	volume	=E19*E20/E13
22	V	cm ³	volume	=E21/1000
23	TND	mm	True Nominal Diameter	=2*(((3*E21)/(PI()*4))^(1/3))
24	TND	cm	True Nominal Diameter	=2*(((3*E22)/(PI()*4))^(1/3))
25	Dd		Dimensionless Size of the Equivalen Sphere	=((E14*E16*E18)^(1/3))*E\$11
26	Dn	cm	True Nominal Diameter according to Le Roux (1997)	=((E14*E16*E18)^(1/3))
27	Wd		Dimensionless Sphere Settling Velocity	=0.375+0.29*E25-0.002*(E25^2)+E\$9*(E25^3)
28	β		Critical Shear Stress	=0.029+0.003*(E27)-9.935*0.00001*(E27^2)
29	Uc*	cm/sec	Critical Shear Velocity	=1.959+0.253*SQRT(((D28*D4)*((D14*D16*D18)^(1/3))/1.32))*((D5-D6)/D6))
30	P _i		Proportion of the Axes	=E13/(E\$15+E\$13+E\$17)
31	P _i		Proportion of the Axes	=E15/(E\$15+E\$13+E\$17)

Appendix A

32	Ps		Proportion of the Axes	=E17/(E\$15+E\$13+E\$17)
33	Hr		Shape Entropy	=- ((D30*LN(D30))+D31*LN(D31))+D32*LN(D32))/1.0986
34	Ws	cm/sec	Settling Velocity of the Equivalent Sphere	=E27/E\$10
35	We	cm/sec	Settling Velocity of a non Spherical Grain	=E34*((E33-0.5833)/0.4167)
36	Re We		Reynold Number Calculated with We	=(E\$6*E14*E35)/E\$7
37	Cd		Drag Coefficient	=(4*E24*E\$4*(E\$5-E\$6))/(3*E\$6*(E34^2))
38	S. height	cm	Slant height	=SQRT(((E14/2)^2)+((E18/2)^2))
39	A	cm ²	Area of the Shell Contrasting Water During Sinking	=(PI()*(E14/2)*((E14/2)+E38))/2
40	v	cm/sec	Settling Velocity	=SQRT(E\$12*E22/(E37*E39))
41	Re Ws		Reynold Number Calculated with Ws	=(E\$6*E14*E34)/E\$7
42	Re v		Reynold Number Calculated with v	=(E\$6*E14*E40)/E\$7

Felix qui potuit rerum cognoscere causas

Publius Vergilius Marus: *Georgica*, II, 490

CURRICULUM VITAE

ANTONINO BRIGUGLIO

Personal:

born: 25.11.1981
nationality: Italian
Marital status: single
Address: Muthgasse 66/127 A-1190 Vienna, Austria
Phone: ++43-1-4277/53546
Mobile: ++43-681-10542198
Email: antonino.briguglio@univie.ac.at
Web: <http://www.girmm.com/staff/antonino/antonino.html>

Education:

Oct 2007 - now PhD at the University of Vienna, Department of Palaeontology

Research Topic: Hydrodynamic behaviour of Larger Benthic Foraminifera.
Supervisor: Ao. Prof. Dr. Johann Hohenegger

Oct 2000 - Dec 2006 Master of Science in Geology (108/110): University of Rome "La Sapienza" Department of Earth Science.
Major Degree Thesis in Micropalaeontology:
Biostratigraphy of Upper Eocene and Oligocene of Majella Mountain (central Italy) with special reference to larger Foraminifers and Corals.
Supervisor: Prof. Dr. Johannes Pignatti
Minor Degree Thesis in Applied Geophysics:
Seismic line in the area of "Caldera di Latera" (Vt)
Supervisor: Dr. Michele di Filippo.

Aug 2000 - Sept 1994 Scientific High School (Liceo Scientifico Statale) Augusto Righi (80/100). Rome, Italy

Work Experience:

Apr 2007 - now Scientific Assistant (*Assistent in Ausbildung*) at the Universität Wien (University of Vienna) in the department of Palaeontology.

Teaching classes

Winter 2007/2008
280492 UE Stratigraphie, Erdgeschichte und Phylogenie (BA16) Teil 1 (PI) - (= BPB 11)
280468 UE Paläobiodiversität (BA04) STEP (PI)
Summer 2008
280025 PR+EX Fossilisation und Paläoökologie

(BA29) (PI)

280046 UE Angewandte Mikropaläontologie

(PP0_28_20) (PI)

Summer 2009

280008 UE Paläobiodiversität (BA04) STEP (PI)

280033 UE Stratigraphie, Erdgeschichte und
Phylogenie (BA16) Teil 2 (PI)

280058 PR+EX Fossilisation und Paläoökologie
(BA29) (PI)

280098 UE Angewandte Mikropaläontologie
(PP0_28_20) (PI)

Summer 2010

280008 UE Paläobiodiversität (BA04) STEP (PI)

280033 UE Stratigraphie, Erdgeschichte und
Phylogenie (BA16) Teil 2 (PI)

280058 PR+EX Fossilisation und Paläoökologie
(BA29) (PI)

280098 UE Angewandte Mikropaläontologie
(PP0_28_20) (PI)

Known languages

English: oral and written very good

German: oral and written very good

Latin: written good

Spanish: basics

Italian: mother tongue

Skills

Software Applications: all MS-Office applications, Windows, statistics (SPSS, Past), 3D imaging and computed microtomography softwares, image processing (Adobe Photoshop, ACD Canvas), w.w.w. and computer mechanics.

Conferences – Symposia - Workshops

2010

W.O.L.F. Working Group on Larger Foraminifera, first meeting. *New insights in shallow marine tropical stratigraphy: integrating progress over the past ten years*, Workshop, Miskolc, (H)

Third International Palaeontological Congress IPC3, London (UK), <http://www.ipc3.org/>;

Forams 2010 - International Symposium on Foraminifera, Bonn (D), <http://www.forams2010.uni-bonn.de/>.

2009

International course on "Applied Facies Analysis in Carbonate rocks", Erlangen (D), <http://www.gzn.uni-erlangen.de/>;

International Course on Carbonate Microfacies", Erlangen (D), <http://www.gzn.uni-erlangen.de/>;

62nd Geological Kurultai of Turkey - Tertiary Larger

- Foraminifera: Evolution, Biostratigraphy, Palaeoecology and Palaeobiogeography; Genesis and Emplacement of Ophiolites, Ankara (TR), <http://www.jmo.org.tr/>;
- Integrated Studies of evolution, taxonomy, ecology and geochemistry: The Foraminifera and Nannofossil Groups Joint Spring Meeting 2009, Zürich (CH), http://www.nhm.ac.uk/hosted_sites/tms/foramnano2009.htm;
79. Jahrestagung der Paläontologischen Gesellschaft Paläontologie Schlüssel zur Evolution, Bonn (D), <http://www.palges2009.uni-bonn.de/>;
- Micro-CT und 3D-Visualisierung Workshop, Bonn (D).
- 2008 European Geosciences Union, Vienna (A), <http://meetings.copernicus.org/egu2008/>;
- Österreichische Paläontologische Gesellschaft, Dornbirn (A), http://www.geologie.ac.at/filestore/download/BR0075_001_A.pdf;
- Giornate di Paleontologia SPI, Siena (I), <http://www.unisi.it/eventi/simspi/presentazione.htm>.
- 2007 2nd International Workshop on the "Neogene of Central and South-Eastern Europe, Kapfenstein (A).
- 2006 Giornate di Paleontologia SPI, Trieste (I), www.spi.unimo.it/giornate06II.doc.

Publications

Briguglio A., Hohenegger J., Pervesler P., Sames B. & Zuschin M. (2008) - Actuopaleontology Course: Palaeoecology and Fossilization. Excursion Guide 2008. Briguglio (ed.). Universität Wien.

Peer-reviewed publications

- Briguglio A.**, Hohenegger J. and Yordanova, E. (submitted) - How To React To Shallow Water Hydrodynamics: The Larger Benthic Foraminifera Solution. *Marine micropalaeontology*
- Briguglio A.**, Metscher B & Hohenegger J (accepted) - Growth Rate Biometric Quantification by X-ray Microtomography on Larger Benthic Foraminifera: Three-dimensional Measurements push Nummulitids into the Fourth Dimension. *Turkish Journal of Earth Science*.
- Briguglio A.** & Hohenegger J. (2009) - Nummulitids hydrodynamics: an example using *Nummulites globulus* Leymerie, 1846. *Bollettino della Società*

Paleontologica Italiana, 48(2): 105-111.

http://www.girmm.com/articoli/Briguglio&Hohenegger_Nummulites_globulus_2009.pdf

Pignatti J., Di Carlo M., Benedetti A., Bottino C., **Briguglio A.**, Falconi M., Matteucci R., Perugini G. & Ragusa M. (2008) - SBZ 2-6 larger foraminiferal assemblages from the Apulian and Pre-Apulian domains. *Atti del Museo Civico di Storia Naturale di Trieste*, 2008 (suppl.): 131-145.
http://www.girmm.com/articoli/Pignatti_etal_SBZ2-6_2008.pdf

Abstracts

* indicates poster

** indicates talk

*** indicates invited talk

***Briguglio A.** & Hohenegger J. (2010) - The Shape entropy Parameter: a Geometric Tool to Approach Larger Foraminifera Accumulation. *Forams 2010 - International Symposium on Foraminifera*.
http://www.forams2010.uni-bonn.de/sites/sessions/pdf/abstracts_forams_2010.pdf
Poster:
http://www.girmm.com/poster/Briguglio_hydrodinamics_2009.pdf

****Briguglio A.** & Hohenegger J. (2010) - Quantifying Forams' Growth with high resolution X-Ray Computed Tomography: Ontogeny, Phylogeny, and Paleoceanographic Applications. *Forams 2010 - International Symposium on Foraminifera*.
http://www.forams2010.uni-bonn.de/sites/sessions/pdf/abstracts_forams_2010.pdf

***Briguglio A.**, & Forchielli A. (2010) - Transportability of Larger Benthic Foraminifera. *Third International Palaeontological Congress IPC3, London*.
<http://www.ipc3.org/docs/ProgrammeAbstractsfull.pdf>
Poster:
http://www.girmm.com/poster/Briguglio&Forchielli_transportability_2010.pdf

***Briguglio A.** & Hohenegger J. (2010) - Functional Test Morphology of larger Benthic Foraminifera: Biometric Quantification by X-Ray Microtomography. *Third International Palaeontological Congress IPC3, London*.
<http://www.ipc3.org/docs/ProgrammeAbstractsfull.pdf>
Poster:
http://www.girmm.com/poster/Briguglio&Hohenegger_biostratinomy_2010.pdf

****Briguglio A.** & Hohenegger J. (2010) - Transportability of Larger Benthic Foraminifera. W.O.L.F. Working Group on Larger Foraminifera, first meeting. *New insights in shallow marine tropical stratigraphy: integrating progress over the past ten years*,

Workshop, Miskolc

<http://www.ipc3.org/docs/ProgrammeAbstractsfull.pdf>

- *****Briguglio A.** (2010) - Quantifying Forams' Growth by high Resolution X-Ray Computed Tomography: Ontogeny, Phylogeny and Paleoceanographic Applications. W.O.L.F. Working Group on Larger Foraminifera, first meeting. *New insights in shallow marine tropical stratigraphy: integrating progress over the past ten years, Workshop, Miskolc*
- ***Briguglio A.** & Hohenegger J. (2010) - Biostratinomy in shallow water environments: how to tackle the larger benthic foraminifera depth distribution. *Third International Palaeontological Congress IPC3, London.*
<http://www.ipc3.org/docs/ProgrammeAbstractsfull.pdf>
Poster:
http://www.girmm.com/poster/Briguglio&Hohenegger_biostratinomy_2010.pdf
- ****Briguglio A.** & Hohenegger J. (2009) - Reconstructing the paleoenvironment of nummulitid strata: transport, erosion and deposition. *79. Jahrestagung der Paläontologischen Gesellschaft, Bonn 5-7/10/2009. Terra Nostra, 2009/3: 24.*
http://www.girmm.com/abstracts/Briguglio&Hohenegger_Bonn2009.pdf
- ****Briguglio A.** (2009) - Mathematical evaluation of the benthic larger foraminifera transport. *Integrated Studies of evolution, taxonomy, ecology and geochemistry: The Foraminifera and Nannofossil Groups Joint Spring Meeting 2009.*
http://www.girmm.com/abstracts/Briguglio_transport_2009.pdf
- **Höck V., Koller F., Hohenegger J., **Briguglio A.**, Ionescu C. & Onuzi K. (2009) - Late Jurassic Clastic Sediments on top of the Luniku Ophiolite Sequence: Southern Albania. *Genesis and Emplacement of Ophiolites, 62nd Geological Kurultai of Turkey, 13–17 April 2009, MTA-Ankara, Türkiye: 863.*
http://www.girmm.com/abstracts/Hock_et_al_Late_Jurassic_2009.pdf
- ***Briguglio A.** (2009) - Hydrodynamic behaviour of nummulitids: numerical explanation and discussed results. *Tertiary Larger Foraminifera: Evolution, Biostratigraphy, Palaeoecology and Palaeobiogeography, 62nd Geological Kurultai of Turkey, 13–17 April 2009, MTA-Ankara, Türkiye: 931.*
http://www.girmm.com/abstracts/Briguglio_hydrodinamics_2009.pdf Poster:

http://www.girmm.com/poster/Briguglio_hydrodinamics_2009.pdf

- *****Briguglio A.** (2009) - In vita and post mortem forams events: hydrodynamic tools for paleoenvironmental reconstructions. *Tertiary Larger Foraminifera: Evolution, Biostratigraphy, Palaeoecology and Palaeobiogeography, 62nd Geological Kurultai of Turkey, 13–17 April 2009, MTA-Ankara, Türkiye*: 890.
http://www.girmm.com/abstracts/Briguglio_hydrodinamics_2009.pdf
- **Benedetti A., **Briguglio A.**, Casieri S., D'Amico C., Di Carlo M., Frezza V., Gianolla D., Pisegna Cerone E. & Succi M.C. (2008) - GIRMM (Gruppo Informale di Ricerche Micropaleontologiche e Malacologiche): una risorsa online per uscire dall'anonimato. *In: Mazzei R., Fondi R., Foresi L., Riforgiato F. & Verducci M. (eds), Riassunti dei lavori Giornate di Paleontologia 2008*: 104.
http://www.girmm.com/abstracts/Benedetti_et_al_girmm_2008.pdf
- ****Briguglio A.** & Hohenegger J. (2008) - Hydrodynamic behaviour of nummulitids: a non -experimental approach. *In: Mazzei R., Fondi R., Foresi L., Riforgiato F. & Verducci M. (eds), Riassunti dei lavori Giornate di Paleontologia 2008*: 14.
http://www.girmm.com/abstracts/Briguglio&Hohenegger_Hydrodynamic_2008.pdf
- ***Briguglio A.** (2008) - New Oligocene coral reef in central Apennines (Majella mt., Italy). *Geophysical Research Abstracts*, Vol. 10, EGU2008-A-00000 EGU General Assembly 2008. Vienna.
<http://www.cosis.net/abstracts/EGU2008/01209/EGU2008-A-01209.pdf> Poster:
http://www.girmm.com/poster/Pignatti_et_al_sbz2-6_2006.pdf
- ****Briguglio A.** (2008) - *Nummulites*: ein einfaches geometrisches Verfahren zur Bestimmung hydrodynamischer Parameter. *Berichte der Geologischen Bundesanstalt*, 75: 8. 14. Jahrestagung Österreichische Paläontologische Gesellschaft. Dornbirn.
http://www.girmm.com/abstracts/Briguglio_Nummulites_2008.pdf
- *Pignatti J., Di Carlo M., Benedetti A., Bottino C., **Briguglio A.**, Falconi M., Matteucci R., Perugini G. & Ragusa M. (2006) - SBZ 2-6 larger foraminiferal assemblages from the Apulian and Pre-Apulian domains. *In: Fonda G., Melis R., Romano R. (eds.)*

Abstracts Giornate di Paleontologia 2006, p. 66.
http://www.girmm.com/abstracts/Pignatti_et_al_SBZ2-6_2006.pdf Poster:
http://www.girmm.com/poster/Pignatti_et_al_sbz2-6_2006.pdf

- Professional membership** Italian Paleontological Society (SPI) since 2003;
Cushman Foundation since 2007;
The Micropalaeontological Society since 2007;
Austrian Palaeontological Society since 2008.
- Journal reviewer** Carnet de Géologie - Notebooks on Geology - 1 review (2009)
- Others** Convenor of the session "Stratigraphy and Ecology of Cenozoic Larger Benthic Foraminifera" during FORAMS 2010, the International Symposium on Foraminifera, Bonn 2010
Award for Student Research of the Cushman Foundation: free one-year subscription to *The Journal of Foraminiferal Research* (2009)
Invited talk at the University of Linz
Online Database for "The Papp's collection on micropaleontology at the university of Vienna" 4000 entries (more than 12000 specimens)
Database for "Biostratigraphische sammlung der Universität Wien für die Vorlesung Biostratigraphie, Erdgeschichte und Phylogenese" 564 entries (more than 800 specimens)